FORM 6K

SECURITIES AND EXCHANGE COMMISSION
Washington, D.C. 20549

Report of Foreign Private Issuer Pursuant to Rule 13a – 16 or 15 d – 16
under the Securities Exchange Act of 1934

For the month of May 12

000-29880 (Commission File Number)

Virginia Mines Inc. 200-116 St-Pierre
Quebec City, QC, Canada G1K 4A7
(Address of principal executive offices)

Virginia Mines Inc.
(Registrant)

Date: May 11, 2012

By:
Name: Noella Lessard
Title: Executive Secretary

Exhibit 1

Technical Report and Recommendations – Summer 2011 Exploration Program – Lac Pau Project, Québec – March 2012

Prepared by: Jérôme Lavoie, M.Sc., P.Geo., Josée-Anne Lévesque, B.Sc. Trainee Geologist, and Paul Archer, M.Sc., Eng.,– Virginia Mines Inc.

8 paper copies

Original Document

000-29880
Commission File Number

ITEM 1 TITLE PAGE

Form 43-101F1
Technical Report

Technical Report and Recommendations
Summer 2011 Exploration Program, Lac Pau Project

MINES VIRGINIA INC.
March 2012

Volume 1

Prepared by:

Jérôme Lavoie, Eng., M.Sc.
Project Geologist
Virginia Mines Inc.

Josée-Anne Lévesque, B.Sc.
Trainee Geologist
Virginia Mines Inc.

And

Paul Archer, Eng., M.Sc.
Vice President, Exploration
Virginia Mines Inc.

TABLE OF CONTENTS

LIST OF TABLES

LIST OF PICTURES

LIST OF FIGURES

LIST OF APPENDICES

ITEM 3 - SUMMARY

The Lac Pau property is situated in the James Bay region (Caniapiscau MRC) just to the north of the Caniapiscau Reservoir, 70 km to the northeast of the Trans-Taiga all season road and Brisay Power House (Figure 1). An airstrip and many outfitters are located on the property which is accessible via a 65 km summer gravel road. The property is 100% owned by Mines Virginia Inc.

Since 2006, successful surface and drilling exploration programs were realized on Lac Pau area and led to discovering of several gold showings. These showings are observed in a kilometric-scale, gold-bearing deformation corridor hosted in a granodiorite with many facies. The Lac Pau Deformation Zone (LPDZ; Simard and *al.*, 2009a) hosts the Tricorne showing: **(9.02 g/t Au over 5.0 m including 17.48 g/t Au over 2.0 m in channeling and 3.43 g/t Au over 6.0 m in drilling)**, the Hope showing **(2.27 g/t Au over 10 m including 3.91 g/t Au over 5.0 m in channeling),** the Jedi and Jedi Extension showings **(2.35 g/t Au over 6.0 m including 5.36 g/t Au over 1.0 m in channeling and 0.53 g/t Au over 44.6 m including 0.71 g/t Au over 10.8 m),** the Beausac-2 showing: **(5.20 g/t Au over 7.0 m including 14.43 g/t Au over 2.0 m in channeling),** the Obiwan showing **(2.10 g/t Au over 5.0 m including 4.73 g/t Au over 2.0 m in channeling)** and the JAL-PPG showing **(2.70 g/t Au over 10.0 m including 10.74 g/t Au over 2.0 m and 10.95 g/t Au over 1.0 m in channeling).**

Following these favourable results, grid-line cutting, induced polarization and ground magnetic surveys were realized during winter of 2011 on Hope and Jedi Extension area. This geophysical program was performed concurrently to a drilling program that took place at the same period on the project. The drilling program confirmed the mineralization at shallow depth on the Jedi, Jedi Extension and Hope showings that returned respectively for the best intersections values of **2.17 g/t Au over 8.5 m including 3.56 g/t Au over 3.0 m (PAU-11-33), 1.32 g/t Au over 5.5 m (PAU-11-040) and 69.78 g/t Au (24.15 cut) over 1.2 m (PAU-11-44).**

Work performed during the summer of 2011 included prospecting, trenching and channelling to test IP (induced polarization) anomalies outlined during winter 2010-2011 that were not tested by drilling, prospecting and mapping of the new gridline, detailed mapping of Jedi and Tricorne showings and finally, regional prospecting. No new showing was discovered during this campaign. On the 13 new trenches performed during 2011 campaign, no significant gold value was returned but some anomalous results were obtained. The best new intersection is located on Beausac-II area and extends the Beausac-II mineralized zone by 45 m toward NW. Channel PAU2011R-002 returned **0.23 g/t Au over 12.0 m including 0.89 g/t Au over 1.0 m.** New channelling performed on 2009-2010 trenches on Jedi and Tricorne areas returned some interesting values but no new mineralized zone was outlined from this work. Best results include **0.74 g/t Au over 6.5 m including 3.48 g/t Au over 1.0 m** in the Jedi zone and **7.57 g/t Au over 3.0 m including 16.45 g/t Au over 1.0 m** in the Tricorne zone.

The highlight of the prospecting campaign amounts essentially to the discovery of a silica-chlorite altered intrusive in the west part of the property (located 24 km NW of Tricorne showing). Alteration is now observed over more than 24 km on the property and indicates a large hydrothermal system associated with regional intrusion (Red stars on Picture 2 and yellow stars Figure 4). Furthermore, a 3x3 meters angular and altered boulder was discovered on Hope area (891 m SSW of Hope showing) and returned **7.91 g/t Au (#205 975).** The presence of IP anomaly (PP-88) combined to the presence of this gold-bearing boulder could indicate that the Hope mineralized zone extends toward SE (Picture 1).

Besides of prospecting, a lithogeochemistry program was performed during this campaign. The results have identified the presence of two intrusive suites: (1) a quartz monzodiorite of regional extent (magnetite bearing) and (2) a granodiorite of more restricted extent, in close association with the mineralization and alteration (sulfides bearing). This latter presents a strong alteration expressed by leaching of Ca-Na, local enrichment in ferro-magnesian, potassic minerals (biotite and K-Feldspars) and silica flooding (Pearson, 2011). Besides the lithogeochemistry program, four (4) trenches were re-mapped in detail to better understand the structural framework in spatial relation with gold-mineralization on Jedi and Tricorne areas.

Finally, a large heliborne high resolution aeromagnetic survey was performed over Lac Pau property during September 2011 (8th to 17th September 2011) by Geo Data Solutions (GDS) Inc. A total of 4 681 km*linear were flown during this survey (Picture 2).

Following the results of the 2011 summer campaign, it appears that additional drilling is required on the property in the Hope and the Jedi, Jedi extension areas. During the next surface exploration program, a special focus should be brought along the western and northern interface of the granodiorite from the Beausac suite and the paragneiss? from the Grosbois complex (contact between low and high magnetic unit). A large lithogeochemistry surface program is strongly suggested to differentiate granodiorite from monzodiorite and to document the numerous alteration facies.

Picture 1 – Location of boulder (#205 975) that returned 7.91 g/t Au SSW of Hope showing. Note the location of IP anomaly PP-88 near the boulder location.

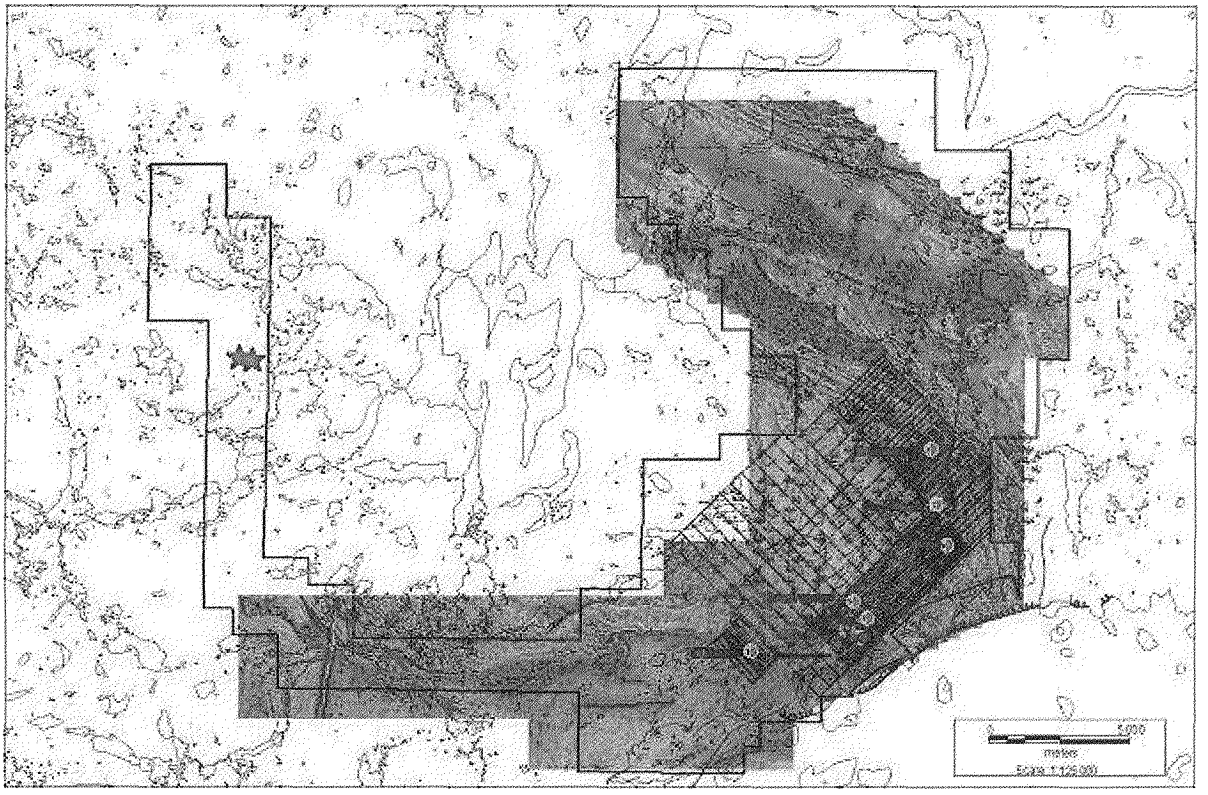

Picture 2 – Heliborne high resolution aeromagnetic survey, Lac Pau Project (Total magnetic field superposed with 50% transparency 1st vertical derivate). The red stars represent new occurrences of altered granodiorite discovered during 2011 summer campaign.

ITEM 4 - INTRODUCTION

Since 2006, many Au±Ag±Cu±Mo±Zn showings have been discovered on Pau Lake property (Lavoie et *al.*, 2007 and 2008, Lavoie and Archer, 2010a and 2010b, Savard and Lévesque, 2011 and Lavoie and *al.*, 2011). Following the 2010 prospecting program and the winter 2011 drilling and IP survey program, Virginia Mines pursued its exploration program during summer of 2011 (July to August). The first objective of this program was to explain IP chargeability anomalies that were not tested by drilling during winter 2011. The second objective was to prospect the new grid line located on Hope and Jedi Extension area looking for additional gold-bearing mineralization and finally, to map in detail some key trenches or outcrops located on Jedi and Tricorne showings. The field work was executed by Jérôme Lavoie (M. Sc. A., eng.), Louis Grenier (B.Sc., Geo), Josée-Anne Lévesque (G.I.T.), Anne-Marie Beauchamp, Tonny Girard, Benoît Martin-Tremblay, Catherine Boudreau, Ludovic Côté, Anne-Laurence Paquet, Alexandre Rodrigue (ungraduate students), Èva-Roy Vigneault (Senior Technologist), Marie-Pier Savard (Cook) and Catherine Provost (Cook) from Virginia Mines Inc. The mechanical shovel was operated by Felco Inc. from St-Félicien.

This report provides the status of current technical geological informations relevant to Virginia Mines' summer 2011 exploration program on the Lac Pau project in Québec and has been prepared in

accordance with the Form 43-101F1 Technical Report format outlined under NI-43-101. The report also provides recommendations for future work.

ITEM 5 – RELIANCE ON OTHER EXPERTS

First author Jérôme Lavoie, engineer with M.Sc. A. in Economic geology and Virginia's Project Supervisor manages the Lac Pau project and supervises all fieldwork conducted by Virginia Mines on the project. Co-author Josée-Anne Lévesque, trainee geologist for Virginia Mines, participated to fieldwork and to the redaction of this report. Co-author Paul Archer is engineer with a M.Sc. in Economic geology and Vice-President of Virginia Mines. This report does not rely on other expert.

ITEM 6 – PROPERTY DESCRIPTION AND LOCATION

The Lac Pau property is located in the James Bay region just to the north of the Caniapiscau Reservoir, 70 km to the northeast of the Trans-Taiga all season road (Figures 1). The property is constituted of 715 designated cells for a total surface area of 347.7 km^2 (Figure 2). The coordinates and maps covered by the project are:

Latitude:	54°87' Nord
Longitude:	-69°96' Ouest
SNRC:	23K/13, 23L/16 and 23N/4
UTM zone:	19 (nad83)
NTS:	446 000 mE
	6084 500 mN

Claims are listed in the appendix 1 (Figure 2).

ITEM 7 – ACCESSIBILITY, CLIMATE, LOCAL RESOURCES, INFRASTRUCTURE AND PHYSIOGRAPHY

The Lac Pau camp is located at kilometre 647 on the Trans-Taïga road and approximately 70 km north-east of the Brisay PowerStation. The Trans-Taïga road is accessible all seasons up to Brisay. From Brisay to Lac Pau, the gravel road is accessible only in summer. To access the camp, vehicles follow the directions to the Duplanter or Air Saguenay and Explo Sylva Outfitters from Brisay. A landing airstrip is present and operational all summer long at 10 km of Lac Pau camp. All gravel roads are privately owned by Hydro-Québec and their maintenance is the responsibility of Les Services Naskapi Enr.

The main showings are located at a maximum of 15 kilometers north-east of the Lac Pau Camp and at a maximum of 10 kilometers to the north-east of the Caniapiscau airstrip. An Astar BA (Canadian Helicopters) and 4x4 trucks were used for crew transportation. All equipments, including fuel and supplies, were carried directly to the campsite by truck. Fontanges airport, also accessible by the Trans-Taïga all-season gravel road, is the nearest all-season facility for aerial transportation.

The landscape of the studied area is relatively uneven with altitude ranging from 400 to 580 meters. The hydrographic system includes many large lakes and a major old river (Caniapiscau River). The hydrographic network was modified by human with dam construction and flooding of the Caniapiscau reservoir. Vegetation is typical of taiga including areas covered by forest and others, typically at the top of hills, devoid of trees.

ITEM 8 – HISTORY

Table 1 summarises all the history of work performed in the area of Lac Pau.

Table 1- Summary of previous work in the Lac Pau project area

SDBJ (1972)
-Évaluation du potentiel minier du bassin de la Baie James (GM 34000).

SDBJ (1974)
-Summary report on mineral resource studies in the James Bay (GM 34002).

SDBJ (1975)
-Lake Sediment Geochemistry. (GM 34036).

SDBJ (1975)
-Geological study of mineral potential (GM 34001).

SDBJ - SERU Nucléaire (Canada) Ltée. (1977)
-Prospecting for Uranium. (GM: 34156, 57676).

SDBJ (1986)
-Lake Sediment Geochemistry (GM 34039).

BHP Minerals Canada Ltd - IOS Services Géoscientifiques Inc. (1998)
-Till Sampling Program (GM 59086)

MRN (2000)
-Geological Mapping (23L) (RG 2000-11).

Mines Virginia Inc. (2006)
-Prospecting and Channeling (GM-63498).
-Discovery of JEDI showing (2.87 g/t Au)
-Channelling of JEDI showing (2.35 g/t Au / 6.0m)

Mines Virginia Inc. (2007)
-Prospecting and Channeling (GM-63495).
-Heliborne MAG-EM Survey (GM-63497) (703 linear km @ N045 & 200m line spacing)
-Discovery of TRICORNE Showing (grab sample up to 4.48 g/t Au; 7.70 g/t Ag & 0.16% Cu)

MRNF (2008)
-Geological Mapping Région du réservoir Caniapiscau (SNRC 23K-23N) (RG 2009-04).
-Discovery of Beausac-2 showing (2.27 g/t Au; 2.45% Cu & 101 g/t Ag)

Virginia Mines Inc. (2009)
-Prospecting, Trenching and Channeling
-Channelling of TRICORNE showing (9.02 g/t Au / 5.0m)
-Channelling of BEAUSAC-2 showing (5.20 g/t Au / 7.0m)
-Discovery of JAL showing (Channel: 2.70 g/t Au / 10.0m)

Virginia Mines Inc. (Winter 2010)
-Drilling Campaign (28 drillholes for 3612 m)
-Line Cutting (304 km)
-Ground Magnetic Survey (99 km)
-Induced Polarization (IP) Survey (213 km)

Virginia Mines Inc. (Summer and Fall 2010)
-Prospecting, Trenching and Channeling
-Trenching and channeling of IP anomalies
-Discovery and channeling of Hope showing (2.27 g/t Au / 10.0 m inc. 3.91 g/t Au / 5.0m)
-Channelling of Jedi Extension showing (1.04 g/t Au / 5.5m)

Virginia Mines Inc. (Winter 2011)
-Drilling Campaign (16 new drillholes and 2 previous holes extended for a total of 2776 m)
-Line Cutting (112 km)
-Ground Magnetic Survey (200 km)
-Induced Polarization (IP) Survey (140 km)

ITEM 9 – GEOLOGICAL SETTING

The Lac Pau property is located in the Archean Superior Province, in the central part of the Ashuanipi high metamorphic-plutonic subprovince near the western contact with the La Grande volcano-sedimentary subprovince.

9.1 – Regional Geology

The Archean rocks of the Ashuanipi high metamorphic-plutonic complex are located in the extension of Opinaca and La Grande volcano-sedimentary subprovinces (Leclair and *al.*, 1998). The first known events in Ashuanipi subprovince correspond to volcanism and sedimentation between 2720 Ma and 2700 Ma and syn-volcanic magmatism (tonalitic in composition) until 2690 Ma (David et *al.*, 2009; Simard, 2008). These rocks were merged between 2682 and 2650 Ma (Leclair and *al.*, 1998; Chevé and Brouillette, 1995; Percival, 1993; Simard and *al.*, 2009a) to produce large diatexite units characteristic of Ashuanipi subprovince (Simard and *al.*, 2009b). These diatexites are cut by granitic to tonalitic intrusions (2650 and 2625 Ma; Simard and *al.*, 2009b). Finally, around 2570 Ma, fluorine-bearing anorogenic granite intrusions took place in Ashuanipi subprovince (Simard and *al.*, 2009b). Most of the

rock units in the area of the Lac Pau property have been metamorphosed to the amphibolite to granulite facies.

For a complete descriptions of the regional geology, the reader is referred to studies by Simard and *al.* (2009a and 2009b), Thériault and Chevé (2001) and Gosselin and Simard (2000), which deal with sheets 23N (Rivière Sérigny) and 23K (Réservoir Caniapiscau), respectively. A simplified description (mainly taken from these studies) of the most abundant lithostratigraphic assemblages mapped during our exploration work is included below.

9.1.1 – Grosbois Complex

The Grosbois complex is a lithodemic complex unit composed of two fractions: an old paleosome, a paragneiss and a more recent neosome of tonalitic to granitic composition, a mobilisate. The complex is subdivided in three (3) units: (1) biotite + orthopyroxene + garnet paragneiss, (2) biotite + orthopyroxene paragneiss and (3) biotite ± garnet paragneiss. The Grosbois Complex is particularly abundant SW of the Lac Pau property. Locally, decimetric to decametric banded iron formations is observed interlayed with paragneiss. Simard (2008) attributes an age of 2700 Ma to the sedimentation period that forms the metasediments of Grosbois Complex. The Grosbois Complex paragneiss and the Raynouard Group paragneiss, observed on Ashuanipi property, could be an equivalent.

9.1.2 – Beausac Suite

Beausac Suite was introduced in Lac Gayot area (Gosselin and Simard, 2000) to describe tonalites, quartziferous monzodiorite and granodiorite. Deformed tonalite sample gave an age of 2698.8 ± 0.8 Ma. This unit is composed of tonalite and granodiorite, fine to medium grained, foliated and affected by linear deformation. These rocks contain between 10 to 20% green hornblende and biotite. The tonalite contains some metric to decametric horizons of quartziferous diorite, 1-3% of centimetric to metric amphibolite or ultramafic enclaves and injected by 10% massive granitic or pegmatite (granitic to tonalitic in composition) dykes.

9.1.3 – Opiscoteo Suite

Opiscoteo Suite is a diatexite unit who characterizes Ashuanipi Subprovince. Leclair and *al.* (1998) subdivided Opiscoteo Suite into six (6) informal units based on these criterions: 1) presence or not of garnet; 2) enclaves and biotite schlierens (<25%: homogeneous and >25%: heterogeneous) and 3) enclaves composition. Numerous U/Pb datations on the Ashuanipi Subprovince place the Opiscoteo Suite diatexites formation between 2682 and 2630 Ma (Chevé et Brouillette, 1995; Percival, 1993; Leclair and *al.*, 1998; David and *al.*, 2009). The Lac Pau area diatexites are homogeneous biotite±garnet intrusive rocks formed by anatexis who result from Grosbois Complex advanced melting. The diatexites contains 10-25% enclaves and biotite schlieren, heterogranulars and injected of pegmatites. The rock composition varies from tonalitic to granitic.

9.1.4 – Caniapiscau Suite

Caniapiscau Suite is composed of tonalitic diatexite with numerous tonalitic, quartziferous dioritic, gabbro, ultramafic and amphibolite enclaves. The field observations suggest that diatexites can represent a partial melting of tonalites and diorites of Beausac Suite. Homogeneous diatexite sample (quartziferous diorite) gave an age U/Pb of 2664 +9/-7 Ma. This result indicates that partial melting of Canipiscau Suite is contemporary with partial melting of Opiscoteo Suite.

9.1.5 – Dervieux Suite

Dervieux Suite group homogeneous to heterogeneous porphyritic granite and granodiorite intrusion composed of 5-10% biotite ± hornblende and 5-20% K-Feldspars porphyry crystals (0,5 to 3 cm). The intrusive rocks are medium to coarse grained, massive to weakly foliated and can contains paragneiss enclaves.

9.1.6 – Joinville Suite

Joinville Suite forms numerous plurikilometric intrusions. The Joinville granite is homogeneous, massive, fine to medium grained, locally pegmatitic or porphyritic and contains 2-5% biotite ± chlorite ± magnetite.

9.2 – Local geology

The geology of Lac Pau property is characterized by the presence of metasedimentary rocks from the Grosbois Complex and granodioritic to quartz monzo-dioritic intrusive rocks from the Beausac Suite. The dominant feature of this belt is the presence of several hectometre-scale (length) gold-bearing zones (Jedi, Jedi Extension, Tricorne, Hope, Obiwan and Beausac-2 gold-bearing zones) hosted in a granodiorite intrusion. Gold mineralization is closely associated with K-Feldspars-Chlorite-Silica-Sillimanite±Cordierite±Sericite±Garnet±Fuchsite pre-metamorphic alteration along a regional open fold with axial plan oriented NW-SE (Picture 3). Metamorphism, deformation and alteration have modified the rocks described above and consequently, additional rock descriptions are required to illustrate the different facies encountered from the Grosbois Complex and the Beausac suite.

Most of the Lac Pau property is poor in outcrop exposure except for the old Caniapiscau riverbed that presents outcrop exposure in continuity. The riverbed exposes most of the contact between the Grosbois Complex metasedimentary rocks (low magnetic unit) and the Beausac suite (high Magnetic unit) and illustrated on Picture 4. Most of the mineralization outlined on the property happens to occur along this contact, mostly hosted within the granodiorite belonging to the Beausac suite rocks. The contact is also characterized by the presence of intense deformation zone, oriented NE to NW, that hosts most of the gold values. The Jedi, the Jedi Extension and the Beausac-2 gold showings all occur along the LPDZ located at the granodiorite / metasediment? interface in the old riverbed of the Caniapiscau river.

The descriptions below include the proposed protolith for each metamorphic rock, based on our present level of understanding. Abbreviations used in the description of rocks come from Sharma (1996).

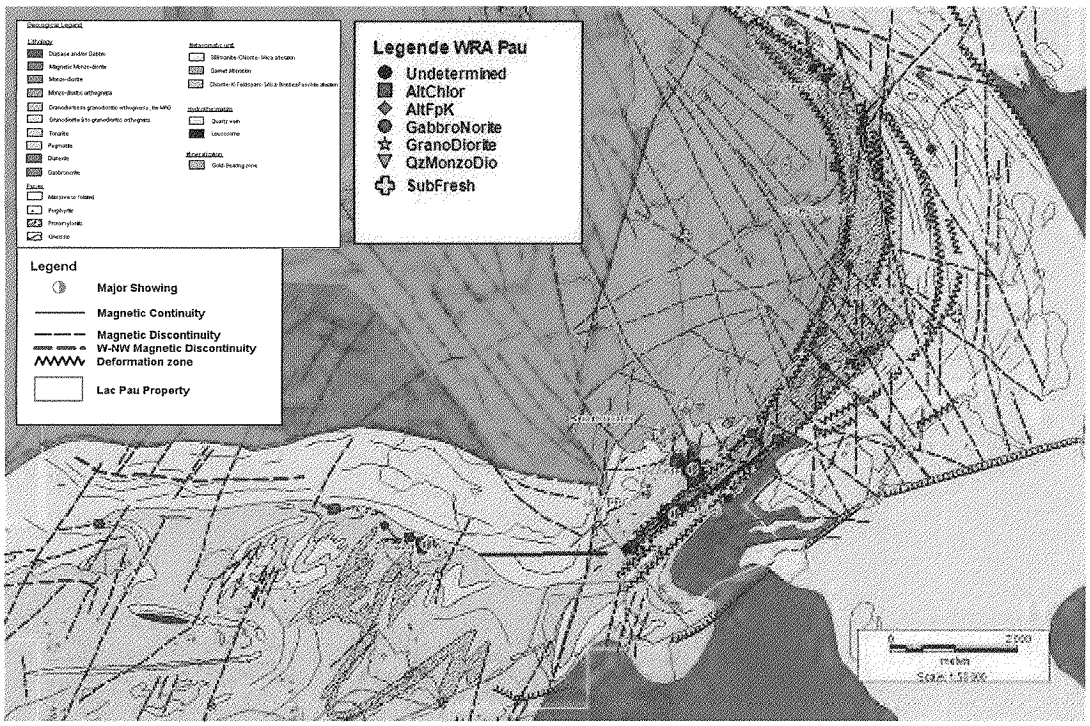

Picture 3 – Location of major showings along Lac Pau Deformation Zone (LPDZ). Contact between quartz monzodiorite and protomylonitic granodiorite is observed along the open fold and well represented by classification of whole rock analyses (WRA).

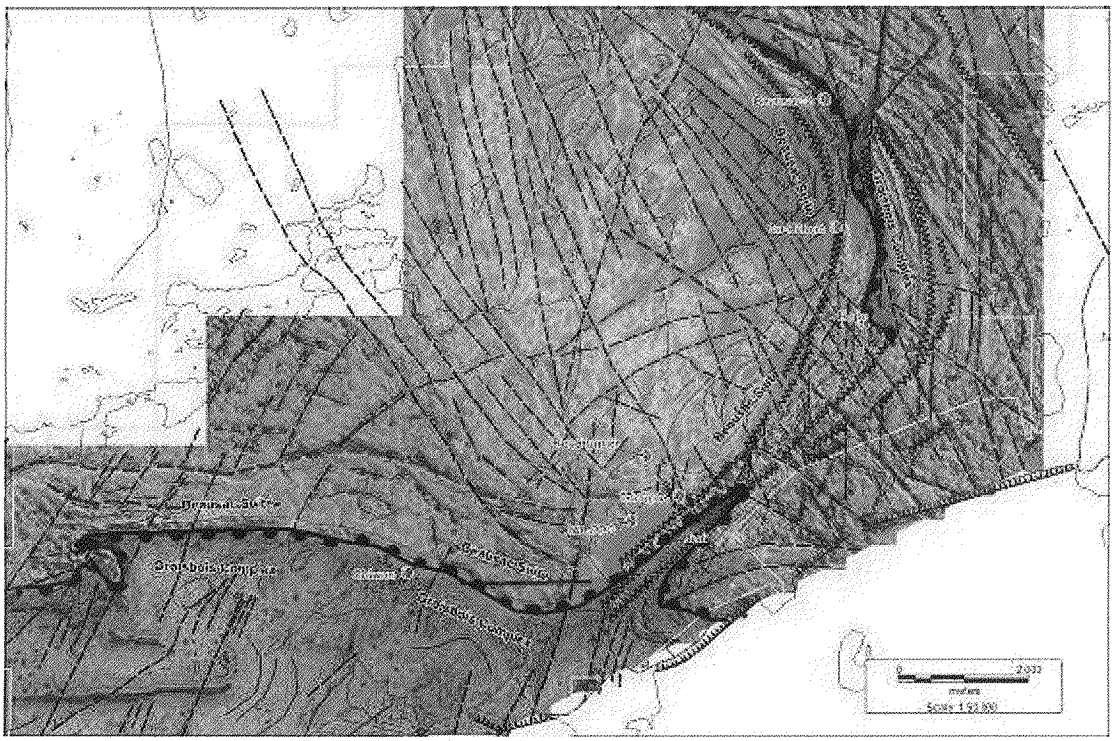

Picture 4 –Magnetic contrast between Grosbois Complex (low magnetic unit) and Beausac Suite (high magnetic unit).

9.2.1 - Facies from Grosbois complex

The rocks from the Grosbois complex encountered on the Property are mostly concentrated in the old riverbed of the Caniapiscau River and in the west section of the property and are constituted by migmatized rock. These rocks, interpreted as paragneiss, are characterized by a brownish to greyish salt and paper colored, fine-grained and granoblastic texture and they contain biotite (15-25%) and local millimeter- to centimeter-scale garnet porphyroblasts. Leucosomes (10-40%) issued from partial melting also compose the paragneiss. Leucosomes occur as irregular millimetric to centimetric bands that form migmatized bands mainly parallel to the paragneiss foliation. Biotite alignment and migmatitic injection form a well-developed schistosity. The consistency of leucosome occurrence and the brownish color makes this unit easy to identify on the field. The 2011 lithogeochemistry program has not allowed though to confirm without any doubt the true sedimentary nature of these rocks, According to Pearson (2011), the identification of the metasedimentary rock through the use of major elements is, at this time, virtually impossible. Although we can't rule out the occurrence of some metasedimentary rocks, it would have been more convincing to observe a specific compositional range.

9.2.2 - Facies from Beausac Suite

Section 9.2.2 to 9.2.4 is a summary of the current understanding of the property geology taken from two (2) internal reports (Pearson and Lavoie, 2011 and Pearson, 2011) written for Virginia Mines Inc. and IAMGOLD Corp. The reader is referred to figure 4 for the geological interpretation map.

Felsic intrusion: Granodiorite (GRD) and Quartz Monzo-diorite (QMD)

The whole rock analysis identifies two (2) distinct intrusions on the Lac Pau Property. (1) A calc-alcaline, per-aluminous **granodiorite (GRD)**, and (2) equally of calc-alcaline affinity, a **quartz monzodiorite (QMD)**, with a meta-aluminous character. Not only these two rock types are readily identifiable on diagrams (Picture 5) but they define coherent mappable units (Figure 4). The QMD is the unaltered and highly magnetic intrusive on the western part of the property (Figure 4), while the GRD represents the porphyry to massive unit host of the mineralization. It is interesting to note that the QMD has a gold content near the detection limit and a zinc content of 44 ppm, while the GRD has a mean gold content of 0.011 ppm and a zinc content of 98 ppm (Pearson, 2011). It must be point out that the validity of this lithogeochemistry process is dependent on an important assumption, namely: the protolith is an igneous rock.

For a majority of outcropping areas, the nature of the protolith is completely obscured by the deformation and the metamorphism, but in places some remnants are preserved and locally convincing primary textures are observed specially on many showings like Obiwan (Picture 6), Jedi (Picture 7) and Tricorne (Picture 8). Examples show such primary texture only affected by an incipient schistosity or not affected by deformation often impregnated by a silicification and/or chlorite-biotite-sericite alterations. The rock is made of mm feldspar phenocrysts set in a fine-grained matrix. In the porphyry, the microgranoblastic matrix is likely to represent a recristallized mesostasis making the texture of the protolith potentially very similar to high level intrusion of Phanerozoic porphyry equivalent. On this basis, the porphyry merits a distinct designation, for short we propose **Pau Porphyry**. One of the main characteristic of this unit is the presence of amphibole±biotite-rich fragments or porphyroblasts. These

fragments are sub-angular to well-rounded and represent 1-2% of the rocks and vary from 2 cm up to 1 meter and are often stretched within main foliation. Some of them are almost completely retrograded in chlorite. Like observed on picture 7, the Pau Porphyry is variably deformed. In this picture, a clear example of grain size reduction caused by deformation is featured. Deformation will be treated in more detail in section 9.2.6.

A second type of intrusive hosting mineralisation is represented by a fine grained granodiorite relatively homogeneous and devoid of porphyritic texture. Whole rock analysis confirmed that this fine-grained facies has the same composition than the primary textured facies (granodiorite in composition) and represents a textural variation of the porphyritic unit. As shown on figure 9, this greyish unit is locally only slightly deformed to locally massive.

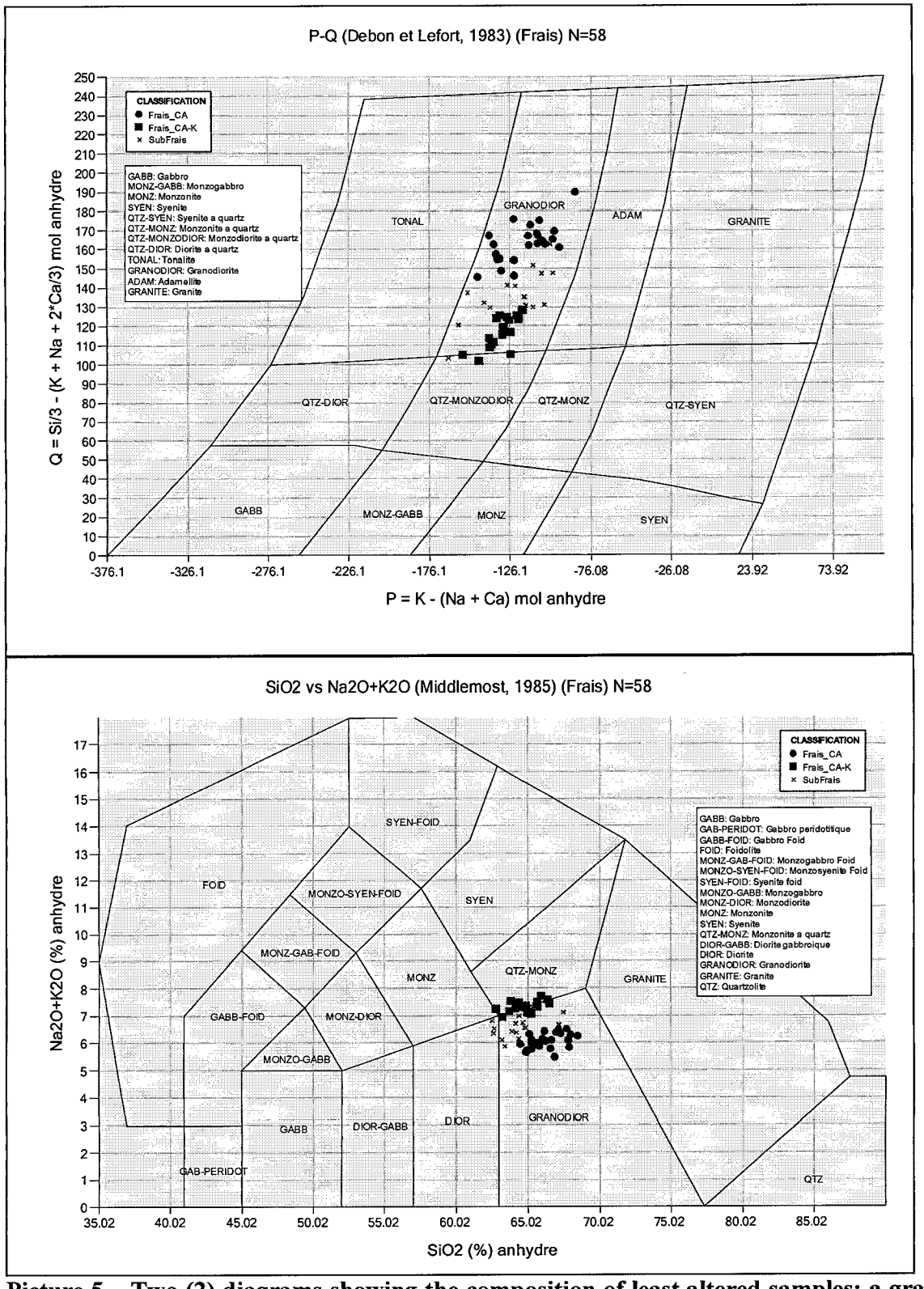

Picture 5 – Two (2) diagrams showing the composition of least altered samples: a granodiorite (GRD) and a quartz monzodiorite (QMD) intrusion.

Picture 6 – Preserved feldspar porphyry rock with 45% of sub-idiomorphic to idiomorphic plagioclase phenocrysts set in a microgranoblastic intermediate matrix. Alteration is observed by sericitization of feldspar phenocryst and occurrence of biotite in the brownish matrix. Color changes from left to right (respectively brownish to greywish) and caused by silicification of the matrix. Obiwan showing (PAU2011TR-001).

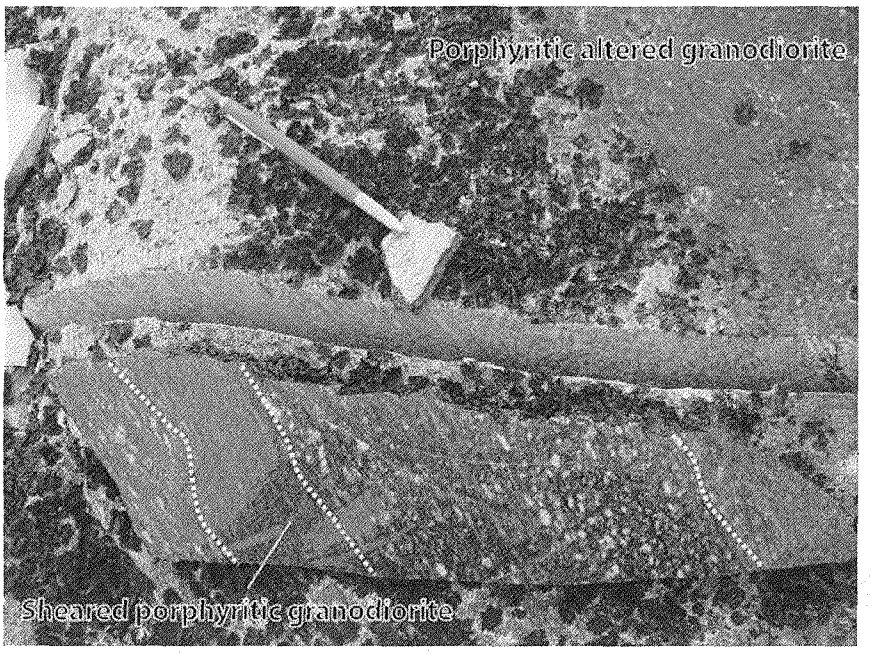

Picture 7 – Granodiorite exhibiting porphyry texture. Deformation is heterogeneously distributed, developing bands of finely laminated protomylonite to mylonite. Jedi showing (PAU2011TR-11).

Picture 8 – Chlorite-sericite-sillimanite massive granodiorite exhibiting porphyry relic texture. Tricorne showing (PAU2009TR-014).

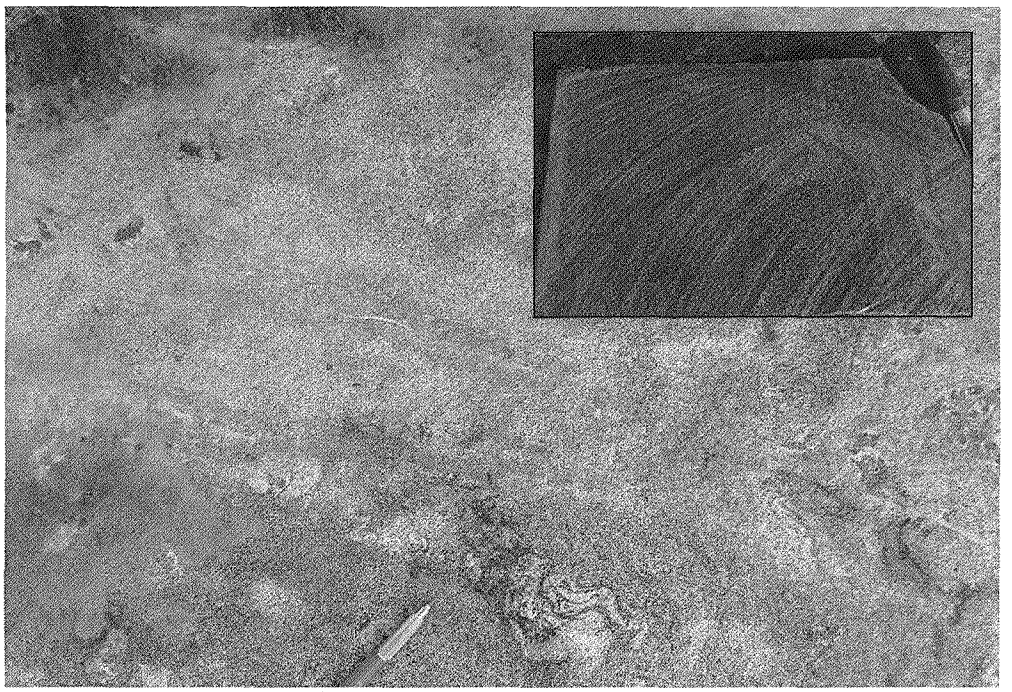

Picture 9 – Fine-grained and massive granodiorite. The protolith appears to be homogeneous and free of primary phenocryst, Tricorne area.

Metasomatized granodioritic rock

As already notified since 2006 from petrographic description, alteration appears to be an early event in the geological history. As mentioned by Tremblay (2007), the cordierite-biotite-sillimanite assemblage with up to a few percent garnet possibly represents a Fe-Mg-K-Al-rich and Na-Ca-poor rock. This composition (plagioclase–quartz±biotite±cordierite±sillimanite±séricite±chlorite±carbonates) also suggests that sericite-chlorite pre-metamorphic metasomatic hydrothermal alteration took place accompanied with sulphides±Au (Tremblay, 2007). Also, presence of cordierite in protomylonitic to mylonitic granodiorite clasts suggests a late deformation (Tremblay, 2007).

Metasomatized granodiorite is usually described where silica, biotite, chlorite, K-Feldspars, sillimanite, cordierite, sericite and garnet are present in association with sulphide mineralization within the granodioritic intrusion. The assessment of alteration is based on the assumption that metasomatism is caused mainly by hydrothermal processes and possibly by slight mobilization from metamorphism (Pearson, 2011). This unit often occurs as corridor (Jedi, Beausac-II, and Jedi Extension) along a deformation zone or occurs as plurimetric folded bands (Tricorne, Hope and Obiwan).

1. Silicification

When considering the normative phases Alb-Fpk-Qtz, the resulting ternary diagram (Picture 10) shows an over representation of quartz expressing silicification. A particularity of that silicification stands on its ubiquitous occurrence. This latter alteration (silicification) doesn't characterize a specific alteration facies, but is present in all of them, i.e. silicification can be associated with sericite facies, chlorite facies or orthose facies (Picture 18). When reported on a geological map, this silicification – i.e. rock having over 50% normative quartz (Picture 18) – is distributed all along the recognized deformation zone, from Obiwan to Beausac and known over 13 km of extent (Pearson, 2011). It's ubiquitous occurrence is best explained if considered as an early alteration stage (Pearson, 2011).

The lithogeochemistry is supported by field observations on Tricorne, Jedi and Obiwan showings. Primary well-preserved phenocrysts are observed in a highly silicified and brecciated granodiorite (Picture 11 and 12). Silicification reaches a climax with large, pluri-metric patches of silica impregnation. Geometric distribution of the silicification on Obiwan and Jedi showings is asymmetric. One edge is irregular with development of elongated patches (Picture 13 and 14), while the other is sharp, curvilinear, faulted and in contact with a deformed but unsilicified feldspar porphyry (Picture 15 and 16). The contrasting nature of the contact on both sides of the silicified area suggests a dislocation of the alteration zone and consequently, a relative chronology where alteration predates at least in part deformation (Pearson and Lavoie, 2011). At the outcrop scale, an incipient schistosity affects the silicification suggesting, once again, an early alteration (Picture 17). It is important to note that the highly silicified zone hosts pyrite-chalcopyrite-molybdenite and gold mineralization.

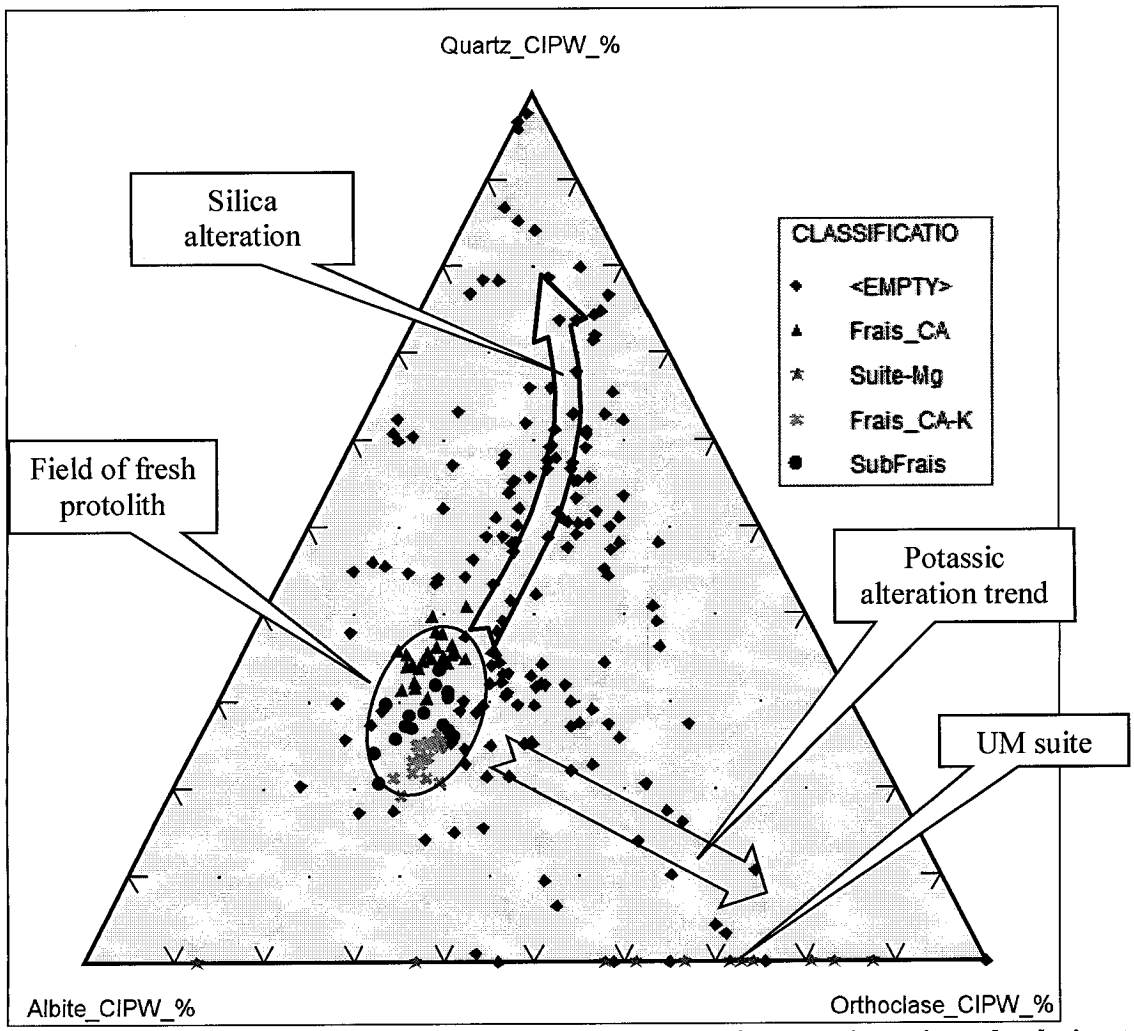

Picture 10 – Ternary diagram showing modification of normative mineral relative to the field of the least altered rocks. Not only can we see the trend toward OR pole, but equally a large number of samples strongly oversaturated in silica, depicting an excess of normative quartz (Pearson, 2011).

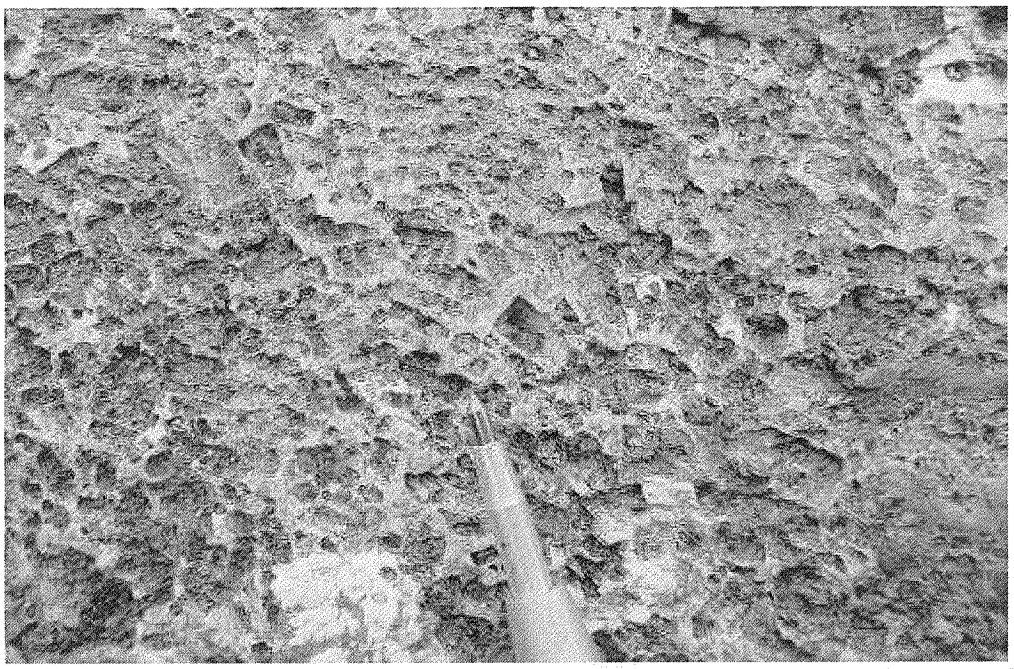

Picture 11 – Extreme silicification of the feldspar porphyry with complete destruction of primary features. Microgranular quartz represents over 80% of the volume (Obiwan showing, PAU2009TR-007).

Picture 12 – Hydrothermal brecciation showing a jigsaw puzzle texture. Extreme silicified fragments (delimited by a red line) of the feldspar porphyry are observed in a chloritized-sericitized-potassic altered granodiorite matrix (Tricorne showing, PAU2009TR-012).

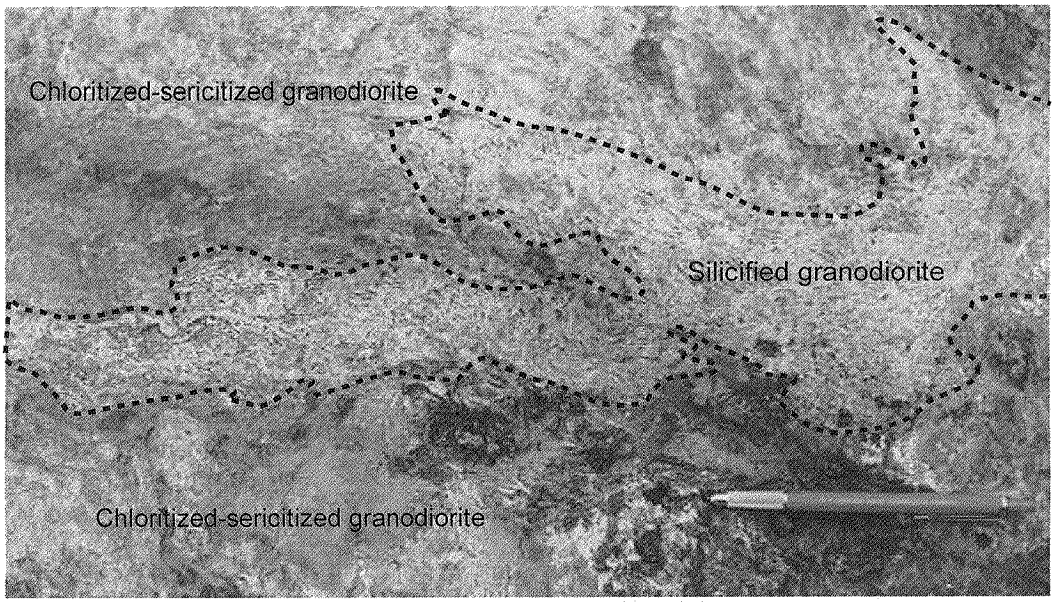

Picture 13 - Elongated patches of silicification bordered by strong chlorite-sericite±sulfidization. These patches are amoeboid and don't follow a specific orientation suggesting a possible primary stockwerk distribution (Obiwan showing, PAU2009TR-001).

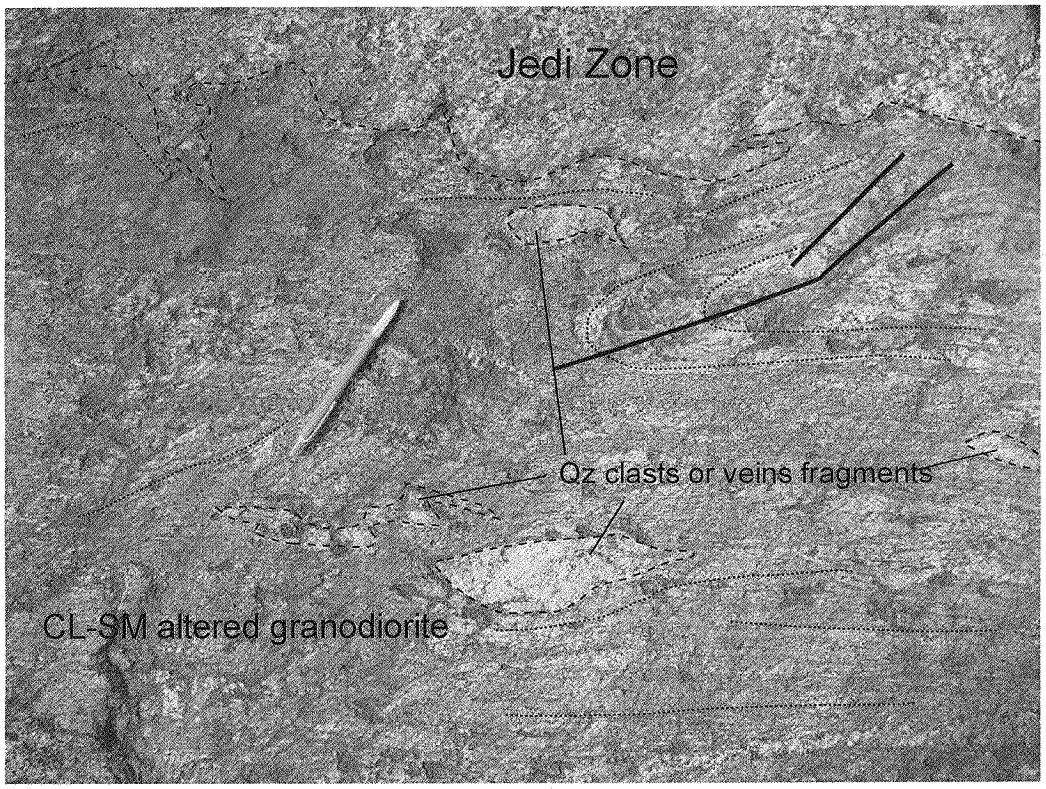

Picture 14 – Assymetric SE contact between Jedi mineralized zone and chlorite-sillimanite altered protomylonitic granodiorite. Quartz fragments observed suggesting a transitional hydrothermal brecciation between mineralized zone and host rock (Jedi showing, PAU2011TR-012).

Picture 15 – Detail of the contact between the strongly altered and deformed feldspar porphyry (to the left) and the highly silicified counterpart (to the right) Obiwan zone. The sharp contact between the two domains differs strikingly from the irregular contact shown on picture 13 and can be related to some late displacement along the contact (PAU2009TR-001).

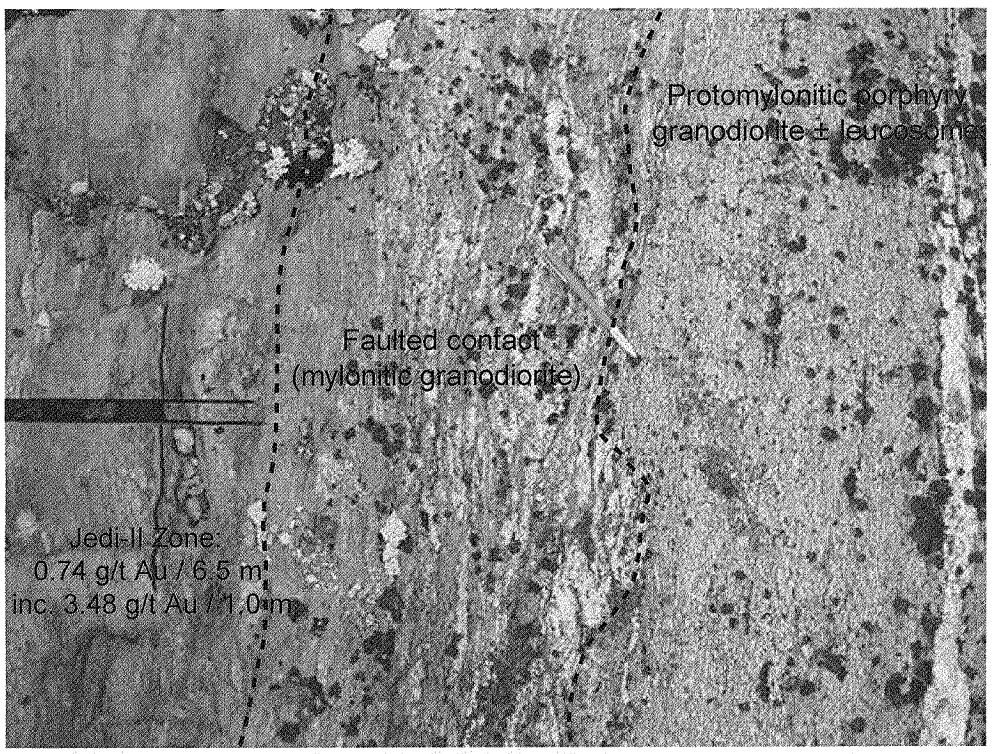

Picture 16 – Detail of the contact between the strongly silicified, deformed and mineralized granodiorite (to the left) and the protomylonitic porphyry (to the right) Jedi-II zone. The sharp contact between the two domains is materialized by a fault zone (mylonite) and differs from the irregular contact shown on picture 14 and can be related to some late displacement along the contact (PAU2011TR-013).

Picture 17 – Close Up of the porphyry texture featuring sericitized plagioclases (subidio- to idiomorphic) set in a highly silicified matrix. Incipient schistosity affects the silicification suggesting an early alteration (Obiwan showing, PAU2009-TR-001).

Silicification occurs equally and much frequently as veining (Picture 18 and 19). This veining is observed in many showings like Obiwan, Jedi, Tricorne and Hope. The deformation affected the veins suggesting the presence of a stockwerk zone in an early stage during mineralization history. It is not surprizing to preserve evidences of veining in the Lac Pau mineralised zone, despite the upper amphibolite to granulite facies metamorphism. The monomineralic nature of the quartz veins differs strikingly from the migmatitic material which results from an eutectic melt at around 600-700°C (Pearson and Lavoie, 2011). The melting point of quartz is around 1670°C, which represents an efficient refractory being well preserved through metamorphism and only affected by deformation (folding, boudinage and dislocation).

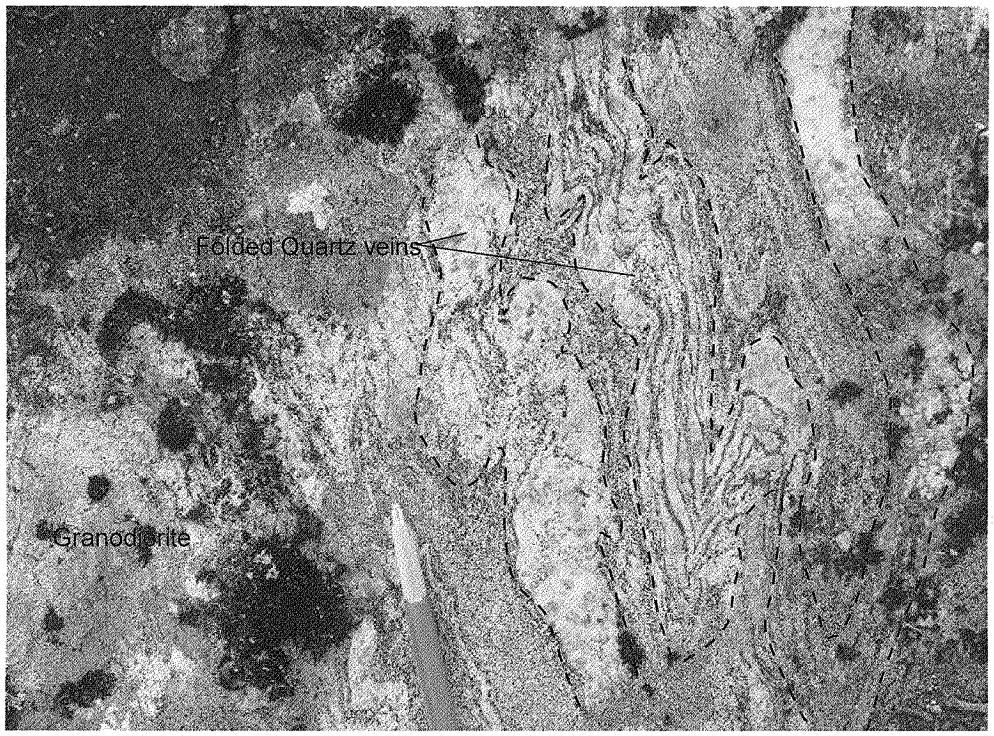

Picture 18 – Fine-grained granodiorite affected by a silicification. Quartz veins are folded indicating an early stage injection during hydrothermal activity (PAU2011JL-005).

Picture 19 – Highly deformed quartz veins hosted in a metasomatized granodiorite strongly altered to silica-chlorite±sillimanite±sulphides (PAU2011JL-052).

2. Potassic and chlorite alterations

Following numerous attempts to classify alteration facies, it appears that the most instructive and coherent representation is through the use of alcalies elements (Hughes diagram's; picture 20). This diagram let's see two alteration trends, one expressing a global enrichment in K2O and the other expressing a depletion in Na2O (with an apparent enrichment in K2O caused by the increase of the ratio K/Na+K. A large proportion of these soda depleted samples are equally enriched in ferro-magnesian elements. Chlorite alteration is quickly visible on the field. This alteration occurs pervasive or as metre scale fractures crosscutting the feldspar porphyry (Picture 21).

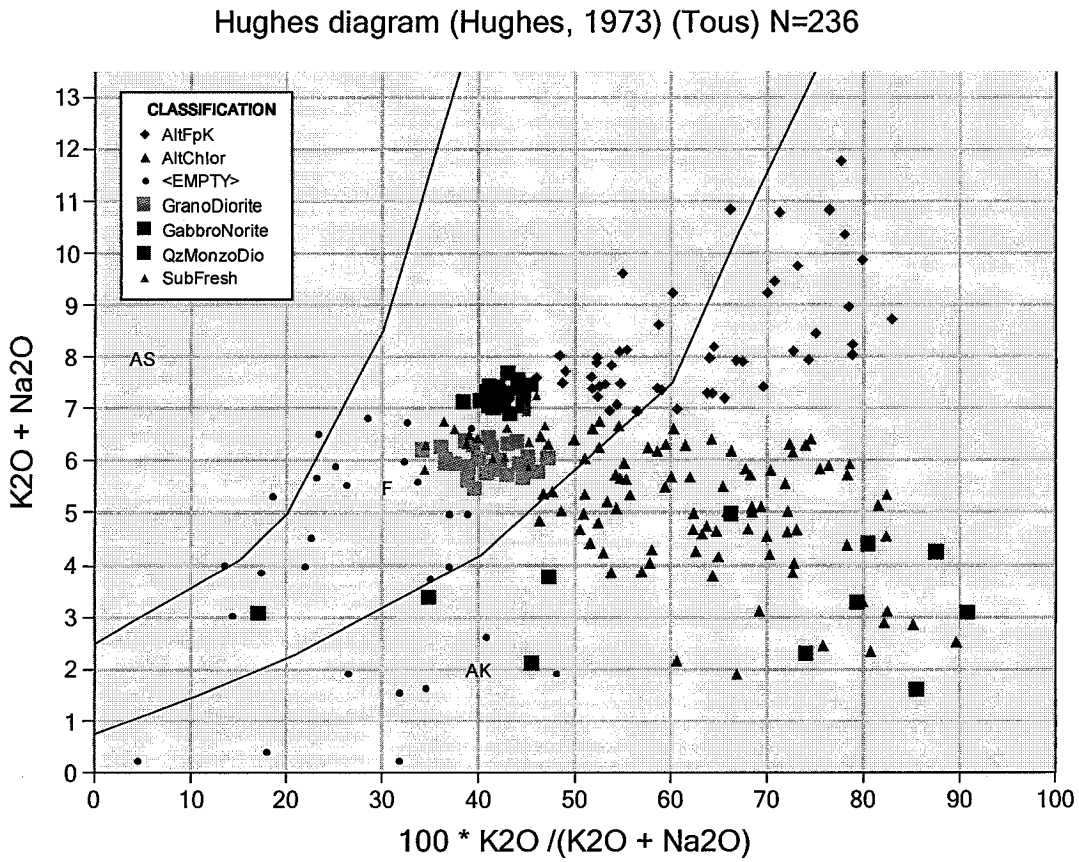

Picture 20 - Hughes diagram originally designed to assess sea floor alterations reveals to be quite efficient in recognizing alteration trend. Here, we can see three trends of alteration: 1) a potassic enrichment trend, 2) an alcalies depletion trend and 3) a mild sodic alteration, (Pearson, 2011).

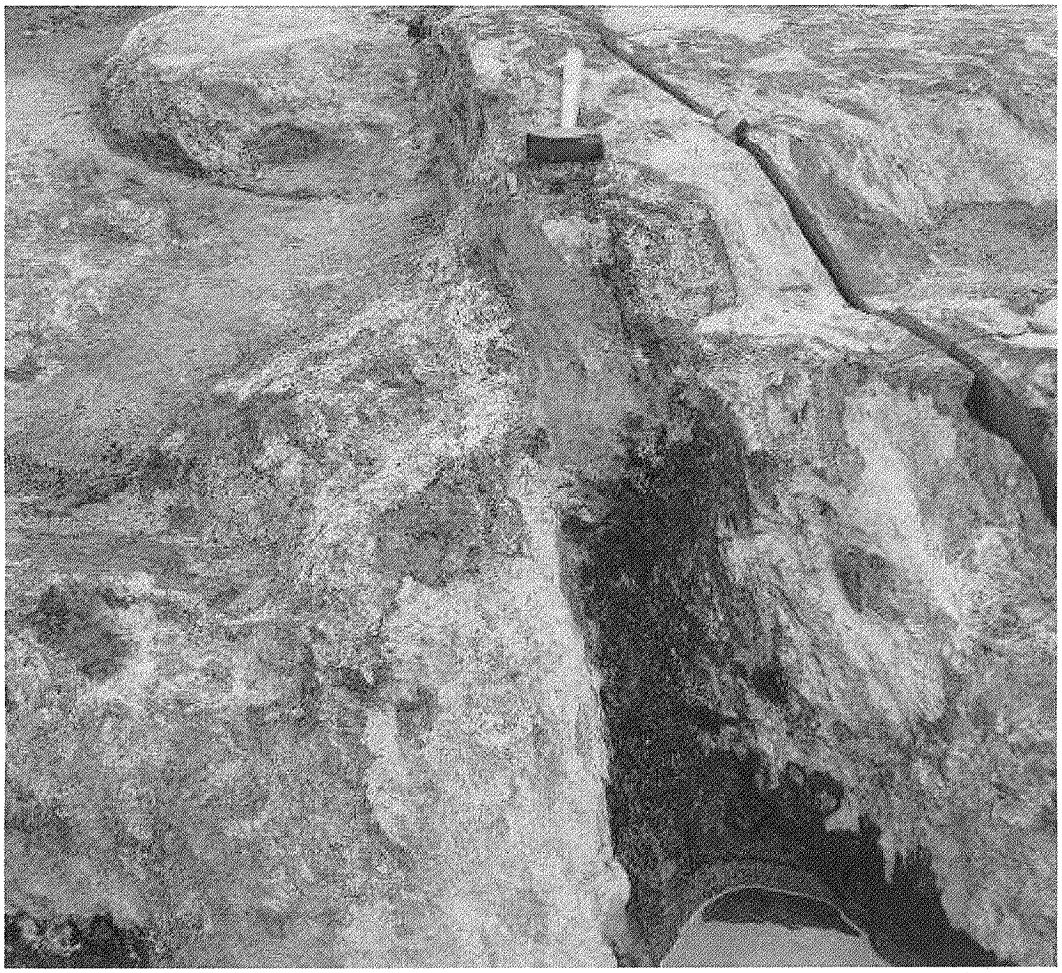

Picture 21 - Highly chloritized fractures on the Hope showing, (Pearson and Lavoie, 2011).

3. Aluminous-Magnesium enrichment

Granodiorite can be affected equally by an Al-Mg enrichment visible by sillimanite in biotite-chlorite lithons (Picture 22), by presence of garnet porphyroblasts in intrusion (Picture 23) or associated with felsic injections and by presence of cordierite in intrusion or felsic pegmatite. Sillimanite is spatially associated with both, chlorite and more rarely potassic alterations. Gold-bearing zones show a spatial association with sillimanite-cordierite metasomatized granodiorite such as Jedi, Tricorne, Hope and Obiwan zones. Garnet alteration is locally associated with gold mineralizations such as in the Hope showing (Savard and *al*, 2010).

Picture 22 – Silica-sillimanite-chlorite-bearing altered granodiorite (PAU2011AMB-181).

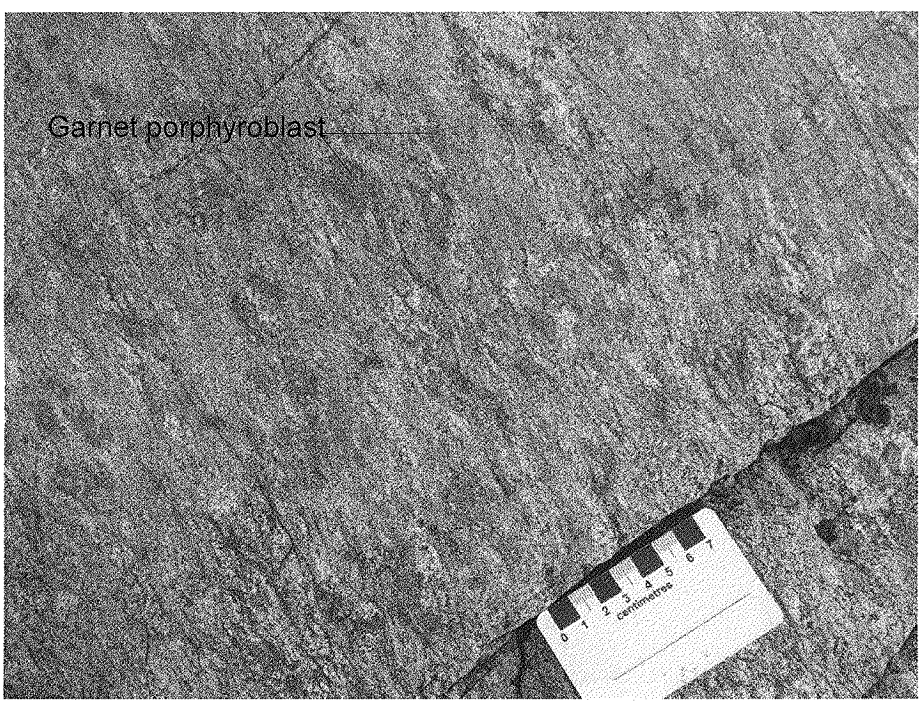

Picture 23 – Granodiorite containing 15-20% garnet porphyroblasts, Jedi area (PAU2011JL-058).

The geographic distribution of the samples using the alteration classification highlights mappable areas (Picture 24). The quartz monzodiorite covers much of the inner intrusive suite and is more or less surrounded to the south-east by the granodiorite. This latter unit is variably affected by the alteration, forming a crescent-shape zone around the quartz monzodiorite. Most of the alterations overlap one unto the other, but a general zoning appears from the south-west toward the north-east; chlorite being more frequent to the south-west and potassic alteration being more frequent to the north-east.

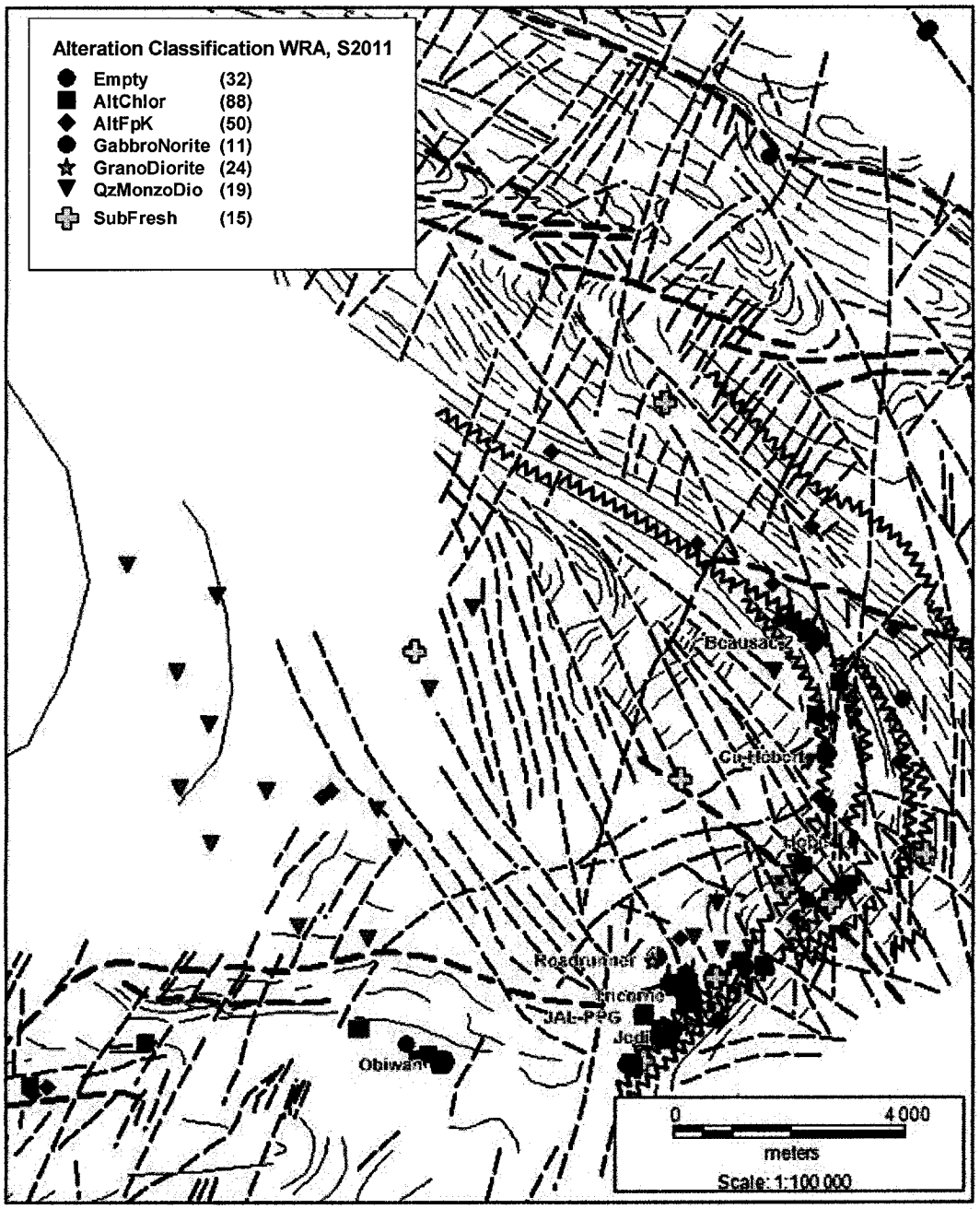

Picture 24 - Field distribution of WRA samples classified by alteration facies. Dash lines represent magnetic discontinuities, while thin lines represent magnetic continuities.

9.2.3 – Alteration and mineralization zonation inside Lac Pau porphyry intrusion

The two following figures (Pictures 25 and 26) are not related to WRA sampling, but to field geological observations in the database. These figures document the observations of sulfides minerals, the controls of these mineralization and finally the alteration. The quartz monzodiorite is magnetite bearing, while the granodiorite is sulfide bearing. Magnetite is also observed in protomylonitic granodiorite. The sulfidation is correlative with an increase of deformation and eventually the occurrence of veining and stockwerk. Furthermore, we identify a mineral zonation in close relationship with the Lac Pau deformation zone. Pyrrhotite-pyrite pyritic shell forms a large external halo in the granodiorite in LPDZ. Superposed at the Pyrite-Pyrrhotite shell, we observed an internal Cu-Mo-bearing phases (more local). Arsenopyrite is marginal and very rare. Like mineralization, alteration shows a zonation (Picture 26). A large chloritic-silica external halo affected the granodiorite with an inner potassic altered core (K-Feldspars-biotite). Local hematization±epidotization±sericitization is also observed and is not illustrated in picture 26. As already noted from the analysis of the geochemistry, these maps equally evidence the occurrence of alteration/mineralization zones in the extreme north-east and south-west of the map area and illustrate very well the zonation in alteration and mineralization inside Lac Pau granodiorite porphyry.

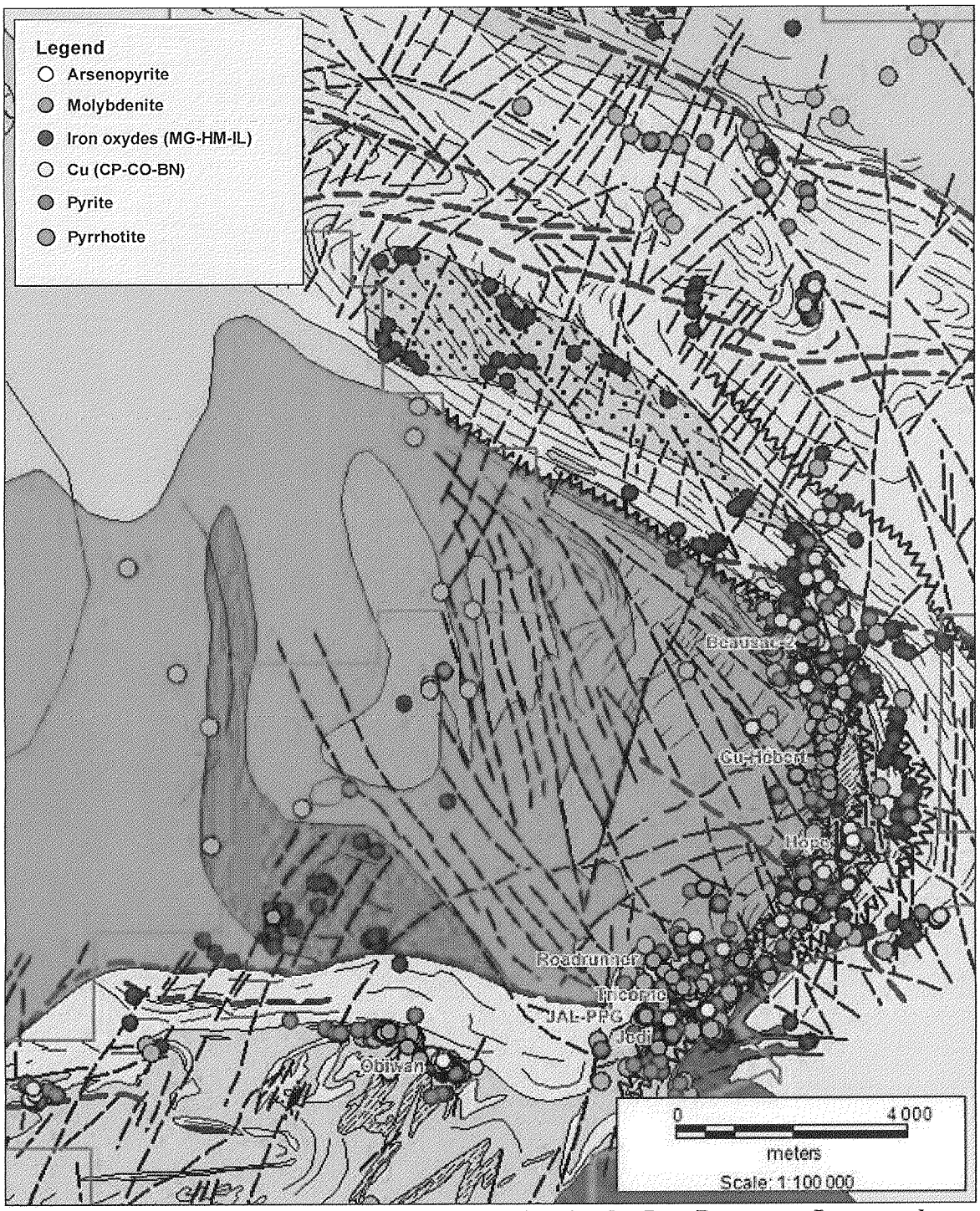

Picture 25 - Field observations of mineralization in the Lac Pau area. Iron oxydes and iron sulfides are nearly exclusive one from the other. The three sulfides phases show a broad zonation from an external pyritic shell, followed by the occurrence of pyrrhotite-pyrite and an internal zone of copper-molybdenite bearing phases. The North-East and South-West limits of the map show clear indication of favorable prospectivity. Dash lines represent magnetic discontinuities, while thin lines represent magnetic continuities.

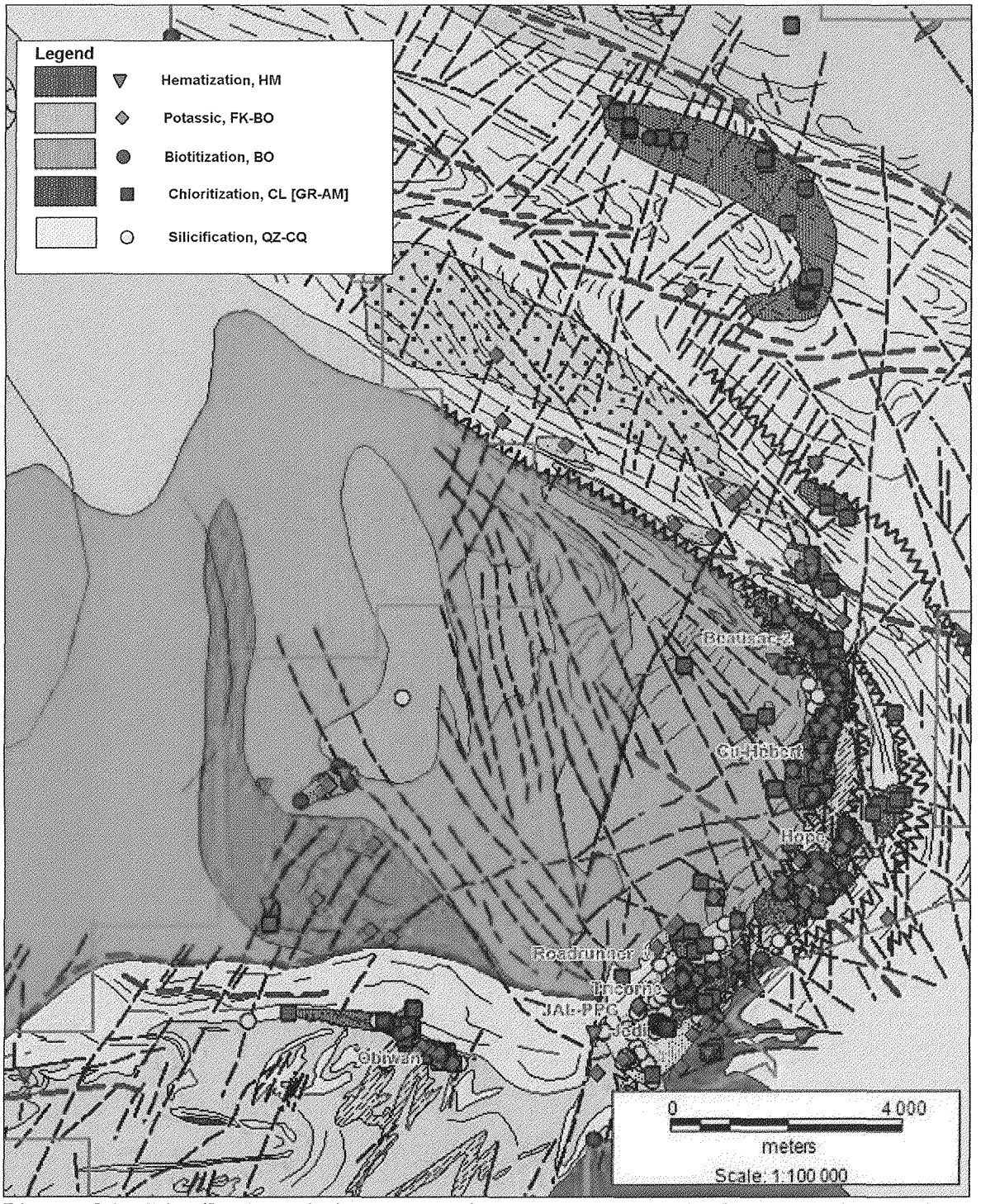

Picture 26 - Distribution of visual alteration as reported in field outcrop description. Again here, we denote a zonation from an inner potassic alteration toward a biotitic, a chloritic and an outward silicification. Dash lines represent magnetic discontinuities, while thin lines represent magnetic continuities.

9.2.4 – Gabbronoritic-pyroxenitic dykes

Along the former Caniapiscau river bed, a suite of outcrops shows occurrences of mafic-ultramafic dykes. These dykes represent a refractory unit marginally affected by the metamorphism but strongly folded and dismembered by the deformation (Pictures 27 and 28). Contact with grandodiorite is generally sharp and well-defined. This rock type has been observed at Cu-Hebert, Obiwan, Jedi Extension, Hope and Beausac-II showings and locally scattered over the property (Figure 4). The dykes are gabbronoritic to pyroxenitic and locally peridotitic in composition. The dykes are likely to mark the contact between the intrusive suite to the West and the so called "paragneiss" to the East, directly in the Lac Pau deformation zone (LPDZ). In fact, being softer than the granodiorite, they are likely to explain the location of the river bed (eroded low ground). An important fact is that gold-bearing zones are spatially associated with these dykes.

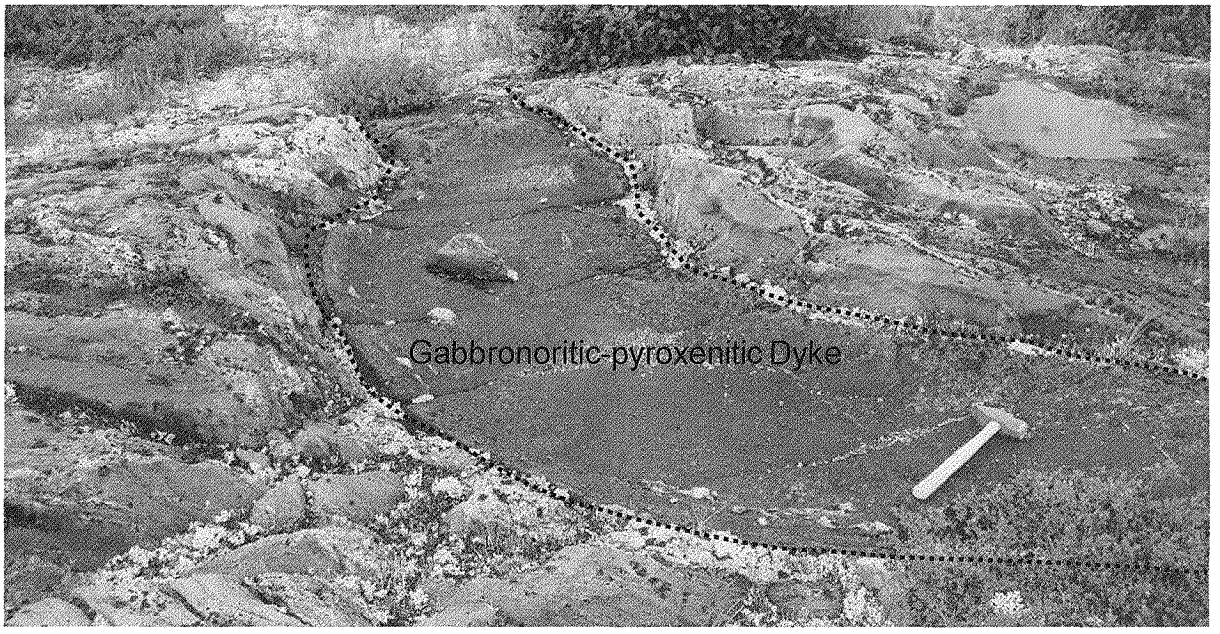

Picture 27 – Schistose and folded mafic dyke composed of Feldspars-amphibole-pyroxene-biotite-chlorite±sulphides locally containing ultramafic or granodiorite enclaves. West of Jedi showing. UTM83-19: 444426; 6077827.

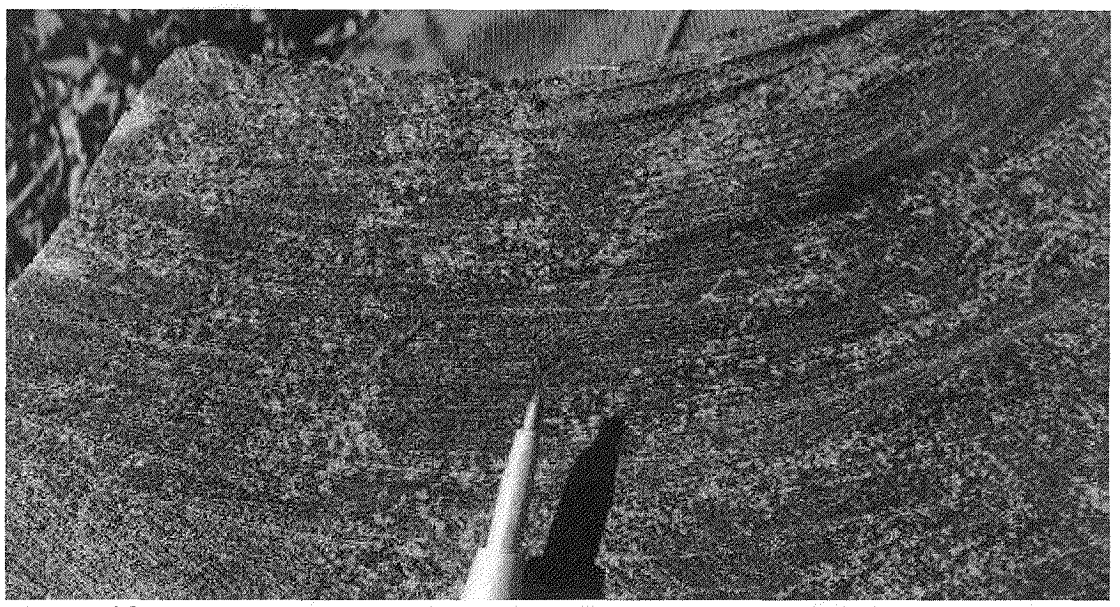

Picture 28 – Fresh slab of a schistose mafic dyke made of Feldspars-chlorite-biotite-pyroxene-amphibole, Jedi area (PAU2011JL-059).

9.2.5 - Potassic brecciated intrusion

Another rock unit in the area is represented by a syenitic intrusion (Picture 29) and observed at Cu-Hébert showing. At first glance, it is not clear if the syenite represents a true rock type (a petrogenetic process) or the product of a potassic alteration (an episyenite). In a number of places, the contact appears gradual and the inner part is extensively altered, with the occurrence of veining and stockwerk (Picture 30) associated with disseminated cupriferous mineralization (Tr-2% chalcopyrite-covelite-bornite). The intrusion is pink to red pinkish colored, medium-grained and foliated. The intrusion or dyke was emplaced in the Lac Pau deformation zone. The syenite is injected by centimeter-scaled stockwerk quartz veins and associated with potassic (K-Feldspars-biotite), chlorite, hematite and carbonates pervasive alterations. The intrusion is highly fractured.

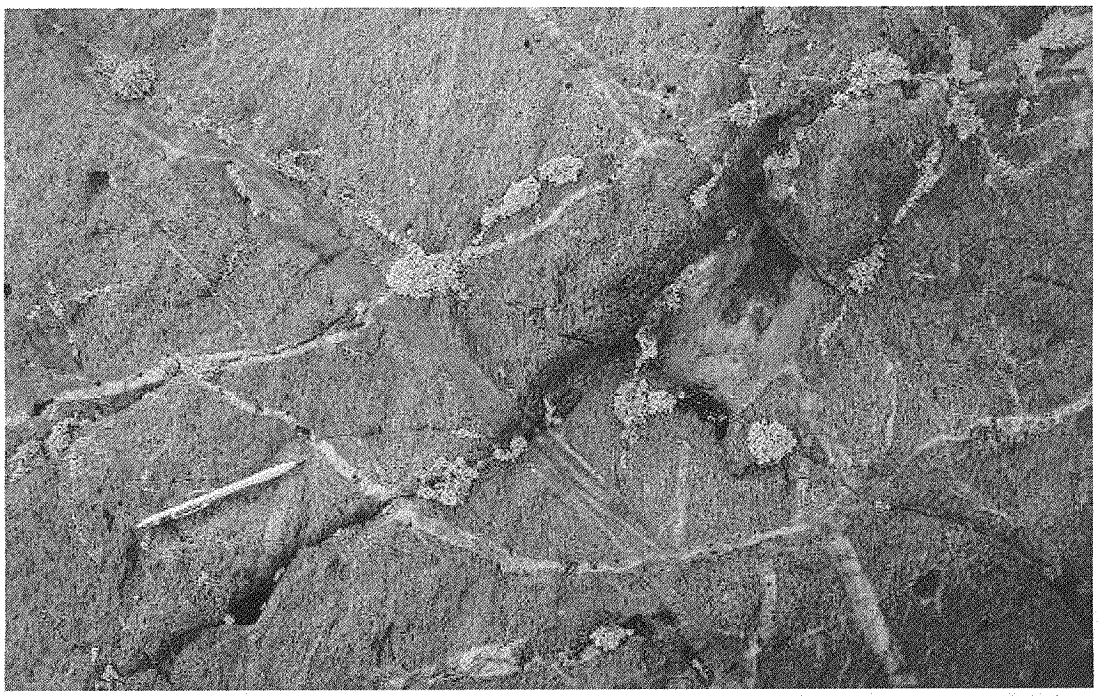

Picture 29 –Foliated syenite at the Cu-Hébert showing. Most exposures of this rock unit are affected by the occurrence of veining, stockwerk and shear veins.

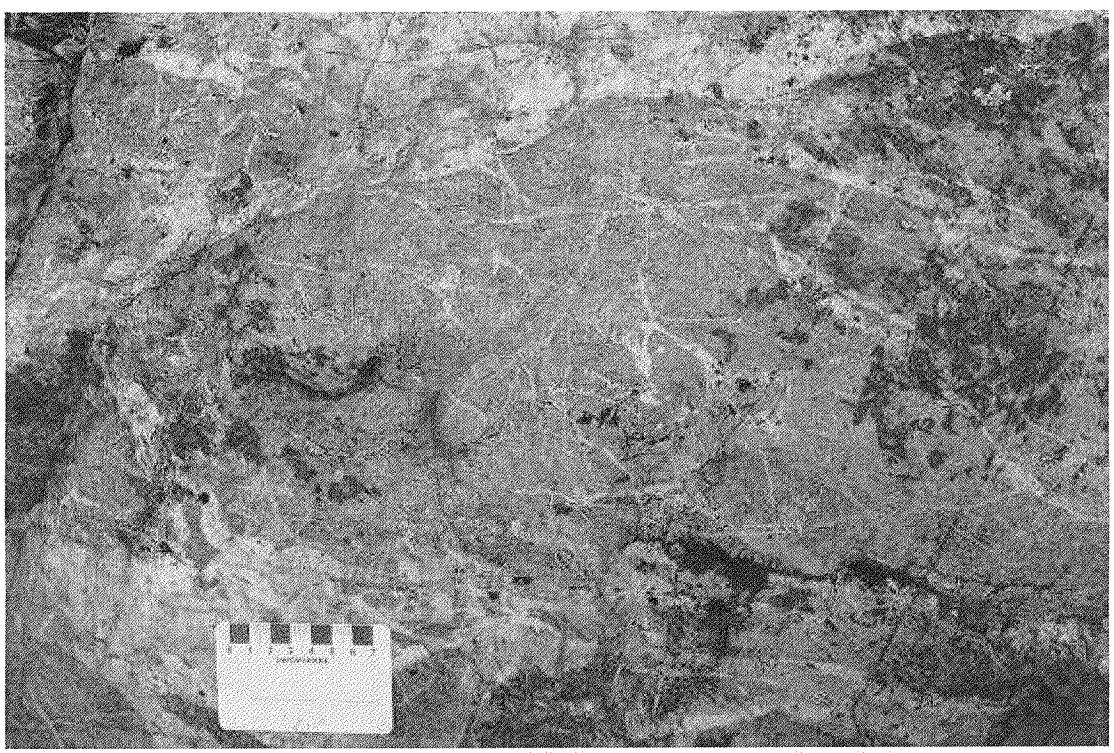

Picture 30 –Strongly altered and brecciated syenite at Cu-Hébert showing.

9.2.6 - Pegmatite

White to pink pegmatites are common throughout the stratigraphic package and composed of plagioclase-quartz-biotite±magnetite. They are ubiquitously massive. An important fact, the pegmatites can be folded (Picture 31) or rectilinear. Folding suggests that pegmatites injection took place in an early stage of the geological story (pre-to syn-deformation). Two (2) kinds of pegmatites are observed on the property. The first one is the **complex pegmatite** composed of Feldspar-quartz-biotite±chlorite±cordierite±garnet±beryl (Picture 32). An hypothesis is the pegmatitic felsic injection could be enriched in Fe-Al by contact with the early altered granodiorite observed on the property during hydrothermal circulation when the Pau Porphyry intrusion took place. The second one is the **simple pegmatite** and composed of Feldspars-quartz-K-Feldspars-biotite±chlorite±magnetite. Sulphides are locally present in pegmatites that crosscut mineralized horizons and can be auriferous.

Picture 31 – "Z" shaped folded, transposed and locally boudinated complex pegmatite composed of Feldspars-quartz±biotite±cordierite±garnet in a sillimanite-biotite-chlorite altered and deformed granodiorite (Jedi area, PAU2009TR-047).

Picture 32 – Complex pegmatite containing 20% cm subidio- to idiomorphic cordierite crystals (Tricorne area, PAU2009TR-037).

9.2.7 – Structural framework and deformation

The structural orientation of the lithologies encountered in the western part of the property is E-W while in the eastern part, the orientation turns to the NE and then to the NW. These orientations form a kilometre-scale open fold with an axial plane oriented NW-SE. According to Simard and *al.* (2009b), four (5) deformation events are observed in Lac Pau area:

A) Primary S_0 structures are obliterated by D1 and D2 events (not observed).
B) D1 is observed and can be separated in 3 events.
B1) D1a: well developed mineral foliation affecting Grosbois Complex and Beausac Suite rocks.
B2) D1b: Tight to isoclinal folds affecting D1a from the Grosbois Complex and Beausac Suite.
B3) D1c: Ductile deformation zones such as the Lac Pau deformation zone: protomylonitic and C-S fabric or stretching sub-horizontal lineation
C) The regional foliation is associated to D2.
D) The axial plane of the Lac Pau deformation zone is associated with deformation D3 and represented by tight folding or axial plan schistosity and oriented NW-SE to NE-SW. Lineations associated with this regional folding are oriented SW in the south flank and oriented NE on the north flank. On north flank, "s"-shape are most frequent and on the other hand, "z"-shape dominated on the south flank (Picture 33).
E) Late fragile deformation and manifested by the presence of faults and fractures (D5).

At the regional scale, the deformation is more complex. Deformation is very heterogeneous in intensity and distribution. It can vary from light to strong in a matter of metres. At first stage, Lac Pau porphyry with light deformation is actually documented and observed on the field (Picture 17). The first step of deformation is through the development of the schistosity, incipient or strong (Picture 34a). It is incrementally followed by the development of a banding texture (Picture 34b). The banding gives place to segregation between melanocratic and leucocratic phases producing a gneissic texture. This gneissic texture is generally associated with shear zone and CS fabric (Picture 35a) producing complex pattern. Locally, the CS fabric develops centimetric- to decimetric-scale "couloir" with a granoblastic texture. Increase of the deformation within the porphyry and the early schistosity which obscured the nature of the protolith is itself deformed through intrafolio folds (Picture 35b). At this deformation facies, kinematic indicators are frequently conflicting and contradictory (Picture 35b). In this case, "z"-shape and "s"-shape folding is observed in the same deformation "couloir" and with fold axis plunge variably in opposite direction.

The contrast of the deformation intensity is triggered by the underlying alteration (Chloritic-Potassic-Sillimanite). This latter is likely to have a higher water content (hydrolysis alteration processes), which lowers the melting point, triggers migmatism, which lowers internal cohesion and finally, enhances deformation ("en cascade" and auto-feedback process; Pearson and Lavoie, 2011).

On the other hand, zones of silicification are refractory to the deformation. Picture 36 expresses in part this relationship where the altered feldspar porphyry (lower part of the picture) shows a folded schistosity, while the strongly silicified area (upper part of the picture) features an attenuation and an almost complete disappearance of the schistosity (Pearson and Lavoie, 2011). This kind of example can explain why in a "homogeneous" intrusion we can observed the occurrence of heterogeneous deformation.

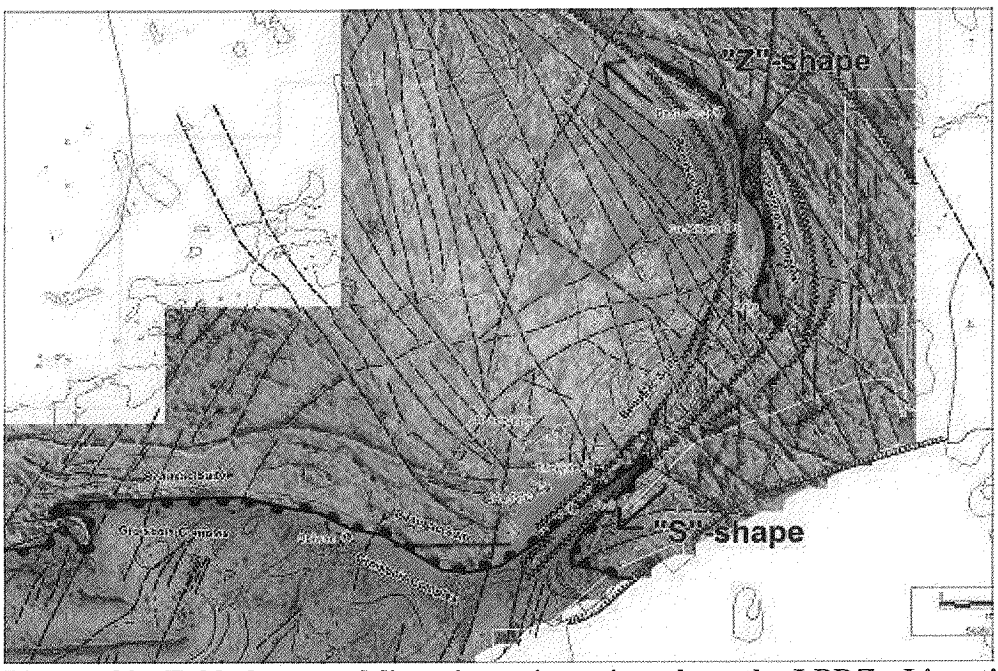

Picture 33 –Fold shape and lineation orientation along the LPDZ. Lineations are represented by black arrows.

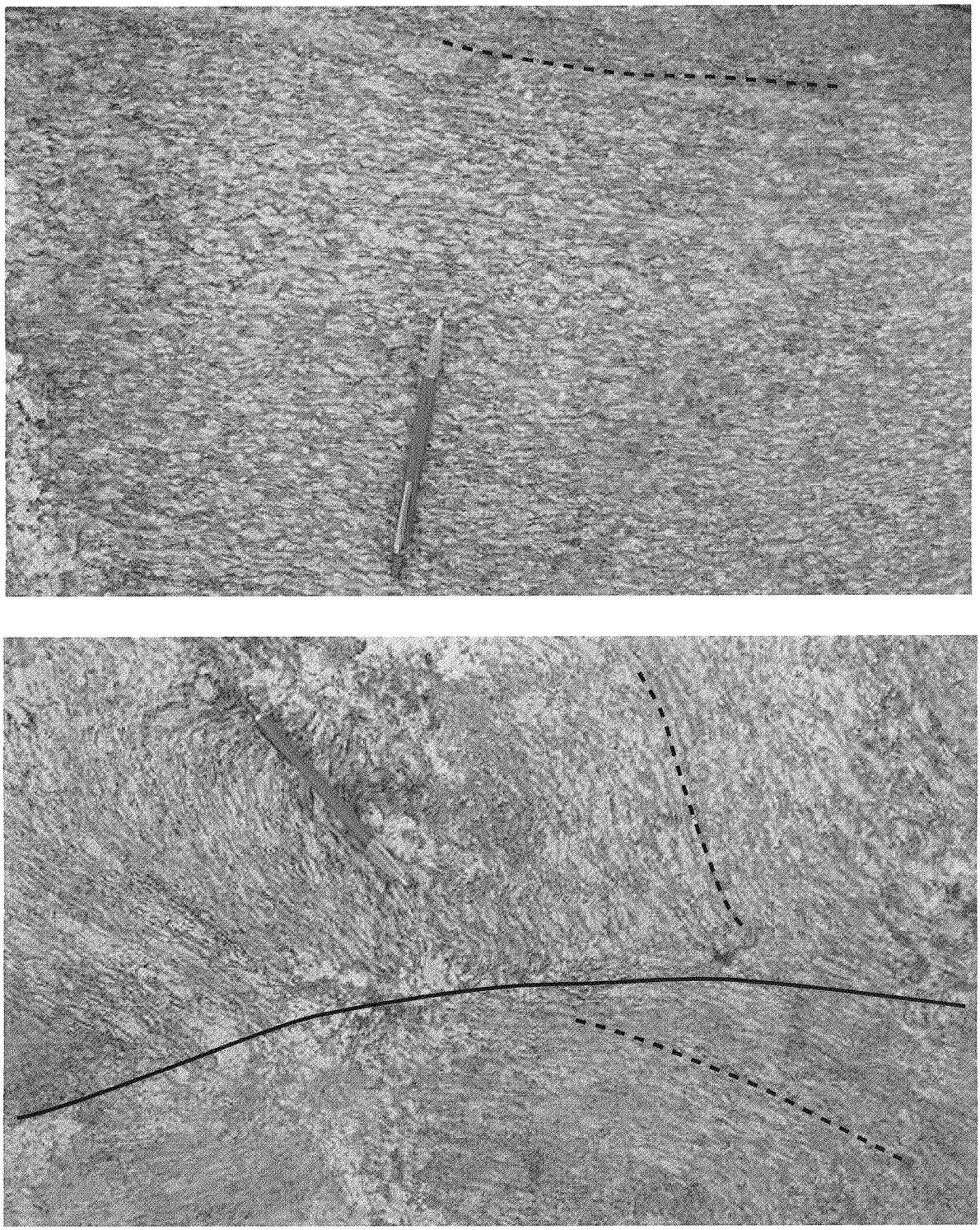

Picture 34 – a) Feldspar porphyry at an incipient stage of deformation. Phenocrysts are flattened and biotite defines a schistosity. Obiwan showing (PAU2009TR-001). b) Feldspar porphyry at a moderate stage of deformation. Obiwan showing (PAU2009TR-001).

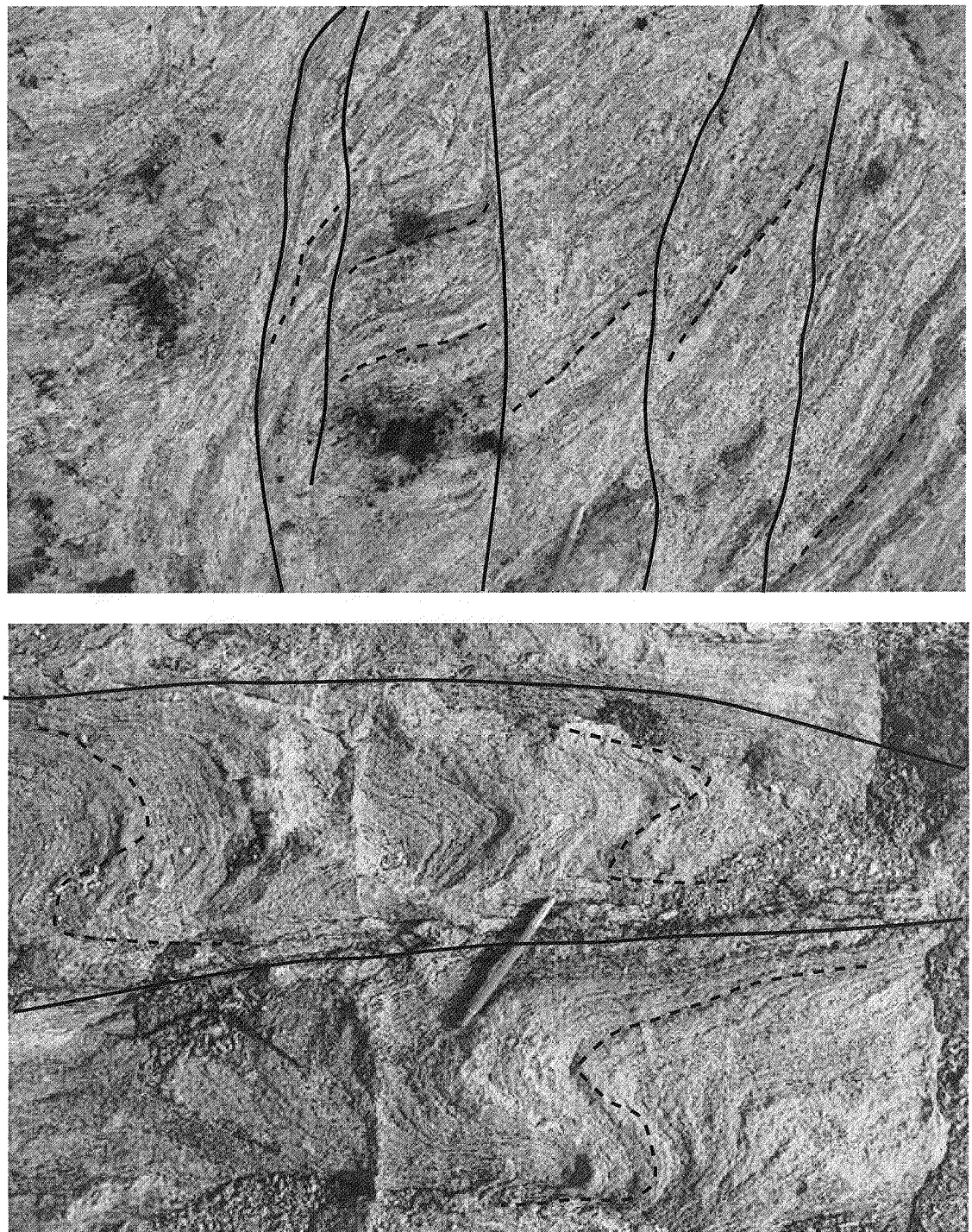

Picture 35 – a) Altered and recristallized feldspar porphyry developing gneissic texture supplemented by the occurences of CS-type fractures (sinistral movement). Obiwan showing; UTM83-19: 440715; 6077222). b) Development of intrafolio folds in the deformation, Tricorne zone. Note the "Z"-shape fold in the upper band and the "S"-shape fold in the lower one. Folds axis plunge variably to the SW or to the NE. Tricorne showing (PAU2009TR-014).

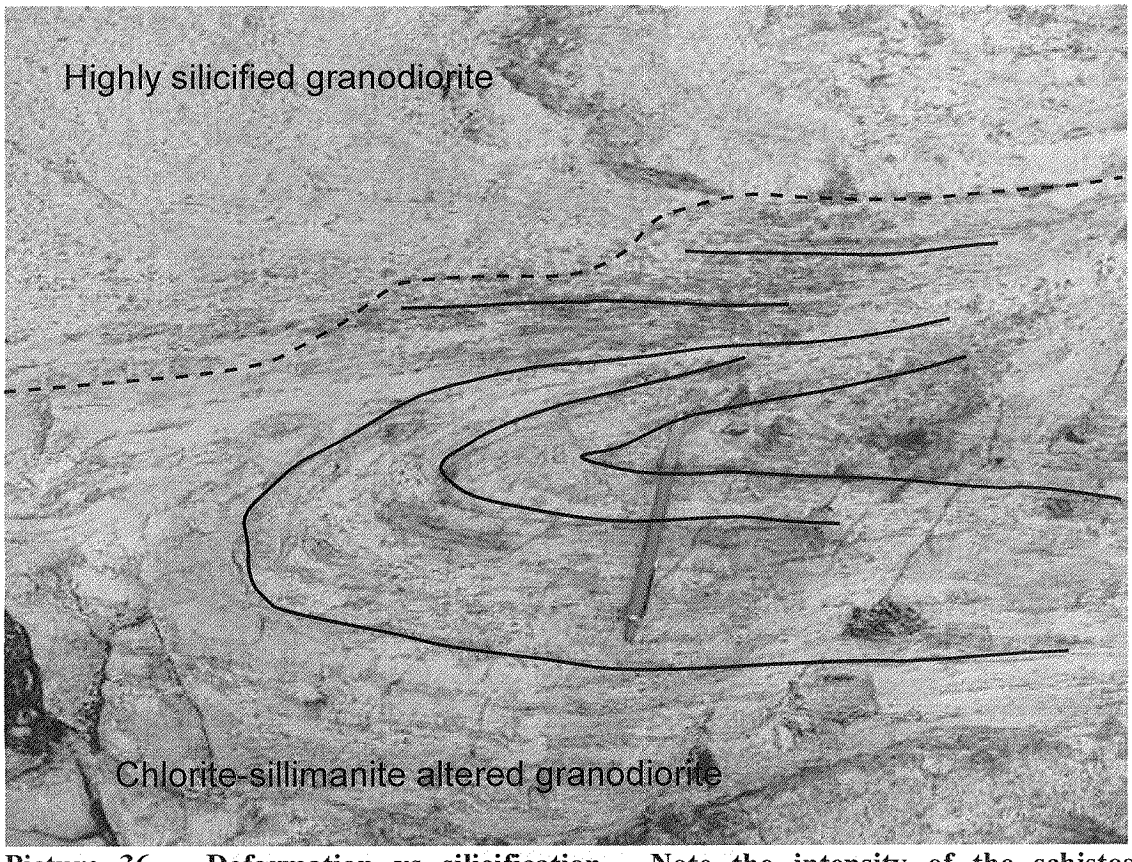

Picture 36 – Deformation vs silicification. Note the intensity of the schistosity while progressing toward the highly silicified upper zone (refractory component of silica). PAU2009-TR-011, Tricorne showing.

9.2.8 - Mineralization

Mineralization appears as disseminations, millimetric-scale stringers, interstitial to silicate (quartz-felspars) crystals, centimetric sulfide-burns, metric-scale amoeboids patches or kilometric-scale sheared corridors. Mineralized zones appear to be in spatial relationship with alteration (Silica-chlorite-potassic-Aluminous), deformation and metamorphism. This observation clearly suggests an early emplacement of the mineralization. Geometric distribution of the mineralization is confined to the periphery of an intrusive complex (Lac Pau porphyry). Except for some short high grade intersections, most of the mineralization is in the range of 1-3 g/t Au. The mineralized zone is often accompanied with a large anomalous halo at around 300-500 ppb Au. Furthermore, a number of high grade results are potentially in close relation with the presence of pegmatites (resulting from small scale remobilization).

ITEM 10 – DEPOSIT TYPES

The overall context of the Lac Pau project presents similarities with Au-Ag±Cu±Mo intrusion-hosted porphyry-type deposit and high-grade metamorphic Archean gold-bearing shear zones and presents a

very good potential for new gold discoveries along the 15 kilometres strike length of favourable stratigraphy. It could be compared to several other Au-Cu±Ag±Mo metamorphosed porphyry-type deposits around the world such as: (1) The 3.315 Ga Spinifex Ridge Porphyry Cu-Mo deposit (Australia, Pilbara craton) which has measured and indicated resources of 652 Mt at 0.8% Cu and 0.05% Mo (cut off at 0.02) or 191 Mt at 0.1% Cu and 0.08% Mo (cut off at 0.05); (2) Malanjkhand (India; multi-phasing batholite injected by aplitic and pegmatitic dykes) with estimated resources of 221 Mt at 1.35% Cu and 790 Mt at 0.83% Cu , 0.2 g/t Au, 6 g/t Ag and 40 ppm Mo; (3) Tallberd-Algtrask (North Sweden; metamorphosed Cu-Au±Mo porphyry injected by felsic pegmatites) with estimated resources of 44 Mt at 0.2 g/t Au and 0.27% Cu; (4) Chapada (Goias Brazil; 40 m thick mylonite zone interpreted as a trust fault associated with a regional faults system) with estimated resources in 2007 of 379 Mt at 0.36% Cu and 0.29 g/t Au and (5) Kopsa (Pohjanmaa area, Finland) a sub-economic deposit with 25 Mt at 0.15% Cu, 0.57 ppm Au and 4 ppm Ag.

ITEM 11 – MINERALIZATION

No new mineralized zone was discovered during 2011 summer campaign. Details mapping of some parts of Jedi and Tricorne showings are discussed in section 12.2 in paragraphs below.

ITEM 12 – EXPLORATION WORK

This section describes prospecting, mapping and trenching work realized during summer 2011 campaign. Field work was realized by Virginia Mines team composed of project geologist Jérôme Lavoie and Louis Grenier, trainee geologist Josée-Anne Lévesque, technicians Ève Roy-Vigneault and Martin Gagnon and finally students in geology Anne-Marie Beauchamp, Anne-Laurence Paquet, Benoit Martin-Tanguay, Ludovic Côté, Alexandre Rodrigue, Tonny Girard and Mathieu Courtemanche. The cooks for the campaign were Marie-Pierre Savard and Catherine Provost. A total of 492 man/days were spent on the property from July to August. During this period, a total of 13 trenches were performed from which 496.4 meters of channel were collected for a total of 579 samples. Most trenches were performed over IP chargeability anomalies outlined by the winter 2010 and 2011 surveys. Trenches and IP anomalies locations are shown in figure 3 and figure 4. Trenches parameters are also listed in table 2. Trenches realized were mapped and a detail mapping was produced for each of them and is presented in this report (Figure 9 to 26).

Prospecting on the property generated a total of 650 outcrop and 30 boulder descriptions (Figure 5 and 8). 810 samples were collected for assays (166 hand samples for MEA and GOLE, 470 channels samples for MEA and 174 for WRA). Grab samples (MEA and WRA) were illustrated on figure 6. Channel samples were illustrated on figures 9 to 26. Best anomalous values (Au-Ag-Cu-Mo-Zn) returned in grab sample are represented in Table 3 and figure 7. To support descriptions and assays, 452 structural measurements (Appendix 7) were taken on outcrops and trenches.

Helicopter support was provided by Héli-Transport from Trois-Rivières (Astar B-2). An excavator used for trenching was provided by Felco Inc. from St-Félicien (Komatsu 200) while a small heliborne excavator was use for remote targets and provided by Services Techniques Géonordic.

The reader can refer to appendix 3 for outcrops and boulders description, appendix 4 for grabs samples results, appendix 5 for channel results, appendix 7 for structural measurement description, appendix 2 for the listing of all abbreviations used in the description of rocks and appendix 8 for assays certificates.

Table 2: Trench performed during Summer 2011 program, Lac Pau Project

TRENCH 2011							
Trench	Utm_E	Utm_N	Status	Surface (m²)	Depth (m)	Volume (m³)	Remaining (m³)
PAU-2011-TR-001	446487	6084517	Opened	12	1.50	18	27.0
PAU-2011-TR-002	446755	6084778	Opened	30	0.50	15	7.5
PAU-2011-TR-003	446280	6085039	Restored and Reforested	20	1.50	30	-
PAU-2011-TR-004	446251	6078919	Opened	350	2.00	700	700
PAU-2011-TR-005	446557	6079237	Opened	585	2.00	1170	700
PAU-2011-TR-006	447701	6080313	Restored and Reforested	192	1.50	288	-
PAU-2011-TR-007	447581	6080242	Opened	315	3.00	945	945.0
PAU-2011-TR-008	447527	6080199	Restored and Reforested	320	3.00	960	-
PAU-2011-TR-009	447422	6080095	Opened	576	3.00	1728	1728.0
PAU-2011-TR-010	447376	6080013	Opened	306	2.00	612	1728.0
PAU-2011-TR-011	443853	6078625	Opened (Manual trench)	40	0.30	12	12.0
PAU-2011-TR-012	444650	6077749	Natural Outcrop				
PAU-2011-TR-013	444603	6077750	Natural Outcrop				
			Total Volume 2011			**6478.0**	**5847.5**
			Volume Restored from 2011 Trenches			**630.5**	

12.1 Prospecting

All the significant showings outlined from outcrops or boulders during 2011 summer are shown in figure 7. The most significant values obtained during summer 2011 are all reported in table 3.

Cu-Hebert Area

Most of the showings found during 2011 campaign are located in Cu-Hebert Area. 9 grabs samples returned anomalous Au-Cu values. The samples #203 460 (PAU2011JAL-019) and #203 462 (PAU2011JAL-023) yielded **1.46 g/t Au** and **1.125 g/t Au** within a decimeter-scale quartz vein included in a protomylonitic granodiorite. The mineralization is composed of 3-5% pyrite-pyrrhotite that occurs penetrative in the quartz veins. The boulder associated to sample #205 901 (PAU2011ERV-001) returned **8.73 g/t Au**. It is described as a massive tonalite composed of quartz-plagioclase-biotite±chlorite. The boulder is subrounded and has a decimeter-scale dimension. The grab samples #205 953 (PAU2011AMB-006), #205 955 (PAU2011AMB-007) and #205 957 (PAU2011AMB-009) returned respectively **0.811 g/t Au**, **0.55 g/t Au** and **4.09 g/t Au.** The descriptions of those outcrops are mostly similar. They are characterized by a protomylonitic texture and granodioritic in composition composed of plagioclase-quartz-biotiteK-feldspars. The mineralization is characterized by presence of 2% pyrite that occurs disseminated. Millimeters- to centimeter-scale granitic injections are locally observed on these outcrops. The sample #205 964 yielded a value of **1.775 g/t Au**. The rock is described as a granodioritic orthogneiss composed of plagioclase-quartz-biotite±hornblende. The

mineralization occurs locally, associated to pegmatitic injections and composed of 1% pyrite and 1% pyrrhotite finely disseminated.

Hope Area

Almost 1 km south from main Hope showing, two grab samples taken from large boulder returned anomalous gold values. Samples are located near of a large IP anomaly that was defined during winter 2011 and could extend Hope mineralized zone toward SE. A grab sample (#205 975) associated to a large boulder (PAU2011AMB-030) of 3 by 3 meter returned a value of **7.91 g/t Au.** It is described as a metasomatic tonalite composed of quartz,-plagioclase-biotite-garnet. An intense silicification was noticed. The mineralization, mostly disseminated, is composed of 3% pyrrhotite and 1% pyrite. The sample #205 998 (PAU2011AMB-090) obtained a value of **0.478 g/t Au** and is described as a protomylonitic granodiorite with pegmatitic injections. It is composed of quartz-plagioclase-biotite-chlorite. A penetrative silicification is also observed. The mineralization, locally associated to pegmatitic injections, is composed of 1% pyrrhotite, 1% pyrite and 1% magnetite, that mostly occur disseminated along main foliation.

Table 3: Significant results obtained from grab samples during Summer 2011 Program.

TagNumber	IdAffleur	X_UTM	Y_UTM	TypeOccurence	Au_ppm	Ag_ppm	Cu_ppm	Mo_ppm	Zn_ppm
205951	PAU2011AMB-002	447856	6083792	Affleurement	0.086	1.8	**1730**	3	48
205953	PAU2011AMB-006	447642	6083587	Affleurement	**0.811**	2.1	398	4	41
205955	PAU2011AMB-007	447587	6083506	Affleurement	**0.545**	1.3	138	0.5	62
205957	PAU2011AMB-009	447564	6083414	Affleurement	**4.09**	3.7	664	41	27
205960	PAU2011AMB-011	447337	6083246	Affleurement	**0.325**	9.4	**1000**	14	17
205964	PAU2011AMB-016	447236	6082878	Affleurement	**1.775**	1.1	299	7	3
205975	PAU2011AMB-030	447579	6080181	Bloc Erratique	**7.91**	2.1	192	3	361
205998	PAU2011AMB-090	447441	6080066	Affleurement	**0.478**	1.9	79	4	693
205901	PAU2011ERV-001	447595	6083521	Bloc Erratique	**8.73**	3.4	887	4	628
203460	PAU2011JAL-019	447132	6083529	Affleurement	**1.46**	1.2	512	12	3
203462	PAU2011JAL-023	447487	6083697	Affleurement	**1.125**	1.4	667	2	3
206559	PAU2011JL-070	444562	6077772	Affleurement	**0.925**	2.1	229	10	124

12.2 Trenching and Channelling

This section describes the trenches performed during summer 2011 and also the channels that have been done in trenches performed during previous campaign. Two Induced polarization (IP) surveys were performed during winter 2010 and 2011. The objective of the 2011 trenching campaign was essentially to explain the IP anomalies outlined in 2010 that was not explained after 2010 trenching campaign and also IP anomaly outlined during 2011 survey. Trenches locations are presented in figure 3 and total IP anomalies in figure 4. Table 4 presents significant Au values obtained from 2011 channel and trenching program. The results obtained from each channel are presented in appendix 5.

Table 4: Significant results obtained from channel sampling during Summer 2011 Program.

Trench ID	Hole Name	From	To	Value (g/t)	Over (m)	Inc. (g/t)	Over (m)
PAU2011TR-001	PAU2011R-001	0,00	1,00	**0,35**	**1,00**		
PAU2011TR-002	PAU2011R-002	3,00	15,00	**0,23**	**12,00**	**0,89**	**1,00**
PAU2011TR-004	PAU2011R-011	0,00	3,00	**0,19**	**3,00**		
PAU2011TR-010	PAU2011R-040	3,00	4,00	**0,41**	**1,00**		
PAU2011TR-010	PAU2011R-042	1,00	2,00	**0,38**	**1,00**		
PAU2011TR-010	PAU2011R-044	6,00	8,00	**0,22**	**2,00**		
PAU2009TR-046	PAU2011R-051	0,00	1,00	**0,30**	**1,00**		
PAU2011TR-013	PAU2011R-083	3,00	4,00	**0,41**	**1,00**		
PAU2011TR-013	PAU2011R-084	1,00	7,50	**0,74**	**6,50**	**3,48**	**1,00**
PAU2011TR-013	PAU2011R-085	4,00	8,00	**0,44**	**4,00**		
PAU2011TR-013	PAU2011R-086	2,00	3,00	**0,40**	**1,00**		
PAU2011TR-011	PAU2011R-090	3,00	4,00	**0,76**	**1,00**		
Natural outcrop	PAU2011R-094	11,00	15,00	**0,23**	**4,00**		
Natural outcrop	PAU2011R-096	5,00	7,00	**0,32**	**2,00**		
Natural outcrop	PAU2011R-097	0,00	9,00	**0,16**	**9,00**		
PAU2009TR-011	PAU2011R-107	1,00	4,00	**0,43**	**3,00**		
PAU2009TR-038	PAU2011R-109	0,00	2,00	**0,75**	**2,00**		
PAU2009TR-038	PAU2011R-111	0,00	1,00	**0,43**	**1,00**		
PAU2009TR-038	PAU2011R-111	1,00	4,00	**7,57**	**3,00**	**16,45**	**1,00**
PAU2009TR-038	PAU2011R-112	0,00	1,00	**1,06**	**1,00**		

PAU2011TR-001 (Figure 9)

The trench PAU2011TR-001 had for objective to explain the IP anomaly PP-150. A grab sample found during previous campaign in this area returned Au value of **3.08 g/t Au** . One channel with a length of 6,0 meters was performed in this trench. The lithology described is a homogeneous granodioritic orthogneiss composed of plagioclase-quartz-biotite-hornblende. Presence of accessory minerals such as chlorite and K-Feldspar is noticed and described as an alteration. Mineralization is constituted of 1% finely disseminated pyrite. Value of **0.35 g/t Au over 1.0 meter** was obtained from channel PAU2011R-001 and value of 3.08 g/t Au wasn't repeated because the grab sample was taken on a big sub-angular boulder.

PAU2011TR-002 (Figure 10)

Purpose of trench PAU2011TR-002 was to explain the presence of IP anomaly PP-152. The rock was described as an orthogneiss tonalitic mainly composed of quartz-plagioclase-biotite-hornblende injected by a felsic pegmatitic meter-scale dyke. The unit is gneissic and characterized by the presence of

leucosomes and biotite shlierens. Centimeter-scale mafic fragments, composed of hornblende and biotite, are noticed locally. Silicification is observed over the trench in veins and also penetrative. Presence of weak chloritic and potassic (revealed by presence of biotite) alterations are noticed (Picture 37). The mineralization, present over the entire trench, is mainly constituted of 3% pyrite-pyrrhotite and occurs disseminated and mainly concentrated in contact with felsic injections. Magnetite is also observed locally in mm-scale blebs. Channel PAU2011R-002 returned a value of **0.23 g/t Au over 12.00 meters including 0.89 g/t Au over 1.0 meter.** That explains the presence of IP anomaly and extends of 45 m the Beausac-II mineralized zone toward NW.

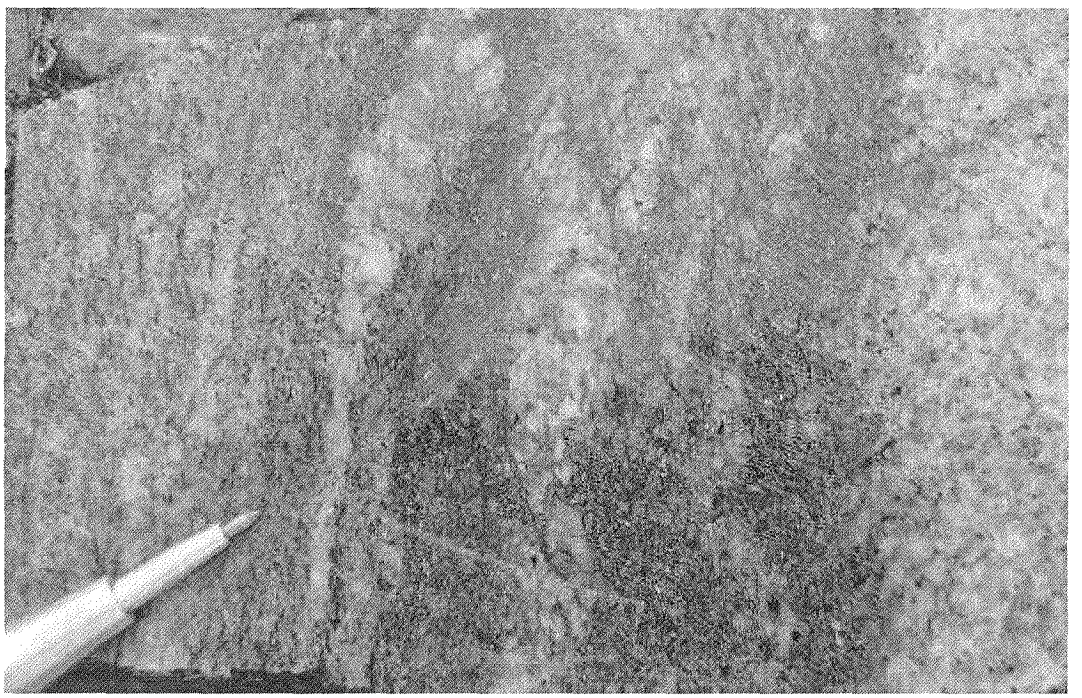

Picture 37 - Granodioritic orthogneiss presenting dissemination of pyrite-pyrrhotite along main foliation and associated with chlorite-biotite alterations.

PAU2011TR-003

The trench PAU2011TR-003 aimed at IP anomaly PP-152. Due to presence of water in the trench at the moment of digging, it was impossible to perform a channel. Only a grab sample was taken. The lithology is described as an orthogneiss tonalitic composed of plagioclase-quartz-biotite. No significant alteration was noticed and pyrrhotite in traces was observed. No significant gold value was obtained from this grab. The IP anomaly remains unexplained.

PAU2011TR-004 (Figure 11)

The trench PAU2011TR-004 had for objective to explain the IP anomaly PP-40. Nine channels were performed on this trench for a total of 30.5 meters. The rock observed is altered and the protolith interpreted is a granodiorite. First lithology encountered is a metasomatic rock altered to silica-biotite-cordierite. The silica alteration is penetrative and the potassic alteration, revealed by presence of biotite, is following main schistosity. This unit is gneissic, banded, medium to fine grained and locally described with protomylonitic texture. Mineralization is constituted of 1-2% pyrite and pyrrhotite that occur locally in mm- to cm-scale blebs and disseminated parallel to principal foliation. Another unit is described as an othogneiss composed of plagioclase-quartz-biotite and accessory minerals such as sillimanite-cordierite. This lithology is homogeneous, medium grained and banded. Protomylonitic texture and anastamosed patterns are also observed locally. Mineralization, composed of 3% pyrite-pyrrhotite, is mostly disseminated in the matrix following main schistosity. The last lithology encountered in trench PAU2011TR-004 is a breccia with quartzo-feldspatic clasts (Picture 38). The matrix is composed of biotite-quartz-amphibole-magnetite. The unit is heterogeneous, medium to coarse grained and foliated. Mineralization is mainly composed of 1-2% pyrite that occurs in blebs and also locally disseminated. Value of **0.19 g/t Au over 3.00 meters** was obtained from channel PAU2011R-011. The mineralization outlined explains the presence of the IP anomaly.

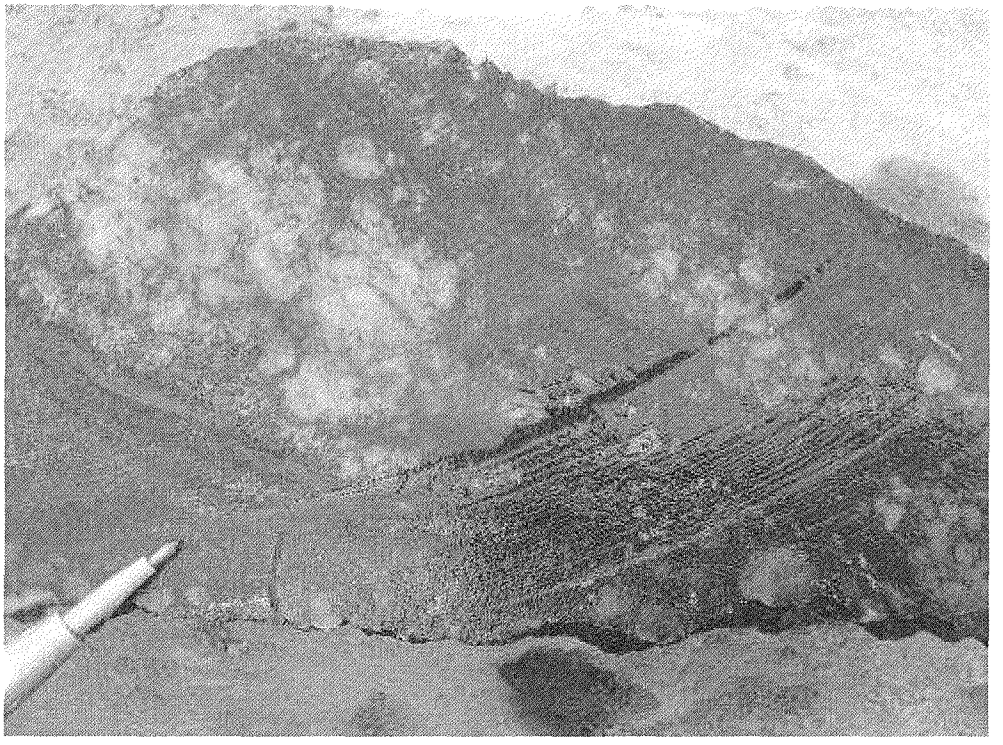

Picture 38 - Coarse-grained granodiorite brecciated by biotite-quartz-hornblende-magnetite matrix. Clasts are well-rounded and mostly composed of quartz-feldspars. Sulphide observed is 2% pyrite occuring as mm- to cm-scale blebs (PAU2011TR-004).

PAU2011TR-005 (Figure 12)

The trench PAU2011TR-005 was performed to explain the IP anomaly PP-40. It is constituted of granodioritic orthogneiss with locally protomylonitic texture. This unit is mainly composed of quartz-plagioclase-biotite. Presence of accessory minerals such as K-Feldspar, chlorite and magnetite is also observed. Coarse grained quartzo-feldspatic injections (leucosomes) are observed. Locally, 1% of centimeter-scale mafic fragments are noticed. Those fragments are elongated following main schistosity. Silicification and chloritization are observed in the intrusion. The sulfides observed are composed of 1-2% pyrite finely disseminated following principal schistosity. The sulphides observed in the intrusive rock don't explain the IP anomaly. The trench location was moved 50 meters from the initial proposition because of the important thickness of overburden. No significant gold value was obtained from that trench and IP anomaly remains unexplained.

PAU2011TR-006 (Figure 13)

Purpose of trench PAU2011TR-006 was to extend trench PAU2010TR-052 that yielded gold value of **1.76 g/t over 1.0 meter** during 2010 summer campaign. The trench is located on the IP anomaly PP-88 on line L78+40N. The main lithology described is a granodioritic orthogneiss layered with meter-scale metasomatic granodiorite. The main unit is composed of quartz-plagioclase-biotite. The metasomatic "bands" are described with strong and pervasive silica-cordierite, garnet porphyroblasts and a potassic alteration, revealed by presence of biotite (Picture 39). Cordierite is partially replaced by chlorite. Sulphides, mainly observed in the metasomatic bands, are composed of 3% disseminated pyrrhotite and chalcopyrite following main schistosity and rare traces of molybdenite and pyrite in blebs. The current mineralization explains the IP anomaly. Unfortunately the channels did not return any significant gold values.

Picture 39 - Metasomatic granodiorite altered to cordierite-silica-garnet-botite and mineralized with 2% pyrrhotite in blebs. Cordierite is partially replaced by chlorite.

PAU2011TR-007 (Figure 14)

The trench PAU2011TR-007 had for objective to explain the IP anomaly PP-88 on line L77+00N. The lithology described is constituted of granodioritic orthogneiss locally injected by pegmatitic veins. Granodiorite is composed of quartz-plagioclase-biotite. Presence of accessory minerals such as chlorite, K-Feldspar and epidote is also noticed. Biotite is partially altered to chlorite. Mineralization is composed of 1% pyrite-pyrrhotite and 2% magnetite that occurs finely disseminated and in irregular blebs. The current mineralization could explain the IP anomaly but no significant gold value was obtained from the channels.

PAU2011TR-008 (Figure 15)

Purpose of trench PAU2011TR-008 was to explain the IP anomaly PP-88 on line L76+32N. The main lithology is described as a protomylonitic granodiorite which contains centimeter-scale felsic injections. The intrusion is composed of quartz-plagioclase-biotite. Chloritization of the biotite grains is noticed locally. The mineralization is constituted of traces of pyrrhotite that occur finely disseminated following principal schistosity. The trench doesn't explain the presence of IP anomaly. No gold value was obtained from those channels.

PAU2011TR-009 (Figure 16)

The trench PAU2011TR-009 aimed at anomaly PP-88 on line L74+85N. The lithology in that trench is very homogeneous and described as a protomylonitic granodiorite. The intrusion is constituted of quartz-plagioclase-biotite±chlorite. The rock is foliated, medium grained, granoblastic and contains centimeter- to decimeter-scale mafic fragments (biotite-hornblende). The protomylonite is characterized by a penetrative silicification that occurs mainly in contact with centimeter-scale felsic injections. Mineralization is composed of 2% finely disseminated pyrite-pyrrhotite that occurs following principal schistosity. Locally, magnetite is also observed in blebs (2%). Current mineralization explains the presence of the IP anomaly. Channels did not return significant gold value.

PAU2011TR-010 (Figure 17)

Purpose of trench PAU2011TR-010 was to explain the IP anomaly PP-88 located on line L74+00N. The lithology described in that trench is a granodioritic orthogneiss with meter-scale altered bands of protomylonitic granodiorite. Orthogneiss is composed of quartz-plagioclase-biotite±chlorite±K-Feldspar±sillimanite±cordierite and locally garnet. Silica, chlorite and potassic alterations are observed and are mainly present in the protomylonitic unit. Veinlets of epidote, hematite and chlorite are also noticed. The sulfides, mainly associated with altered protomylonite (Si-EP-CL), are composed of 2% pyrite-pyrrhotite that occurs finely disseminated with traces of chalcopyrite. Locally, up to 8% sulfides are noticed. Sulphides explain the anomaly PP-88. Channels PAU2011R-040, PAU2011R-042 and PAU2011R-044 returned anomalous gold values of **0.41 g/t Au over 1.0 meter**, **0.38 g/t Au over 1.0 meter** and **0.22 g/t over 2.0 meter**.

PAU2011TR-011 (Figure 18)

Purpose of trench PAU2011TR-011 was principally to return to a value of **1.47 g/t Au** (#133 125) that was recorded by a grab sample during 2010 summer campaign. The lithology described is a protomylonitic diorite composed of plagioclase-quartz-chlorite-biotite. The unit is characterized by a strong chloritization and the presence of centimeter-scale felsic injections (leucosomes). Mineralization is composed of pyrrhotite in finely disseminated traces. Channel PAU2011R-090 returned anomalous gold value of **0.76 g/t over 1.00 meter**. This value obtained in channel corresponds with the 2010 anomalous grab sample.

PAU2011TR-012 and PAU2011TR-013, Jedi showing (Figure 19)

Trench PAU2011TR-012 and PAU2011TR-013 are part of a natural outcrop hosting the Jedi discovery showing (Figure 19). During 2011 campaign, detail mapping was performed on these two outcrops and channeling was done on PAU2011TR-013. No new channel was performed on PAU2011TR-012.

Detail mapping of Jedi showed the distribution of pegmatites (in black on Figure 19) inside the mineralized zone. Jedi mineralized zone is in close association with a large number of pegmatitic dykes or quartz veins (Picture 40). Most pegmatites are highly deformed, globally featuring a "Z"-shape pattern (highlighted in red in Figure 19). "Z"-shape is also observed in mafic dyke fragments incorporated in protomylonitic granodiorite near the sharp contact between two lithologies (west part of the map). Locally fold hinges are observed inside the mineralized zone (Picture 41a). Breccia texture with weakly deformed granodiorite fragments is observed in mineralized zone (Picture 41b) combined with well preserved porphyritic texture associated with a chloritic alteration (Picture 7) suggesting, one more time, an early stage for the alteration and probably for auriferous mineralization? Some discontinuities in dykes distribution, oriented N020°, suggest the presence of faults (P-shear in the Riedel nomenclature; paralleling the short limb of fold), actually welded through metamorphism (Lavoie and Pearson, 2011).

Picture 40 - Metasomatic granodiorite injected by felsic leucosomes, pegmatitic dykes and/or quartz veins, Jedi showing, PAU2011TR-013.

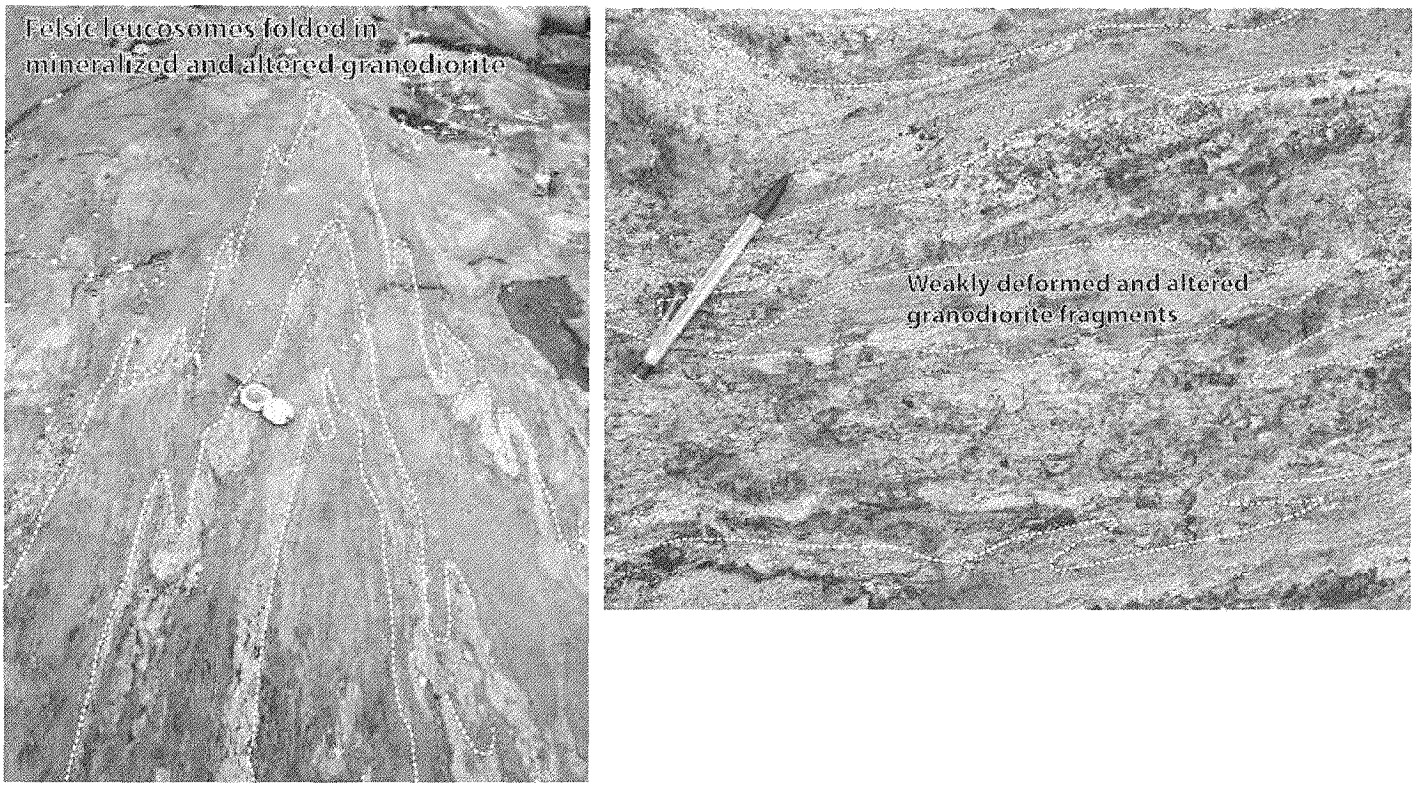

Picture 41 – A) Fold hinge in Jedi mineralized zone represented by felsic injections, PAU2011TR-013. Note the "Z"- and "S"-shape on each flanks of the fold. B) Breccia texture represented by weakly deformed and altered granodiorite fragments in a quartz-feldspars-cordierite-bioite-chlorite-sillimanite matrix in Jedi mineralized zone, PAU2011TR-012.

Channels were performed during previous campaign and 5 new channels were done this year on PAU2011TR-013. The lithology that was channeled corresponds to a metasomatic unit strongly deformed and composed of quartz-plagioclase-biotite and accessory minerals such as chlorite, epidote, cordierite and sericite. That unit is characterized by the presence of several pegmatitic and quartz veins injections. The alterations noticed are a strong penetrative silicification, biotitization and sericitization on PAU2011TR-013 and a silica-biotite-chlorite-sillimanite alteration on PAU2011TR-012. In this latter, silicification is observed pervasively and by locally up to 60% quartz veins. Porphyritic textures revealed by the presence of relics of plagioclase phenocrysts are locally observed. The mineralization is composed of 1-3% finely disseminated pyrite-pyrrhotite and locally traces of chalcopyrite in close association with a large number of pegmatitic dykes. The Jedi zone is in contact with a protomylonitic granodiorite and clearly less injected by felsic pegmatites to the north and with an altered proyomylonitic granodiorite (silica-biotite-chlorite-sillimanite) to the south. The protomylonitic granodiorite is in contact to the north with a gabbronorite and/or pyroxenite dyke injected by a few pegmatitic injections. Values of **0.41 g/t Au over 1.00 meter, 0.74 g/t Au over 6.50 meter including 3.48 g/t over 1.0 meter, 0.44 g/t Au over 4.0 meter** and **0.4 g/t over 1.0 meter** were obtained from channel PAU2011R-083 to PAU2011R-086 (Figure 19).

PAU2009TR-046 (Figure 20)

Channels PAU2011R-049 to PAU-2011R-064 were realized in trench PAU2009TR-046 (Figure 20) that was not sampled in previous campaign. The main lithology noticed in that trench is a granodioritic orthogneiss mainly composed of quartz-plagioclase-biotite-chlorite injected by decameter-scale pegmatitic injections. At the SE extremity of the trench, the granodiorite is in contact with an altered granodiorite (sillimanite-chlorite-silica-sericite). The altered granodiorite is characterized by gneissic texture, granoblastic fine grained rock with presence of biotite schlieren. Locally, protomylonitic texture is observed. No significant gold values were obtained from those channels.

PAU2009TR-047 (Figure 21)

During summer 2011, channels PAU2011R-065 to PAU2011R-082 were realized in trench PAU2009TR-047 (Figure 21). The lithology described is a metasomatic rock with granodioritic protolith composed of quartz-plagioclase-biotite-sillimanite. Presence of accessory minerals such as chlorite and locally cordierite is also noticed. Several folded pegmatitic cordierite-rich injections with meter-scale thickness are present. Penetrative silicification, sillimanite and a weak potassic alteration, revealed by presence of biotite, characterize the granodiorite. Mineralization is observed locally and is defined by traces of pyrrhotite that occurs disseminated. The granodiorite is probably a part of the alteration halo in Jedi area. No significant gold values were obtained from those channels.

Additional Channels on natural outcrop

PAU2011R-094 to PAU2011R-097 (Figure 22)

Channels PAU2011R-094 to PAU2011R-097 (Figure 22) were performed over a gossan zone discovered in 2006 on natural outcrop in the old Caniapiscau riverbed and located 100 meters South East of Tricorne showing. Channel PAU2006R-010 performed in 2006 returned anomalous gold of 0.34 g/t Au over 1.0 m (Lavoie et *al*, 2007). The alteration zone corresponds with IP anomaly PP-36. The alteration zone corresponds with an altered granodiorite (silica-garnet-biotite-sericite-sillimanite) hosted in a fresh, fine-grained granodiorite to the west and by an altered protomylonitic granodiorite to the east (silica-chlorite-potassic alterations). The lithologies encountered in channels are constituted of granodioritic orthogneiss in alternance with metasomatic bands with different alterations. The units are mainly constituted of quartz-plagioclase-biotite-sericite and accessory minerals such as sillimanite-garnet. Mineralization is variable along the channels, up to 5% pyrite-pyrrhotite is noticed but generally the sulfides represent 1% of the rock and traces of molybdene are observed locally. Anomalous gold values such as **0.23 g/t over 4.00 meters**, **0.32 g/t over 2.00 meters** and **0.16 g/t over 9.00 meters** were obtained from channels PAU2011R-094, PAU2011R-096 and PAU2011R-097.

PAU2011R-098 to PAU2011R-104 (Figure 23)

Channels PAU2011R-098 to PAU2011R-104 (Figure 23) were performed on natural outcrop, located 170 meters NW of Jedi showing. This figure features a deformed mineralized "band" where axial plane fractures are preferentially invaded by pegmatitic material. Pegmatitic dykes follow the trend of the mineralized "band" oriented N020°. Their locations are clearly influenced by the mineralized "band" or by faults that dislocated the alteration zone and observed on the field (Figure 23). The fold hinge is depicted on picture 42. Some mineralization occurs into the pegmatite, most likely representing remobilization. But generally, sulphides are associated with dismembered and folded quartz veins as well-illustrated in picture 43. The angular relation with Sp and quartz veins at the contact and breccia texture suggests an early stockwerk zone.

The lithology described is a granodioritic orthogneiss with intense alteration. The mineralogy is mainly constituted of quartz-plagioclase-biotite±cordierite±garnet±sericite±chlorite. The alteration is composed of silicification, grenatization, chloritization and biotitization with variable intensity. Distribution of alteration is heterogeneous along the channels. Mineralization occurs mostly disseminated and is generally composed of 2% pyrrhotite, 1% pyrite and locally traces of molybdenum. No significant gold value was obtained from those channels.

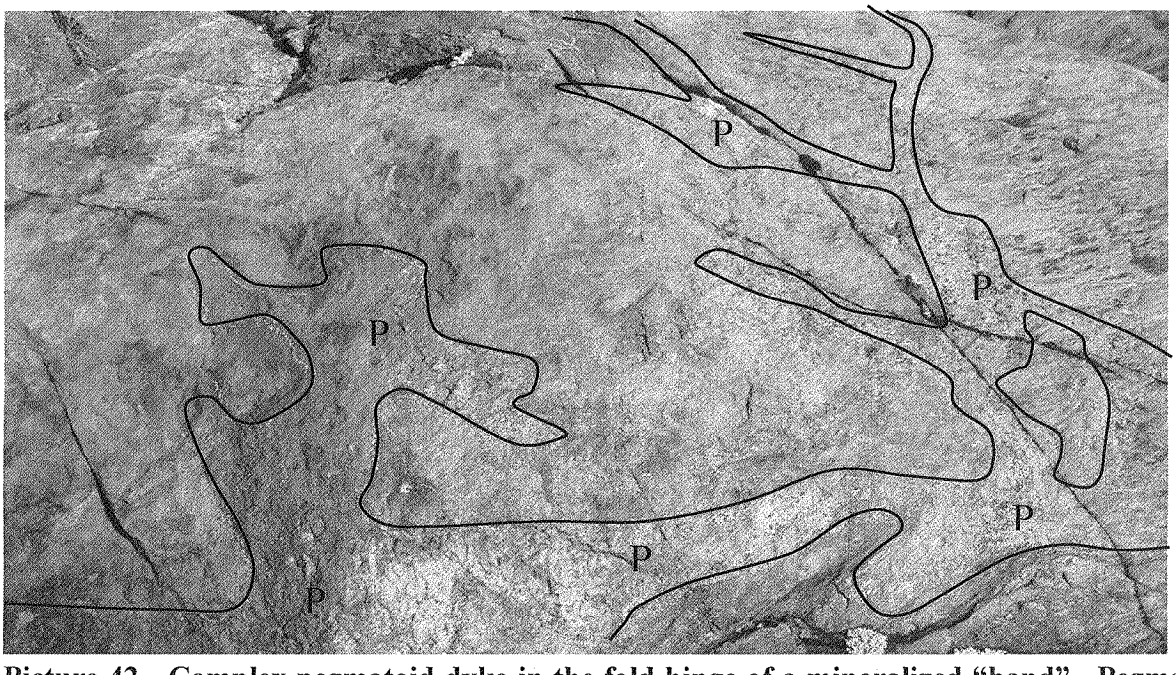

Picture 42 - Complex pegmatoid dyke in the fold hinge of a mineralized "band". Pegmatite is equally mineralized. "P" = pegmatite. Picture location from the fold hinge of figure 23.

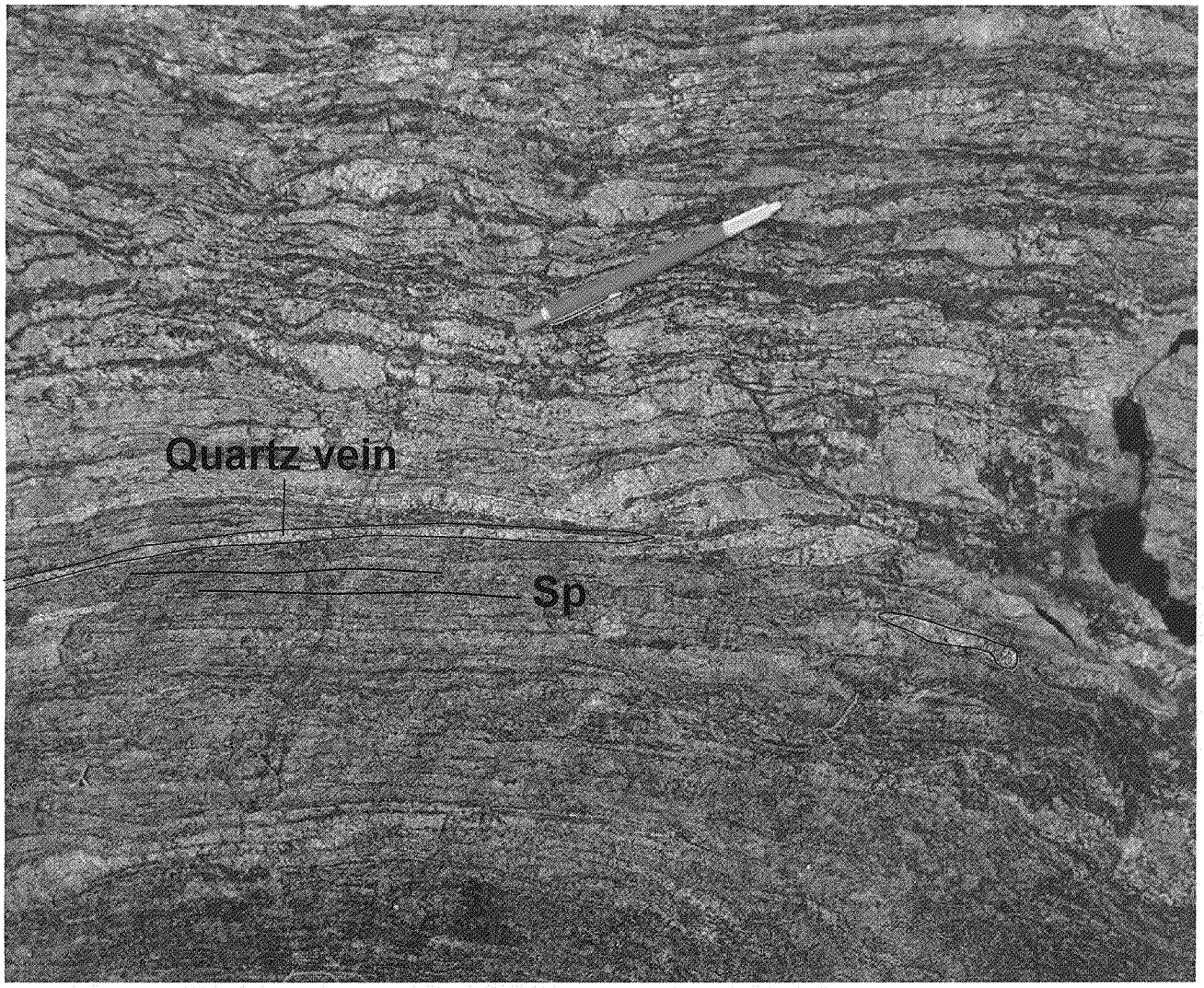

Picture 43 - Contact between sulphidation zone injected by 40-50% dismembered and folded quartz veins in contact with fresh and fine grained foliated granodiorite, North Jedi area. Quartz veins directly at the contact are dislocated and crosscut Sp in hosted rock.

PAU2009TR-014 (Figure 24)

Trench PAU2009TR-014 was already channeled during 2009 campaign but during summer 2011, channels PAU2011R-105, PAU2011R-106, PAU2011R-115 (PAU2009TR-013) and extension of channel PAU2009R-113 were performed. A detail mapping was also done and is described in paragraph below (Figure 24). No significant gold value was obtained from those channels.

Initially, Tricorne mineralized zone was interpreted as a tight fold open toward SW with a fold axis toward SW with moderate plunge varying from 55° to 60°. Axial plane is oriented NE-SW with dip toward NW (70° to 80°). The flanks of this fold are oriented toward NE with a dip varying from 30° to

80° (mean 60° to 70°). Metric pegmatite injections took place parallel to axial plane. PAU2009TR-014 is located directly in the fold hinge.

Many lithologies are observed with several degrees of alteration and deformation. The protolith is often obliterated. A series of faults oriented NE-SW could explain the presence of granodiorite blocs with different facies. In spite of the high intensity of alteration and deformation, it is possible to observe locally porphyritic relic texture with incipient schistosity in granodiorite (Picture 44). Deformation such as intra-folio folding, transposition of principal schistosity along an axial plan schistosity oriented NE-SW and fold axis with contradictory orientation (oriented SW, S or NE with plunge varying of 45° to 85°) are also observed. These observations suggest that Tricorne zone is directly located in a large anastomosed shear zone and could explain conflicting sheared movement indicators . New mapping, new structural data and new interpretation suggest that Tricorne zone on PAU2009TR-014 could be in reality a folded sigmoid (Picture 45d). The bloc diagram on figure 45 shows a possible interpretation of Tricorne zone at this location. Initially, a mineralized zone is present in a porphyritic and altered granodiorite (Figure 45a). A first stage of deformation created schistosity and could elongate the mineralized zone (Figure 44b). A second deformation stage (compressive with $\sigma 1$ oriented NW-SE) developed a second schistosity (axial plane) oriented NE-SW. Pegmatite magnetite-rich were emplaced parallel to this axial plane schistosity (Figure 45c). At last, the shape of the mineralized zone is a "Z"-shaped folded sigmoid. An "en-echelon" model and/or stacking structure could develop other mineralized zones at shallow depth. This model could explain why the drilling campaign wasn't successful on Tricorne area during previous campaigns.

Picture 44 – Porphyritic texture observed in altered granodiorite (chlorite-potassic±sillimanite). Tricorne zone, PAU2009TR-014.

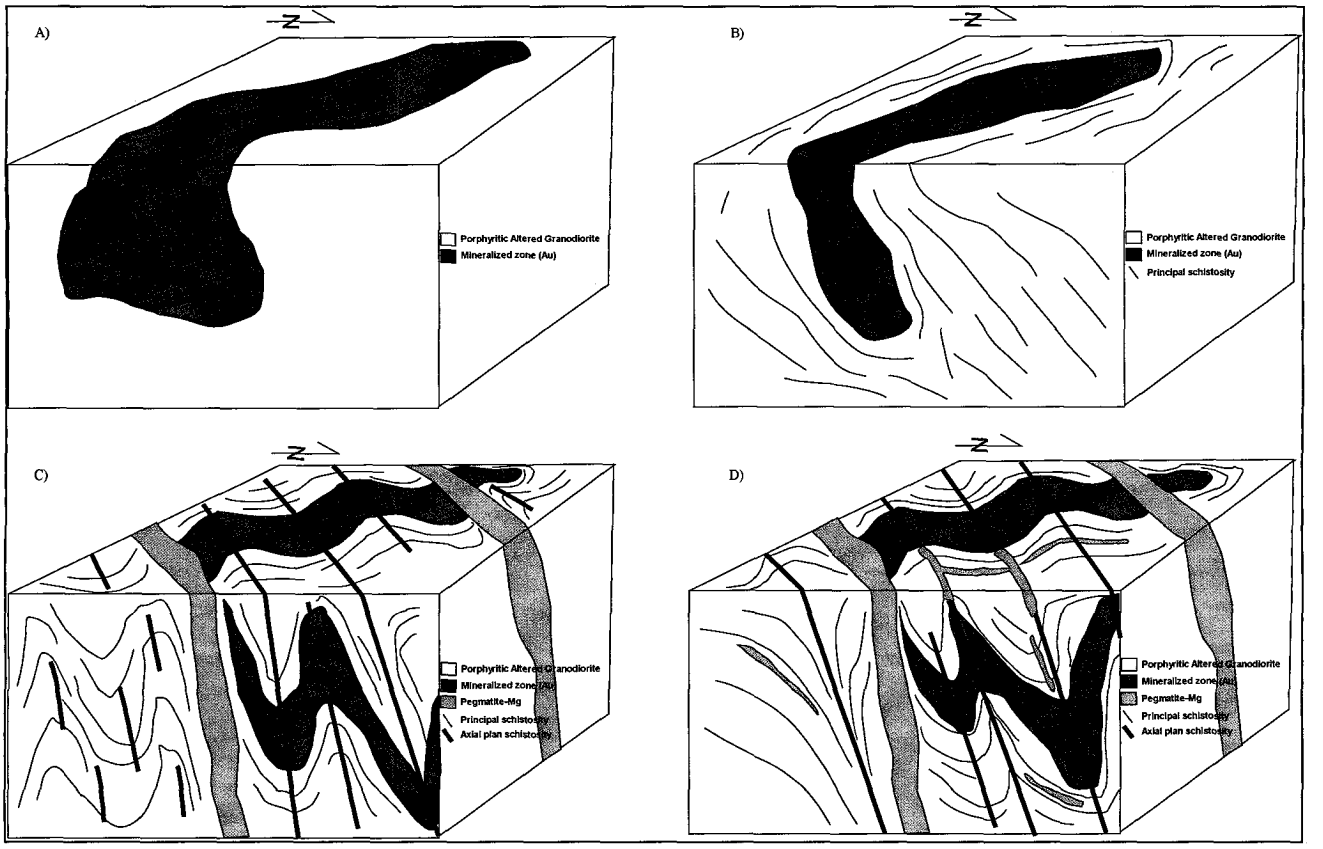

Picture 45 – Bloc diagram showing a possible explanation for the formation and the final morphology of Tricorne mineralized zone on PAU2009TR-014.

PAU2009TR-011 (Figure 25)

New channels PAU2011R-107 and PAU2011R-108 were performed in trench PAU2009TR-011 from Tricorne showing. A new detail mapping of the trench was also done (Figure 25). The lithology described in channels is a granodiorite with quartz veins and pegmatitic injections. The principal lithology is mainly composed of plagioclase-quartz-biotite-chlorite and locally hornblende. Among the alterations present in that unit, silicification, chloritization, sericitization and biotitization are described. Mineralization is mainly characterized by presence of 2% pyrite and 1% pyrrhotite that occurs disseminated, penetrative and in blebs. Traces of molybdenum are observed locally. Value of **0.43 g/t Au over 3.0 meters** was obtained from channel PAU2011R-107.

Like PAU2009TR-038, porphyritic relic texture is also observed in altered granodiorite. Detail mapping shows a high concentration of leucosomes and quartz veins in periphery of Tricorne mineralized zone. The orientation of leucosomes fits with Riedel pattern observed in shear zone. "Z"-shaped folding is

observed with sillimanite-bearing unit in contact with chloritic-potassic altered granodiorite (south contact). Sub-horizontal fractures and pegmatite contact locally observed suggest that high grade zone could be corresponding with some discontinuous fragments incorporated in felsic pegmatite and spatially associated with Tricorne zone in this trench.

PAU2009TR-039 (Figure 26)

Channels PAU2011R-109 to PAU2011R-114 and extension toward NNE of PAU2009R-131 (8 to 16 meter) were performed (Figure 26). This trench wasn't channeled during previous campaign. Channel PAU2011R-109 is described as a pegmatite with plagioclase-quartz-K-Feldspars-chlorite and accessory minerals such as sillimanite and cordierite. Mineralization is composed of 2% pyrite in blebs and traces of molybdenum associated to chlorite alteration. The other channels are described as quartz diorite with presence of metasomatic alteration with pegmatitic injection and quartz veins. The mineralogy is mainly composed of plagioclase-quartz-biotite and accessory minerals such as chlorite, sillimanite and cordierite. The intensity of the alteration and deformation is heterogeneous along the channels and locally the protolith is difficult or impossible to identify. When altered, pervasive silicification, sericitization and chloritization accompanied by sillimanite are observed (Picture 46). Mineralization is mainly composed of 1% pyrite and 1% pyrrhotite that occur disseminated and in stringers following principal schistosity. Channels PAU2011R-109 returned gold value of **0.75 g/t Au over 2.0 m**, channel PAU2011R-111 returned **0.43 g/t Au over 1.0m** and **7.57 g/t Au over 3.0 meter including 16.45 g/t Au over 1.0 meter**. Channel PAU2011R-112 obtained a value of **1.06 g/t Au over 1.0 meter.** No gold value was obtained for the extension of PAU2009R-131.

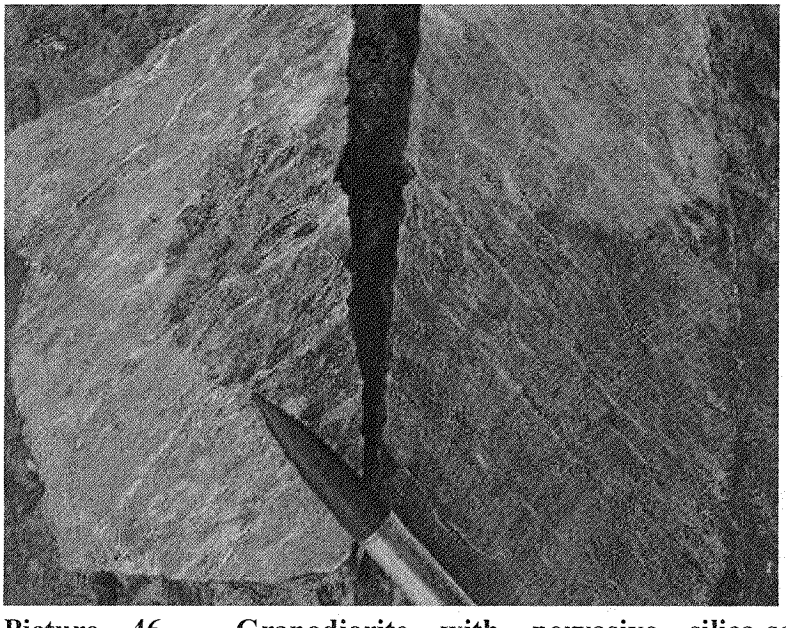

Picture 46 - Granodiorite with pervasive silica-sericite-chlorite-sillimanite-cordierite alterations, which returned 16,45 g/t Au over 1.0 meter, PAU2011R-111.

ITEM 13 – DRILLING

This section is not applicable to this report.

ITEM 14 – METHODS AND APPROACH

Rock samples collected during the 2011 program were obtained to determine the elemental concentrations in a quantitative way by ALS Chemex, Val d'Or or Thunder Bay. These included both mineralized and barren rocks, the latter of which were selected for lithological controls. Samples have been collected at the bedrock surface by either a hammer or a rock saw. Rocks collected with a hammer have been located with the use of a GPS Garmin 76Map. Samples picked up from channel have been positioned relative to each other using measuring tape with an anchor point located using the GPS positioning of their respective trenches. Individual bagged samples were then placed in shipping bags and stored in a secure area at the camp.

For surface sampling, most of the weathered crust was removed before samples were bagged. All samples were placed in individual bags with their appropriate tag number and the bags sealed with fibreglass tape. Individual bagged samples were then placed in shipping bags. The authors are not aware of any sampling or recovery factors that would impact the reliability of the samples.

ITEM 15 - SAMPLE PREPARATION, ANALYSIS AND SECURITY

15.1 - Sample security, storage and shipment

Samples were collected and processed by the personnel of Virginia Mines. Samples were immediately placed in plastic sample bags, tagged and recorded with unique sample number. Sealed samples were placed in shipping bags, which in turn were sealed with plastic tie straps or fibreglass tape. Bags remained sealed until the ALS Chemex personnel (Val-d'Or or Thunder Bay) opened them.

All samples were initially stored at the campsite. Samples were not secured in locked facilities, this precaution deemed unnecessary due to the remote location of the camp. Samples were then loaded onto a cube van for transport to Val-d'Or where Virginia personnel delivered them to the ALS Chemex sample preparation facility.

15.2 - Sample preparation and assay procedures

After logging in, the samples were crushed in their entirety at the ALS Chemex preparation laboratory in Val-d'Or to >70% passing 2 mm (ALS Chemex Procedure CRU-31). A 200 to 250-g sub-sample was obtained after splitting the finer material (<2 mm). The split portion derived from the crushing process was pulverized using a ring mill to >85% passing 75 µm (200 mesh - ALS Chemex Procedure PUL-31). From each such pulp, a 100-g sub-sample was obtained from another splitting and shipped to the ALS Chemex laboratory for assay. The remainder of the pulp (nominally 100 to 150 g) and the rejects are held at the processing lab for future reference. Three types of analytical packages have been used: WRC, Au+ and GOLE. Each package is discussed below.

The Au+Scan package includes Au, Ag, Al, As, B, Ba, Be, Bi, Ca, Cd, Co, Cr, Cu, Fe, Ga, Hg, K, La, Mg, Mn, Mo, Na, Ni, P, Pb, S, Sb, Sc, Sr, Th, Ti, Tl, U, V, W and Zn. All elements, except Au, were determined by the ME-ICP41 Procedure. Au was determined by the AA23 Procedure. For the sample with the value higher than 10 g/t Au, the analysis was repeated with the GRA21 Procedure. For the sample with the value higher than 0.5% Cu or Zn, the analysis was repeated with the OG62 Procedure.

The WRC package was selected to perform lithogeochemistry on lithological samples. These samples have been analyzed for Si, Al, Fe^{3+}, Ca, Mg, Na, K, Cr, Ti, Mn, P, Sr and Ba, reported as oxides, and for Y, Zr, Zn, Cu and Au. Major elements, Y and Zr were assayed using the ME-XRF06 method which consists in a lithium meta or tetra borate fusion followed by XRF. Cu and Zn from this package were obtained using AAS, following aqua regia digestion, according to the AA45 Procedure. Au was determined by the AA23 Procedure, a 30-g fire assay followed by AAS. Loss on ignition was calculated by the gravimetric method applied after heating at 1000°C.

The GOLE package includes concentrations in Al, Fe, Mg, Cr and Ca, reported as oxides, and Ag, Co, Cu, Ni, Au, Pt, Pd and S. It was used for sampling of ultramafic rocks. Base metals of economic interest (Ni, Cu, Co) and Ag were determined using the ME-AA61 Procedure, a HF-HNO_3-$HClO_4$ digestion and HCl leach followed by AAS. Precious metals Au, Pt and Pd were determined by the PGM-ICP23 Procedure, a 30-g fire assay followed by ICP-AES. Elements of more general and geochemical interest such as Al, Fe, Mg, Cr and Ca were determined using the ME-XRF06 Procedure, a lithium meta or tetra borate fusion followed by XRF. Total sulphur was determined using a Leco sulphur analyzer (Geochemical Procedure S-IR08). For this method, the sample (0.5 to 5.0 g) is heated to approximately 1350 °C in an induction furnace while passing a stream of oxygen through the sample. Sulphur dioxide released from the sample is measured by an infrared spectrometer and the total sulphur result is provided.

ITEM 16 - DATA VERIFICATION

Data verification procedures were performed by the staff of Virginia Mines on the assay results, standard, blank assays and duplicates. The authors were involved in the collecting, recording, interpretation and presentation of data in this report and the accompanying maps. The data has been reviewed and checked by the authors and is believed to be accurate. During the collection of channel samples, standards, blanks and reject duplicates were inserted for each batch of 20 samples as a part of Virginia quality control program. ALS Chemex, as part of their standard quality control, also ran duplicate check samples and standards. No sample was assayed at other laboratories. All assays results were received from the laboratory at the time that this report was written in April 2012. Samples 236267 to 236280 and 205882 were not received to the laboratory and are believed to be lost after sampling. Standards used were SK52, SQ48 and SI54 (Appendix 9) and an uncertified blank material made of calcite (Dolomite).

Table 5 shows results obtained from assays of standards and blanks provided by Virginia Mines to ALS Chemex laboratory as a part of its quality control. All the blanks assayed returned values inferior to 0.005 ppm Au (detection limit) except three (3) samples which returned 0.009 ppm (#236 185 and #236 619) and 0.006 ppm (#236 443). Considering that the detection limit is at 0.005 ppm and that the blank

are uncertified, the assays are considered to be accurate and clean of any contamination during the laboratory procedures.
Standard samples assaying highlights some laboratory failures as shown in table 6. Standard assays are considered a failure when the Au value obtained differs by 3 times or more the standard deviation of the standard (Au Obtained – Au Expected = < 3 X Standard Deviation of Standard Sample). Detailed from the gold expected results for each standard sample are displayed in appendix 9.

Regarding the standard assay results, seven (7) standard assays returned variations above the "3 x standard deviation". One assay from standard SI54 (expected gold value of 1.78 ppm) returned 1.675 ppm (#236 169) from batch assays TB11182326. Three assays from standard SK52 (expected gold value of 4.11 ppm) returned 3.59 mm (236 464), 3.83 ppm (236 603) and 3.72 ppm (236 646) from batch assays TM11194891, TM11194898 and TM11194901. And three (3) assays from standard SQ48 (expected gold value of 30.25 ppm) obtained value of 27.7 ppm (236 525), 28.1 ppm (236 579) and 28.7 ppm (236 626). According to the fact that the other blanks, standards and duplicates analysed in the same batches were evaluated precisely, the reassaying was not required.

Table 5: Analytical results and statistic treatment for all blank and standard samples taken during the channelling program

Type	Sample	Voucher	Std Au ppm	Std Dev	3xStd Dev	Au Lab ppm	Variation	Status
Blank	236111	TB11159979	0.00	0	0	<0,005	bdl	OK
SK52	236116	TB11159979	4.11	0.088	0.264	4.07	0.04	OK
Blank	236122	TB11161056	0.00	0	0	<0,005	bdl	OK
SQ48	236134	TB11161056	30.25	0.51	1.53	29.2	1.05	OK
Blank	236004	TB11161441	0.00	0	0	<0,005	bdl	OK
SK52	236018	TB11161441	4.11	0.088	0.264	4.13	-0.02	OK
SQ 48	236045	TB11161442	30.25	0.51	1.53	29.6	0.65	OK
Blank	236047	TB11161442	0.00	0	0	<0,005	bdl	OK
Blank	236030	TB11161443	0.00	0	0	<0,005	bdl	OK
SI 54	236038	TB11161443	1.78	0.034	0.102	1.83	-0.05	OK
SK 52	236086	TB11161444	4.11	0.088	0.264	4.14	-0.03	OK
Blank	236093	TB11161444	0.00	0	0	<0,005	bdl	OK
SI 54	236064	TB11161445	1.78	0.034	0.102	1.73	0.05	OK
Blank	236079	TB11161445	0.00	0	0	<0,005	bdl	OK
Blank	236145	TB11182325	0.00	0	0	<0,005	bdl	OK
SQ48	236152	TB11182325	30.25	0.51	1.53	29.5	0.75	OK
SI54	**236169**	**TB11182326**	**1.78**	**0.034**	**0.102**	**1.675**	**0.11**	**> 3xStd Dev**
Blank	236179	TB11182326	0.00	0	0	<0,005	bdl	OK
Blank	236185	TB11182327	0.00	0	0	0.009	/	OK
SK52	236199	TB11182327	4.11	0.088	0.264	3.91	0.20	OK
SQ48	236208	TB11182328	30.25	0.51	1.53	29.4	0.85	OK
Blank	236215	TB11182328	0.00	0	0	<0,005	bdl	OK
Blank	236306	TB11182329	0.00	0	0	<0,005	bdl	OK

SK52	236312	TB11182329	4.11	0.088	0.264	3.97	0.14	OK
Blank	236331	TB11182680	0.00	0	0	<0,005	bdl	OK
SQ48	236338	TB11182680	30.25	0.51	1.53	29.4	0.85	OK
SI54	236225	TB11184659	1.78	0.034	0.102	1.69	0.09	OK
Blank	236234	TB11184659	0.00	0	0	<0,005	bdl	OK
Blank	236245	TB11185720	0.00	0	0	<0,005	bdl	OK
SQ48	236251	TB11185720	30.25	0.51	1.53	29.9	0.35	OK
SK52	236285	TM11194867	4.11	0.088	0.264	3.86	0.25	OK
Blank	236296	TM11194867	0.00	0	0	<0,005	bdl	OK
SK52	236404	TM11194868	4.11	0.088	0.264	3.84	0.27	**OK**
Blank	236418	TM11194868	0.00	0	0	<0,005	bdl	OK
SQ48	236433	TM11194869	30.25	0.51	1.53	28.8	1.45	OK
Blank	236437	TM11194869	0.00	0	0	<0,005	bdl	OK
Blank	236443	TM11194890	0.00	0	0	0.006	/	OK
SK52	236458	TM11194890	4.11	0.088	0.264	4.08	0.03	OK
SK52	**236464**	**TM11194891**	**4.11**	**0.088**	**0.264**	**3.59**	**0.52**	**> 3xStd Dev**
Blank	236471	TM11194891	0.00	0	0	<0,005	bdl	OK
SK52	236484	TM11194892	4.11	0.088	0.264	4.04	0.07	OK
Blank	236496	TM11194892	0.00	0	0	0.005	/	OK
Blank	236503	TM11194893	0.00	0	0	<0,005	bdl	OK
SI54	236518	TM11194893	1.78	0.034	0.102	1.735	0.04	OK
SQ48	236525	TM11194894	30.25	0.51	1.53	27.7	2.55	**> 3xStd Dev**
Blank	236532	TM11194894	0.00	0	0	<0,005	bdl	OK
Blank	236551	TM11194895	0.00	0	0	<0,005	bdl	OK
SK52	236558	TM11194895	4.11	0.088	0.264	3.92	0.19	OK
Blank	236565	TM11194896	0.00	0	0	<0,005	bdl	OK
SQ48	**236579**	**TM11194896**	**30.25**	**0.51**	**1.53**	**28.1**	**2.15**	**> 3xStd Dev**
SI54	236583	TM11194897	1.78	0.034	0.102	1.72	0.06	OK
SK52	**236603**	**TM11194898**	**4.11**	**0.088**	**0.264**	**3.83**	**0.28**	**> 3xStd Dev**
Blank	236619	TM11194898	0.00	0	0	0.009	/	OK
SQ48	**236626**	**TM11194900**	**30.25**	**0.51**	**1.53**	**28.7**	**1.55**	**> 3xStd Dev**
Blank	236636	TM11194900	0.00	0	0	<0,005	bdl	OK
SK52	**236646**	**TM11194901**	**4.11**	**0.088**	**0.264**	**3.72**	**0.39**	**> 3xStd Dev**

For duplicates assays, the relative percent difference (RPD) was calculated to evaluate the precision of the results. The formula to calculate the RPD is defined by:

Absolute value of ((C1-C2)/((C1+C2)/2))x100

Where C1 is defined by the concentration of the element in the sample and C2 the concentration of the same element in the duplicates. If values have a RPD greater than 20%, the values are not considered to

be within precision standard. When the difference between the sample and duplicates assays for an element is equivalent or lower than the detection limit of this element, the RPD was not considered. The table 6 shows results obtained for duplicates and the RPD calculated for each element (Au-Ag-Cu-Mo-Zn). Regarding the duplicates assays results, five (5) duplicates have a RPD higher than 20% in one or several elements. The sample #236 320, duplicates of #236 319, has a relative percent difference of 31.58% for the copper from batch assays TB11182329. The sample #236 264, duplicates of #236 263 has a RPD of 59.65% for gold and 55.32% for zinc. It is included in batch assays TB11185721. The duplicate #236 289 from sample #236288, from batch assays TM11194867, has a relative percent difference of 24.66% for gold and 66.67% for molybdenum. The samples #236408 and #236 407, from batch assays TM11194868, has a relative difference of 27.91% for gold. And finally, the duplicates #236 451 of sample #236450 has a relative percent difference of 27.12% for copper and 20.59% for zinc and is included in batch assays TM11194890. According to the fact that the other blanks, standards and duplicates analysed in the same batches were evaluated precisely, the reassaying was not required.

Table 6: Analytical results and statistic treatment for all duplicates samples taken during the channelling program

Sample	Type	Voucher	Au (ppm)	Ag (ppm)	Cu (ppm)	Mo (ppm)	Zn (ppm)	RPD % (Au)	RPD % (Ag)	RPD % (Cu)	RPD % (Mo)	RPD % (Zn)	Comments
236105	Expected Duplicated Result	TB11159979	0.015	0.6	59	2	106						
236106	Duplicata de 236105	TB11159979	0.017	0.4	61	2	106	12.50	40.00	3.33	0.00	0.00	OK
			0.002	0.2	2	0	0						
236130	Expected Duplicated Result	TB11161056	0.005	0.1	8	0.5	68						
236131	Duplicata de 236130	TB11161056	0.005	0.1	8	0.5	73	0.00	0.00	0.00	0.00	7.09	OK
			0	0	0	0	5						
236009	Expected Duplicated Result	TB11161441	0.189	3.2	419	0.5	68						
236010	Duplicata de 236009	TB11161441	0.179	3.3	435	0.5	72	5.43	3.08	3.75	0.00	5.71	OK
			0.01	0.1	16	0	4						
236057	Expected Duplicated Result	TB11161442	0.199	0.7	159	3	103						
236058	Duplicata de 236057	TB11161442	0.196	0.7	159	4	102	1.52	0.00	0.00	28.57	0.98	OK
			0.003	0	0	1	1						
236023	Expected Duplicated Result	TB11161443	0.168	1.3	396	0.5	67						
236024	Duplicata de 236023	TB11161443	0.158	1.3	391	0.5	65	6.13	0.00	1.27	0.00	3.03	OK
			0.01	0	5	0	2						
236098	Expected Duplicated Result	TB11161444	0.027	0.4	40	0.5	67						
236099	Duplicata de 236098	TB11161444	0.023	0.5	41	0.5	68	16.00	22.22	2.47	0.00	1.48	OK
			0.004	0.1	1	0	1						
236069	Expected Duplicated Result	TB11161445	0.006	0.4	31	0.5	303						
236070	Duplicata de 236069	TB11161445	0.005	0.2	30	0.5	310	18.18	66.67	3.28	0.00	2.28	OK
			0.001	0.2	1	0	7						
236159	Expected Duplicated Result	TB11182325	0.0025	0.1	21	0.5	37						
236160	Duplicata de 236159	TB11182325	0.0025	0.1	20	0.5	36	0.00	0.00	4.88	0.00	2.74	OK

			0	0	1	0	1						
236162	Expected Duplicated Result	TB11182326	0.021	1.3	340	1	1040						
236163	Duplicata de 236162	TB11182326	0.021	1.4	354	1	1055	0.00	7.41	4.03	0.00	1.43	OK
			0	0.1	14	0	15						
236192	Expected Duplicated Result	TB11182327	0.208	0.5	70	0.5	81						
236193	Duplicata de 236192	TB11182327	0.209	0.5	69	0.5	78	0.48	0.00	1.44	0.00	3.77	OK
			0.001	0	1	0	3						
236203	Expected Duplicated Result	TB11182328	0.0025	0.1	30	1	56						
236204	Duplicata de 236203	TB11182328	0.0025	0.1	30	1	57	0.00	0.00	0.00	0.00	1.77	OK
			0	0	0	0	1						
236319	Expected Duplicated Result	TB11182329	0.012	0.4	55	2	68						
236320	Duplicata de 236319	TB11182329	0.01	0.3	40	2	57	18.18	28.57	31.58	0.00	17.60	??
			0.002	0.1	15	0	11						
236324	Expected Duplicated Result	TB11182680	0.0025	0.3	56	2	80						
236325	Duplicata de 236324	TB11182680	0.0025	0.2	55	2	79	0.00	40.00	1.80	0.00	1.26	OK
			0	0.1	1	0	1						
236226	Expected Duplicated Result	TB11184659	0.0025	0.2	49	1	94						
236227	Duplicata de 236226	TB11184659	0.0025	0.1	49	1	94	0.00	66.67	0.00	0.00	0.00	OK
			0	0.1	0	0	0						
236256	Expected Duplicated Result	TB11185720	0.008	0.1	6	0.5	16						
236257	Duplicata de 236256	TB11185720	0.005	0.1	5	0.5	15	46.15	0.00	18.18	0.00	6.45	OK
			0.003	0	1	0	1						
236263	Expected Duplicated Result	TB11185721	0.02	0.2	37	2	51						
236264	Duplicata de 236263	TB11185721	0.037	0.2	37	1	90	59.65	0.00	0.00	66.67	55.32	??
			0.017	0	0	1	39						
236288	Expected Duplicated Result	TM11194867	0.032	0.2	66	4	106						
236289	Duplicata de 236288	TM11194867	0.041	0.2	72	2	107	24.66	0.00	8.70	66.67	0.94	??
			0.009	0	6	2	1						
236407	Expected Duplicated Result	TM11194868	0.049	0.5	83	0.5	96						
236408	Duplicata de 236407	TM11194868	0.037	0.6	85	0.5	95	27.91	18.18	2.38	0.00	1.05	??
			0.012	0.1	2	0	1						
236424	Expected Duplicated Result	TM11194869	0.515	1.2	103	8	123						
236425	Duplicata de 236424	TM11194869	0.452	1.1	102	7	125	13.03	8.70	0.98	13.33	1.61	OK
			0.063	0.1	1	1	2						
236450	Expected Duplicated Result	TM11194890	0.005	0.4	67	2	150						
236451	Duplicata de 236450	TM11194890	0.005	0.3	51	2	122	0.00	28.57	27.12	0.00	20.59	??
			0	0.1	16	0	28						
236477	Expected Duplicated Result	TM11194891	0.069	0.9	165	2	66						
236478	Duplicata de 236477	TM11194891	0.072	0.9	163	2	65	4.26	0.00	1.22	0.00	1.53	OK

			0.003	0	2	0	1						
236487	Expected Duplicated Result	TM11194892	0.0025	0.1	5	1	5						
236488	Duplicata de 236487	TM11194892	0.0025	0.1	5	1	6	0.00	0.00	0.00	0.00	18.18	OK
			0	0	0	0	1						
236508	Expected Duplicated Result	TM11194893	0.013	0.6	112	3	58						
236509	Duplicata 236508	TM11194893	0.012	0.7	110	3	57	8.00	15.38	1.80	0.00	1.74	OK
			0.001	0.1	2	0	1						
236537	Expected Duplicated Result	TM11194894	0.124	0.3	43	4	108						
236538	Duplicata 236537	TM11194894	0.118	0.1	43	5	108	4.96	100.00	0.00	22.22	0.00	OK
			0.006	0.2	0	1	0						
236543	Expected Duplicated Result	TM11194895	0.251	1.6	397	14	63						
236544	Duplicata 236543	TM11194895	0.271	2.2	447	14	70	7.66	31.58	11.85	0.00	10.53	OK
			0.02	0.6	50	0	7						
236570	Expected Duplicated Result	TM11194896	0.16	0.6	124	1	103						
236571	Duplicata 236570	TM11194896	0.169	0.5	123	2	102	5.47	18.18	0.81	66.67	0.98	OK
			0.009	0.1	1	1	1						
236590	Expected Duplicated Result	TM11194897	0.074	1.4	116	7	428						
236591	Duplicata 236590	TM11194897	0.075	1.3	108	8	365	1.34	7.41	7.14	13.33	15.89	OK
			0.001	0.1	8	1	63						
236627	Expected Duplicated Result	TM11194900	0.012	0.1	31	1	80						
236628	Duplicata 236627	TM11194900	0.007	0.2	32	0.5	78	52.63	66.67	3.17	66.67	2.53	OK
			0.005	0.1	1	0.5	2						

ITEM 17 – ADJACENT PROPERTIES

This section is not applicable to this report.

ITEM 18 – MINERAL PROCESSING AND METALLURGICAL TESTING

This section is not applicable to this report.

ITEM 19 – MINERAL RESOURCE, MINERAL RESERVE ESTIMATES

This section is not applicable to this report.

ITEM 20 – OTHER RELEVANT DATA AND INFORMATION

Trench restoration was performed during summer 2011 program. From the ten (10) trenches realized using an excavator in 2011, three (3) were completely restored and reforested for a total of 1278 m^3.

Several trenches that were performed during previous campaigns (2009 and 2010) were also restored and reforested. In tables 7 to 9, the trenches highlighted in bold are those that were restored during 2011 campaign. From 2010 trenches, fourteen (14) trenches for a total volume of 1395 m³ were completely restored and reforested. From 2009 trenches, six (6) new trenches were restored and reforested for a total of 234 m³. During summer 2011, 2000 black spruces were planted on the different trenches.

Table 7: Trenches performed during 2011 campaign

TRENCH 2011							
Trench	**Utm_E**	**Utm_N**	**Status**	**Surface (m²)**	**Depth (m)**	**Volume(m³)**	**Remaining (m³)**
PAU-2011-TR-001	446487	6084517	Opened	12	1.50	18	27.0
PAU-2011-TR-002	446755	6084778	Opened	30	0.50	15	7.5
PAU-2011-TR-003	**446280**	**6085039**	**Restored and Reforested**	**20**	**1.50**	**30**	-
PAU-2011-TR-004	446251	6078919	Opened	350	2.00	700	700
PAU-2011-TR-005	446557	6079237	Opened	585	2.00	1170	700
PAU-2011-TR-006	**447701**	**6080313**	**Restored and Reforested**	**192**	**1.50**	**288**	-
PAU-2011-TR-007	447581	6080242	Opened	315	3.00	945	945.0
PAU-2011-TR-008	**447527**	**6080199**	**Restored and Reforested**	**320**	**3.00**	**960**	-
PAU-2011-TR-009	447422	6080095	Opened	576	3.00	1728	1728.0
PAU-2011-TR-010	447376	6080013	Opened	306	2.00	612	1728.0
PAU-2011-TR-011	443853	6078625	Opened (Manual trench)	40	0.30	12	12.0
PAU-2011-TR-012	444650	6077749	Natural Outcrop				
PAU-2011-TR-013	444603	6077750	Natural Outcrop				
			Total Volume 2011			**6478.0**	**5847.5**
			Volume restored in 2011			**1278.0**	

Table 8: Trenches performed during 2010 campaign

TRENCH 2010							
Trench	**Utm_E**	**Utm_N**	**Status**	**Surface (m²)**	**Depth (m)**	**Volume(m³)**	**Remaining (m³)**
PAU-2010-TR-001	**444469**	**6079146**	**Restored and Reforested**	**60**	**0.50**	**30**	-
PAU-2010-TR-002	444332	6079011	Opened	320	0.60	192	192.0
PAU-2010-TR-003	445071	6078528	Restored and Reforested	60	0.25	15	-
PAU-2010-TR-004	444528	6077937	Opened	158	1.50	237	237.0
PAU-2010-TR-005	**445123**	**6079054**	**Restored and Reforested**	**71**	**0.50**	**36**	-
PAU-2010-TR-006	**445303**	**6079167**	**Restored and Reforested**	**88**	**0.30**	**26**	-
PAU-2010-TR-007	**445057**	**6079414**	**Restored and Reforested**	**93**	**0.75**	**70**	-
PAU-2010-TR-008	444818	6079568	Restored and Reforested	71	0.30	21	-
PAU-2010-TR-009	445237	6080227	Restored and Reforested	130	1.50	195	-
PAU-2010-TR-010	446452	6081859	Restored	40	1.75	70	-
PAU-2010-TR-011	446487	6081872	Opened	170	1.50	255	255.0
PAU-2010-TR-012	446791	6082187	Opened	250	1.50	375	375.0
PAU-2010-TR-013	447010	6082397	Opened	260	1.40	364	364.0
PAU-2010-TR-014	**445456**	**6079978**	**Restored and Reforested**	**186**	**0.25**	**47**	-
PAU-2010-TR-015	**445481**	**6079977**	**Restored and Reforested**	**105**	**0.50**	**53**	-
PAU-2010-TR-016	445834	6079614	Opened	135	0.50	68	67.5
PAU-2010-TR-017	444901	6079860	Restored and Reforested	30	1.50	45	-
PAU-2010-TR-018	444208	6079134	Restored	30	2.00	60	-

PAU-2010-TR-019	444263	6077497	Restored	30	2.00	60	-
PAU-2010-TR-020	445723	6078432	Restored	21	5.00	105	-
PAU-2010-TR-021	445883	6078575	Restored	21	5.00	105	-
PAU-2010-TR-022	446031	6078707	Restored	21	5.00	105	-
PAU-2010-TR-023	441326	6077203	Restored and Reforested	107	0.30	32	-
PAU-2010-TR-024	**440978**	**6077124**	**Restored and Reforested**	**153**	**0.75**	**115**	-
PAU-2010-TR-025	**440962**	**6077105**	**Restored and Reforested**	**108**	**0.50**	**54**	-
PAU-2010-TR-026	**440841**	**6077276**	**Restored and Reforested**	**246**	**1.00**	**246**	**246.0**
PAU-2010-TR-027	**440560**	**6077427**	**Restored and Reforested**	**140**	**1.00**	**140**	-
PAU-2010-TR-028	**440479**	**6077405**	**Restaured**	**472**	**0.75**	**354**	-
PAU-2010-TR-029	**440536**	**6077262**	**Restored and Reforested**	**91**	**0.15**	**14**	-
PAU-2010-TR-030	**440278**	**6077294**	**Restored and Reforested**	**95**	**0.75**	**71**	-
PAU-2010-TR-031	**440145**	**6077560**	**Restored and Reforested**	**156**	**0.90**	**140**	-
PAU-2010-TR-032	446326	6083122	Opened	23	0.50	12	11.5
PAU-2010-TR-033	446026	6082999	Opened	25	0.30	8	7.5
PAU-2010-TR-034	444931	6083986	Opened	90	1.20	108	108.0
PAU-2010-TR-035	447253	6080507	Opened	60	0.25	15	15.0
PAU-2010-TR-036	447600	6080865	Opened	82	0.30	25	24.6
PAU-2010-TR-037	447764	6081063	Extended	39	0.40	16	-
PAU-2010-TR-038	447766	6081026	Restored	25	0.50	13	-
PAU-2010-TR-039	447870	6081129	Extended	60	0.50	30	-
PAU-2010-TR-066	447750	6081063	Opened	1005	0.30	301.5	301.5
PAU-2010-TR-067	447729	6081014	Restored up to 60%	286	0.50	143	57.2
PAU-2010-TR-068	447794	6081093	Opened	239.5	0.40	95.8	95.8
PAU-2010-TR-069	447716	6081095	Opened	574	0.50	287	287.0
PAU-2010-TR-070	447830	6080966	Opened	333	0.75	249.75	249.8
PAU-2010-TR-071	447782	6081003	Opened	303	0.35	106.05	106.1
PAU-2010-TR-072	447744	6081151	Opened	396	0.75	297	297.0
PAU-2010-TR-073	447874	6081125	Opened	405	0.60	243	243.0
PAU-2010-TR-074	447715	6081219	Opened	155	0.30	46.5	46.5
PAU-2010-TR-075	447645	6080841	Opened	337.5	0.30	101.25	101.3
			Total Volume 2010			**5794.2**	**3688.2**
			Volume restored in 2011			**1394.7**	

Table 9: Trenches performed during 2009 campaign

TRENCH 2009							
Trench	**Utm_E**	**Utm_N**	**Status**	**Surface (m²)**	**Depth (m)**	**Volume(m³)**	**Remaining**
PAU-2009-TR-001	440772	6077278	Restaured at 75%	900	0.50	450	112.5
PAU-2009-TR-002	440755	6077313	Restored and Reforested	75	0.50	38	-
PAU-2009-TR-003	440749	6077250	Restored and Reforested	60	0.30	18	-
PAU-2009-TR-004	440743	6077152	Restored and Reforested	90	0.50	45	-
PAU-2009-TR-005	440686	6077182	Restored and Reforested	150	1.00	150	-
PAU-2009-TR-006	440341	6077317	Restored and Reforested	200	0.75	150	-
PAU-2009-TR-007	440677	6077323	Opened	450	1.00	450	450.0
PAU-2009-TR-008	440511	6077393	Opened	225	0.30	68	67.5
PAU-2009-TR-009	440763	6077190	Restored and Reforested	20	0.30	6	-
PAU-2009-TR-010	440873	6077352	Restored and Reforested	180	0.35	63	-
PAU-2009-TR-011	444894	6078432	Opened	1700	0.15	255	255.0

PAU-2009-TR-012	444956	6078472	Opened	944	0.20	189	188.8
PAU-2009-TR-013	444931	6078493	Opened	120	0.10	12	12.0
PAU-2009-TR-014	444941	6078526	Opened	770	0.30	231	231.0
PAU-2009-TR-015	445076	6078543	Restored and Reforested	184	0.40	74	-
PAU-2009-TR-016	444884	6078536	Restored and Reforested	135	0.50	68	-
PAU-2009-TR-017	444800	6078589	Opened	514	0.75	386	385.5
PAU-2009-TR-018	444753	6078560	Restored and Reforested	49	0.30	15	-
PAU-2009-TR-019	444675	6078475	Restored and Reforested	230	0.75	173	-
PAU-2009-TR-020	444413	6078312	Restored and Reforested	67	0.30	20	-
PAU-2009-TR-021	444383	6078308	Restored and Reforested	98	0.25	25	-
PAU-2009-TR-022	444331	6078314	Restored and Reforested	705	0.75	529	-
PAU-2009-TR-023	444748	6078628	Opened	129	0.30	39	38.7
PAU-2009-TR-024	**444794**	**6078518**	**Restored and Reforested**	**174**	**0.30**	**52**	**-**
PAU-2009-TR-025	444246	6078199	Opened	220	0.50	110	110.0
PAU-2009-TR-026	444204	6078101	Opened	593	0.20	119	118.6
PAU-2009-TR-027	444186	6078058	Opened	443	0.25	111	110.8
PAU-2009-TR-028	444809	6078493	Opened	240	0.25	60	60.0
PAU-2009-TR-029	**444697**	**6078356**	**Restored and Reforested**	**114**	**0.30**	**34**	**-**
PAU-2009-TR-030	**444848**	**6078391**	**Restored and Reforested**	**125**	**0.30**	**38**	**-**
PAU-2009-TR-031	**444530**	**6078482**	**Restored and Reforested**	**139**	**0.40**	**56**	**-**
PAU-2009-TR-032	444797	6078558	Restored and Reforested	75	0.40	30	-
PAU-2009-TR-033	**444793**	**6078467**	**Restored and Reforested**	**83**	**0.30**	**25**	**-**
PAU-2009-TR-034	444791	6078279	Restored and Reforested	69	0.25	17	-
PAU-2009-TR-035	444775	6078456	Restored and Reforested	75	0.50	38	-
PAU-2009-TR-036	444965	6078546	Restored and Reforested	75	0.50	38	-
PAU-2009-TR-037	444920	6078548	Opened	407	0.20	81	81.4
PAU-2009-TR-038	445416	6078969	Opened	335	0.20	67	67.0
PAU-2009-TR-039	**444781**	**6078544**	**Restored**	**100**	**0.30**	**30**	**-**
PAU-2009-TR-040	444470	6079090	Restored and Reforested	105	0.50	53	-
PAU-2009-TR-041	444433	6079076	Opened	101	0.30	30	30.3
PAU-2009-TR-042	444414	6079065	Opened	210	0.30	63	63.0
PAU-2009-TR-043	444390	6079033	Opened	127	0.50	64	63.5
PAU-2009-TR-044	443775	6077331	Opened	90	0.30	27	27.0
PAU-2009-TR-045	443810	6077292	Opened	96	0.20	19	19.2
PAU-2009-TR-046	443884	6077227	Opened	170	0.25	43	42.5
PAU-2009-TR-047	443985	6077273	Opened	142	0.30	43	42.6
			Total Volume 2009			**4695**	**2576.9**
			Volume restored in 2011			**234**	

ITEM 21 – INTERPRETATION AND CONCLUSIONS

Exploration during summer 2011 did not outline new major gold-bearing zone but a few highlights were obtained while resampling previously known mineralized zone. Beausac-II mineralized zone was extended by 45 meters toward NW with channel PAU2011R-002 returning **0.23 g/t Au over 12.0 m including 0.89 g/t Au over 1.0 m**. Channel PAU2011R-084 performed on Jedi zone returned **0.74 g/t Au over 6.5 m including 3.48 g/t Au over 1.0 m** on trench PAU2011TR-013 and channel PAU2011R-111 performed on Tricorne zone returned **7.57 g/t Au over 3.0 m including 16.45 g/t Au over 1.0 m**. In grab sample, two (2) boulders returned high gold values. The first one, located in Cu-Hébert area returned **8.73 g/t Au (#205 901)**. The second boulder is located in Hope area and returned **7.91 g/t Au (#207 975)**. This latter is located near IP anomaly PP-88. The presence of IP anomaly (PP-88) combined to the presence of high grade boulder could indicate that the Hope mineralized zone extends toward SE. An outcrop located in Cu-Hébert area, in the old Caniapiscau riverbed yielded **4.09 g/t Au (#205 957)**. One of the more interesting fact is the discovery of new silica-chlorite altered intrusive rock in the west part of the property (Picture 2). The discovery of this altered intrusive opens a new area for exploration. Alteration is now observed over more than 24 km on the property and indicates a large hydrothermal system associated with regional intrusion (Picture 47).

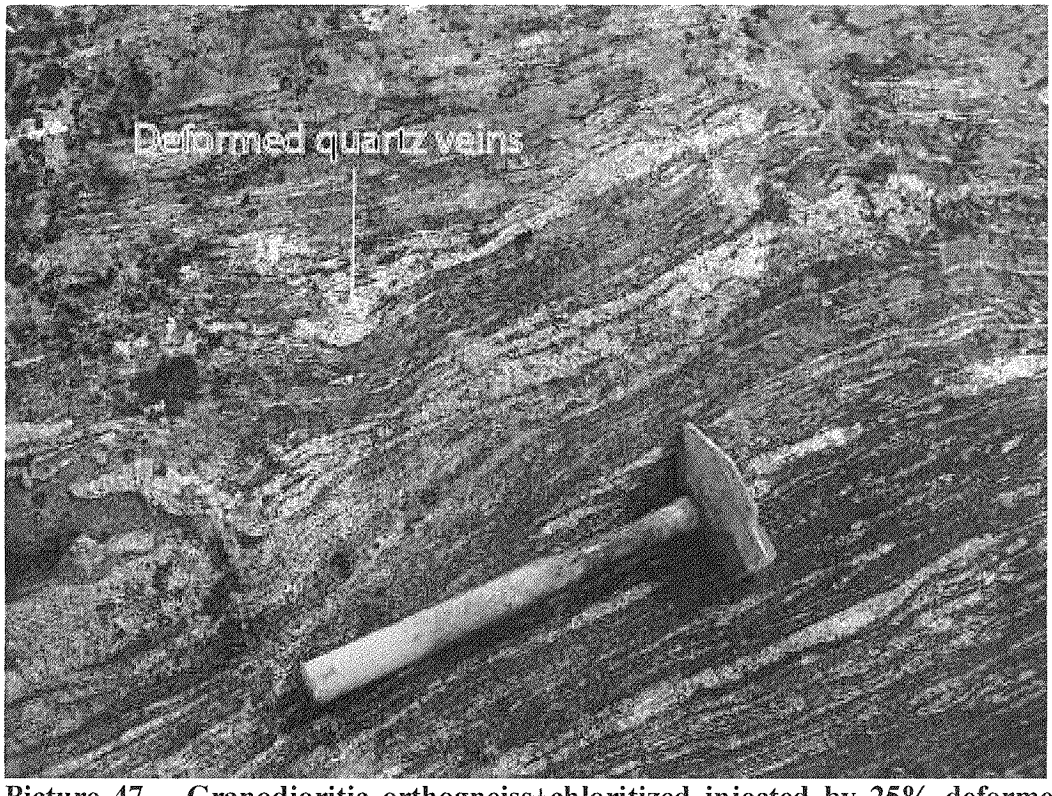

Picture 47 – Granodioritic orthogneiss±chloritized injected by 25% deformed quartz veins, PAU2011AMB-137, West area. Hammer pointed toward North.

The lithogeochemistry program for evaluating the context of mineralization in the area proved to be efficient. A specific rock type, the porphyritic granodioritte (GDA), is in spatial relationship with gold mineralization. The granodiorite borders a more voluminous intrusion of quartz monzodiorite

composition (QMD). The quartz monzodiorite is generally fresh and characterized by a high magnetic contrast (magnetite bearing suite, Pearson, 2011). The granodiorite is characterized by a low magnetic signature. The low magnetic signature observed toward south-west and north-west of the property may represent the extension of granodiorite intrusion. Futhermore, the granodiorite is affected by a strong and early-stage silicification (calco-sodic alteration), superimposed by a chloritization (ferro-magnesian enrichment) and potassic alteration. The potassic alteration facies corresponds with the highest metal enrichment (Pearson, 2011). Secondary alteration facies are also observed in metasomatized granodiorite such as garnet-sillimanitte-cordierite (aluminous and magnesium enrichment) and fuchsite (chrome enrichment). At first view and on the basis of lithogeochemistrical data, gold mineralization is related to a single unit, the granodiorite. The WRA sampling program also defined a mafic-ultramafic unit, a gabbronorite-pyroxenite dyke. This unit is in close relationship with altered and/or gold-bearing zones. This mafic-ultramafic dyke could represent deep fractures or crustal scale fault and probably pre-existing anisotropy for hydrothermal circulation?

Picture 33 could summarize the observations made during 2011 summer campaign. The central intrusive complex (quartz monzodiorite Mg-bearing) is relatively homogeneous, granoblastic, poorly mineralized and affected by a regional schistosity (Pearson and Lavoie, 2011). Molded around this complex, we observe an older? feldspar porphyry diorite to granodiorite forming a 15 km long favorable unit and high level intrusive complex. The presence of mafic-ultramafic dykes along the same trend points to some asthenospheric input through crustal scale fault (Pearson and Lavoie, 2011). Pau porphyry suite has been affected by hydrothermal alteration, brecciation and mineralization represented and observed by numerous showings along this fertile "corridor".

During deformation, stress has been focused on altered rocks, already softened by alteration or migmatization (Pearson and Lavoie, 2011). At regional scale, from north to south and along LPDZ, we observed a shift from "S"-shape to a "Z"-shape drag fold. Lineations are oriented toward NW in north and toward SW in south. When you are directly inside shear zone (generally associated with altered and/or mineralized zone), conflicting shear sense indicators are noted. The deformation is too intense to allow interpreting the orientation of σ_1. We suggest, in first of all, that the central intrusive complex acted as a buttress and partitioned the deformation style. In second hand, the heterogeneity inside altered and mineralized granodiorite acted equally as a buttress and partitioned deformation style. It is probably why the "homogeneous" intrusion is now so much heterogeneous (alteration-deformation-metamorphism impregnation) and why the protolith is locally so difficult to identify. Field observations suggest strongly that deformation superposed alteration and mineralization in Pau porphyry.

The large heliborne high resolution aeromagnetic survey done during fall 2011 shows the continuity of magnetic contrast to the south and to the north of the Lac Pau property. Furthermore, this area is poorly prospected. The "Z"-shape fold observed to the north of the property (Picture 2) could duplicate favorable horizons inside Pau porphyry intrusion.

ITEM 22 – RECOMMENDATIONS

Recommendations for future exploration campaign are:

GEOLOGY:

- Define the geometry of Pau porphyry (granodiorite);
- Prospecting the south, the west and the north parts of the property (magnetic contrast);
- Define geometry of the different alteration halos (silicic, chloritic, potassic, sericitic, pyritic, aluminous);
- Define high migmatism area in granodiorite. Migmatism can be spatially associated with alteration halo.
- Mapping of mafic-ultramafic dykes. Those dykes could represents the limits between two structural and lithological domains in close relationship with alteration and mineralization;
- Rigorous structural survey, especially outside the LPDZ. Data collected outside LPDZ will help understand the regional constrains;
- Pursue detail mapping of major showings to eventually produce kinematic indicators maps (domains of dextral, senestral, dip slip movement, riedel system, etc.);
- Define the syenitic intrusion of Cu-Hébert area (if the intrusion is episyenite, potassic alteration associated with Cu mineralization could be interesting);
- Verify all occurrences of alteration, especially sillimanite-cordierite-silica alterations, all over the property.

GEOCHEMISTRY:

- Develop an extensive WRA program (database) to (1) verify chemical variations relative to alterations and (2) identify chemical signature of the batholit (especially to define porphyry granodiorite);
- A large till survey over the south part of the property (picture 48);

GEOPHYSIC:

- A high definition magnetic survey (75 meters line spacing) to complete coverage of the core of the intrusion (the quartz monzodiorite complex) and the west part of the property;
- Induced polarization survey along high-low magnetic contrast.

DRILLING:

- Drilling program (3 000 to 5 000 meters) to test Hope-Jedi extension and Jedi altered "corridor" (drillhole spacing about 250 meters).

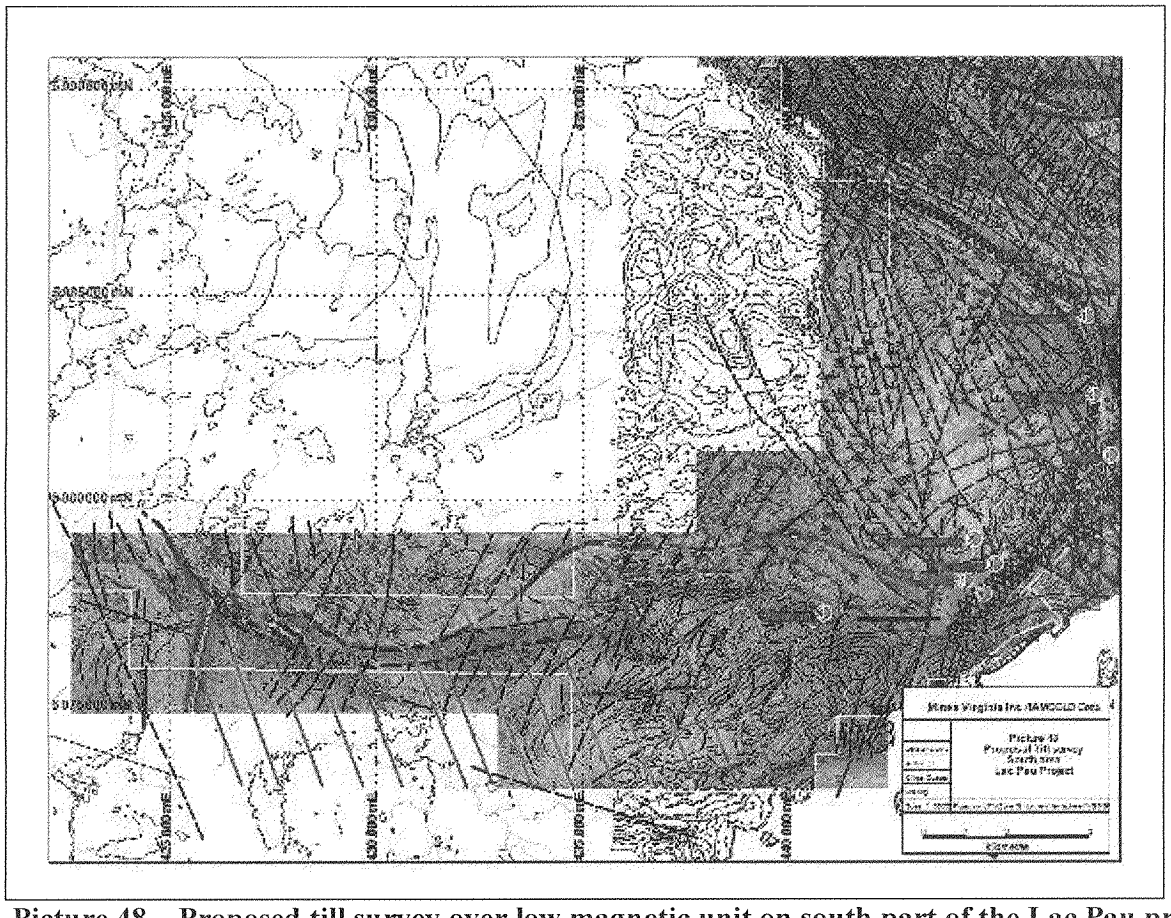

Picture 48 – Proposed till survey over low magnetic unit on south part of the Lac Pau property (red lines represent till survey, sample spacing = 250 m).

ITEM 23 – REFERENCES

BEAUMIER, M., 1987. Géochimie des sédiments de lac, région de la rivière Caniapiscau. Ministère de l'Énergie et des Ressources, Québec; DP 86-23.

BÉLANGER, M., 1987. L'or dans la région de Schefferville. Ministère de l'Énergie et des Ressources, Québec; PRO 86-23.

CHEVÉ, S. et BROUILLETTE, P., 1995. Géologie et métallogénie de la partie nord-est de la Sous-province d'Ashuanipi (Nouveau-Québec) – Carte synthèse – 23J, 23K, 23N et 23O. Ministère des Ressources Naturelles, Québec; MM 95-01, carte synthèse au 1/100 000.

CHOINIÈRE, J., LAMOTHE, D. et CLARK, T., 1995. Cibles d'exploration géochimiques dans le Moyen-Nord québécois, secteur Caniapiscau-Ashuanipi. Ministère des Ressources Naturelles, Québec; PRO-95-05.

DAVID, J., MAURICE, C. et SIMARD, M., 2009. Datations isotopiques effectuées dans le nord-est de la Province du Supérieur, travaux de 1999, 2000 et 2001. Ministère des Ressources naturelles et de la Faune, Québec; DV 2009-05.

GOSSELIN, C. et SIMARD, M., 2000. Géologie de la région du lac Gayot (SNRC 23M). Ministères des Ressources naturelles, Québec; RG 99-06, 29 pages.

LAVOIE, J., SAVARD, M. et ARCHER, P., 2007. Rapport techniques et Recommandations, Programme de Reconnaissance, Projet Lac Pau. Ministère des Ressources naturelles et de la Faune, Québec; GM 63498.

LAVOIE, J., SAVARD, M. et ARCHER, P., 2008. Rapport techniques et Recommandations, rapport 43-101, programme de Reconnaissance, Projet Lac Pau. Ministère des Ressources naturelles et de la Faune, Québec; GM 63495.

LAVOIE, J., ARCHER, P., 2010, Technical Report and Recommandations, 2009 Exploration Program, Lac Pau Project, Québec, 442 pages and maps.

LAVOIE, J., ARCHER, P., 2010, Technical Report and Recommandations, Winter 2010 Drilling Program, Lac Pau Project, Québec, 747 pages and maps.

LAVOIE, J., ROY, I., LÉVESQUE, J-A. and ARCHER, P., 2011. Technical Report and Recommendations, Winter 2011 Drilling Program, Lac Pau Project, Quebec. In deposition Ministère dees Ressources Naturelles et de la Faune.

MORITZ, R.P. and CHEVÉ, S.R., 1992. Fluid inclusion studies of high-grade metamorphic rocks of the Ashuanipi complex, eastern Superior Province: constraints on the retrograde P-T path and implication for gold metallogeny. Journal canadien des Sciences de la Terre, volume 29, pages 2309-2327.

PEARSON, V., 2011. Lac Pau Project, Lithogeochemical Interpretation. Virginia Mines Inc. Internal Report, 21 pages.

PEARSON, V. and LAVOIE, J., 2011. Field visit report, lac Pau Project. Some Geological observations. Virginia Mines Inc. Internal Report, 33 pages.

PERCIVAL, J.A., 1993. Géologie, Complexe d'Ashuanipi, région de Schefferville, Terre-Neuve-Québec. Commission Géologique du Canada ; carte 1785A, échelle 1 :125 000.

SAVARD, M. and LÉVESQUE, J.-A., 2011. Technical Report and Recommendations, Summer-Fall 2010 Exploration Program, Lac Pau Project, Quebec. Ministère des Ressources naturelles et de la Faune, Québec, GM-65714, 471 pages and 29 plans.

SDBJ, 1978. Cartes géochimiques des sédiments de lac de la région de la Baie James. Ministère des Ressources naturelles, Québec ; GM-34039.

SIMARD, M., 2008. Stratigraphie et géochronologie du nord-est de la Province du Supérieur. Dans : Synthèse du nord-est de la Province du Supérieur, M. Simard (coordonnateur). Ministère des Ressources naturelles et de la Faune, Québec ; RG 2009-02, 196 pages.

SIMARD, M., GOSSELIN, C., et LAFRANCE, I., 2009a. Géologie de la région de la rivière Sérigny (SNRC 24C et 23N). Ministère des ressources naturelles et de la Faune, Québec ; RG 2009-02, 38 pages.

SIMARD, M., PARENT, M., PAQUETTE, L. et LAFRANCE, I., 2009b. Géologie de la région du réservoir de Caniapiscau (SNRC 23K-23N). Ministère des Ressources naturelles et de la Faune, Québec, 37 pages ; RG 2009-04.

THÉRIAULT, R. et CHEVÉ, S., 2001. Géologie de la région du lac Hurault (SNRC 23L). Ministère des Ressources naturelles, Québec ; RG 2000-11, 49 pages.

TREMBLAY, L. Étude pétrographique de trois échantillons de roche, Projet Lac Pau. Rapport interne produit par IOS Services Géoscientifiques Inc, 28 pages.

SHARMA, K.N.M., 1996. Légende générale de la carte géologique ; édition revue et augmentée. Ministère des Ressources Naturelles ; MB 96-28.

TSHIMBALANGA, S., 2010, Levés de polarisation provoquées et de magnétométrie, Propriété du Lac Pau, Secteur Grid W2010, Région de la Baie-James, MRC Caniapiscau,Québec, SNRC 23K/13, Rapport, 24 pages.

ITEM 24 – DATE AND SIGNATURE

CERTIFICATE OF QUALIFICATIONS

I, *Jérôme Lavoie*, resident at 1304 Richard-Turner, Québec, Qc, G1W 3N2, do hereby certify that:

- I am presently employed as a Project Geologist with Virginia Mines Inc., 116 St-Pierre, Suite 200, Québec, Qc, G1K 4A7.
- I have received a B.Sc. in Engineering Geology in 2000 from the *Université du Québec à Chicoutimi* (U.Q.A.C.) and a M. Sc. A. in Economic Geology in 2008 from *Université du Québec à Chicoutimi* (U.Q.A.C.).
- I have been working as a geologist in mineral exploration since 2004.
- I am a professional geologist presently registered to the board of the *Ordre des Ingénieurs du Québec*, permit number #127 127.
- I am a qualified person with respect to the Lac Pau Project in accordance with section 5.1 of the national instrument 43-101.
- I worked in the region since 2006.
- I am responsible for writing the present technical report in collaboration with the other author, utilizing proprietary exploration data generated by Mines Virginia Inc. and information from various authors and sources as summarized in the reference section of this report.
- I am not aware of any missing information or changes, which would have caused the present report to be misleading.
- I do not fulfil the requirements set out in section 5.3 of the National Instrument 43-101 for an «independent qualified person» relative to the issuer being a direct employee of Mines Virginia Inc.
- I have been involved in the Lac Pau project since 2006.
- I have read and used the National Instrument 43-101 and the Form 43-101A1 to make the present report in accordance with their specifications and terminology.

Dated in Québec, Qc, this 2nd day of April 2012.

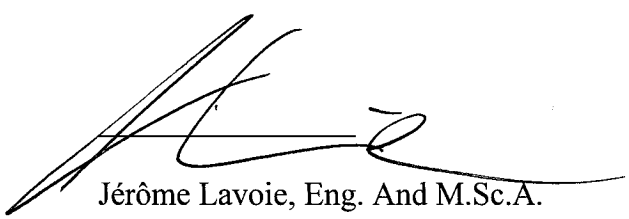

Jérôme Lavoie, Eng. And M.Sc.A.

CERTIFICATE OF QUALIFICATIONS

I, *Josée-Anne Lévesque*, resident at 1212 rang Edmour Lavoie, Ferland-et-Boilleau, Qc, G0V 1H0, hereby certify that:

- I am presently employed as a Geologist in training with Virginia Mines Inc., 116, rue St-Pierre, Suite 200, Québec (Québec), G1K 4A7.
- I received a B.Sc. in Geology in 2009 from *Université du Québec à Chicoutimi* (UQAC).
- I have been working as a mineral exploration geologist since 2009.
- I am a professional geologist presently registered to the board of the *Ordre des Géologues du Québec*, permit number 1442.
- I worked on the Lac Pau project since 2009.
- I am responsible participated to the writing the present technical report in collaboration with the other first author, utilizing proprietary exploration data generated by Virginia Mines Inc. and information from various authors and sources as summarized in the reference section of this report.
- I am not aware of any missing information or changes, which would have caused the present report to be misleading.
- I do not fulfil the requirements set out in section 5.3 of the National Instrument 43-101 for an « independent qualified person » relative to the issuer being a direct employee of Virginia Mines Inc.
- I read and used the National Instrument 43-101 and the Form 43-101A1 to make the present report in accordance with their specifications and terminology.

Dated in Québec, Qc, this 2nd day of April 2012.

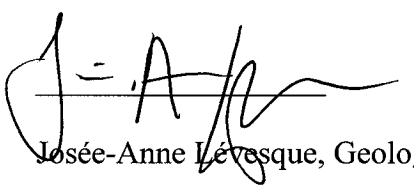

Josée-Anne Lévesque, Geologist in training

CERTIFICATE OF QUALIFICATIONS

I, *Paul Archer*, resident at the 4772 rue du Courlis, St-Augustin-de-Desmaures, Qc, G3A 2B5, hereby certify that:

- I am presently the Vice President, Exploration with Mines Virginia inc., 116 St-Pierre, Suite 200, Québec, Qc, G1K 4A7.
- I received a B.Sc. in Geological Engineering from the Université du Québec à Chicoutimi in 1979 and a M.Sc.A. in Earth Sciences from the Université du Québec à Chicoutimi in 1982.
- I have been working as a professional geologist in exploration since 1980.
- I am an active professional engineer in geology presently registered to the board of the *Ordre des Ingénieurs du Québec*, permit number 36271.
- I am a qualified person with respect to the Lac Pau Project in accordance with section 5.1 of the national instrument 43-101.
- I have already visited the immediate region where the exploration activities were undertaken during summer 2009 and summer 2011.
- In collaboration with the authors, I am responsible for writing the present technical report, utilizing proprietary exploration data generated by Virginia Mines inc. and information from various authors and sources as summarized in the reference section of this report.
- I am not aware of any missing information or change, which would have caused the present report to be misleading.
- I do not fulfil the requirements set out in section 5.3 of the National Instrument 43-101 for an «independant qualified person» relative to the issuer being a direct employee of Virginia Mines inc.
- I have been involved in the Lac Pau project since 2006.
- I read and used the National Instrument 43-101 and the Form 43-101A1 to make the present report in accordance with their specifications and terminology.

Dated in Québec, Qc, this 2nd day of April 2012.

Paul Archer, M.Sc., P. Eng.

ITEM 25 – ADDITIONAL REQUIREMENTS FOR TECHNICAL REPORTS ON DEVELOPMENT PROPERTIES AND PRODUCTION PROPERTIES

This section is not applicable to this report.

ITEM 26 – ILLUSTRATIONS

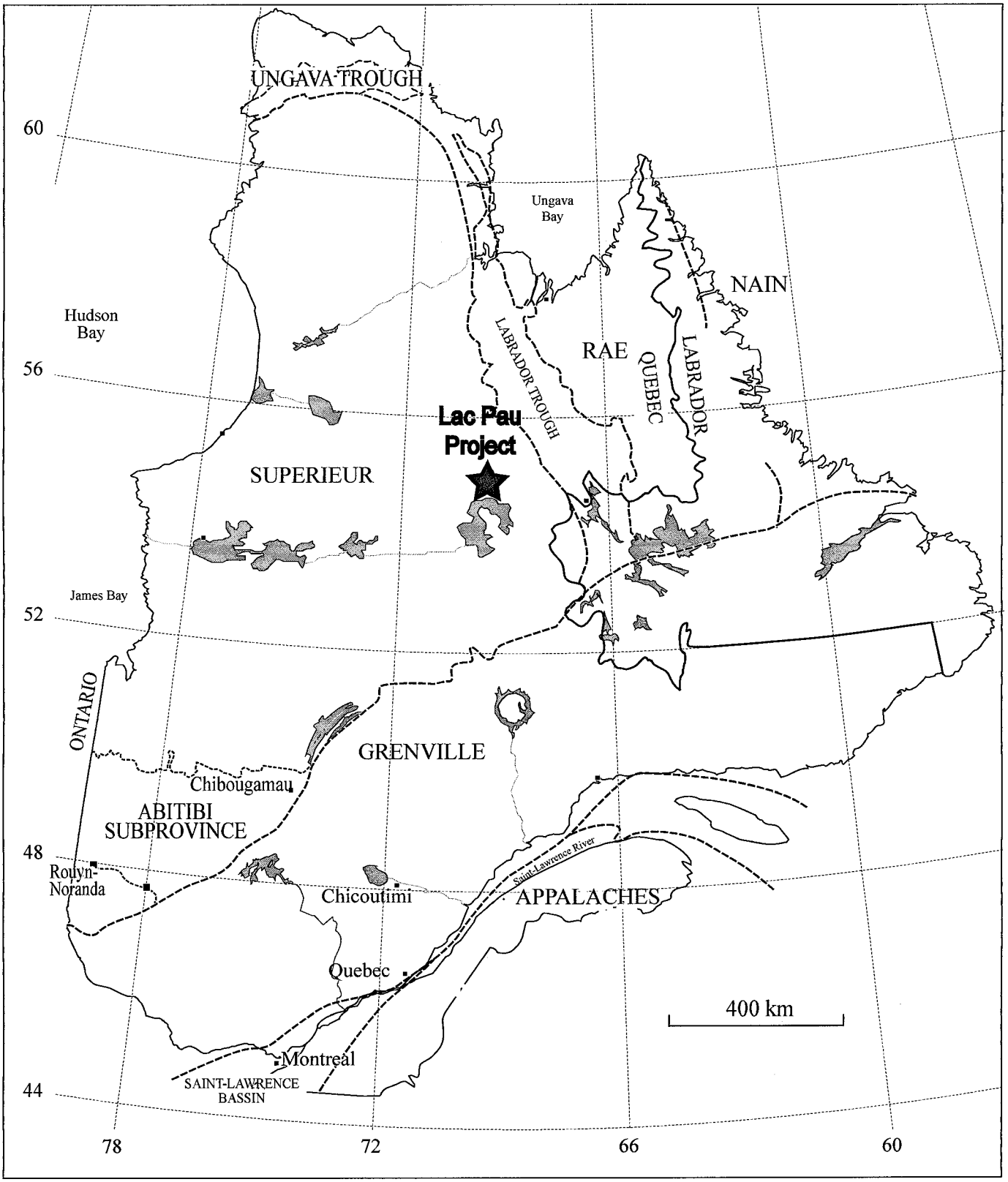

Figure 1 : Lac Pau project location

420000 mE

430000 mE

440000 mE

450000 mE

6095000 mN

6085000 mN

6075000 mN

Legend

- Claim
- Gravel road
- Dam
- Airstrip

Virginia Gold Mines

Figure 2
Lac Pau project 2011
Claims and facilities location

Date: 1/6/2011	
Author:	
Office: Quebec City	
Drawing:	
Scale: 1:150000	Projection: UTM Zone 19 (NAD 83)

0 1.25 2.5 5

kilometres

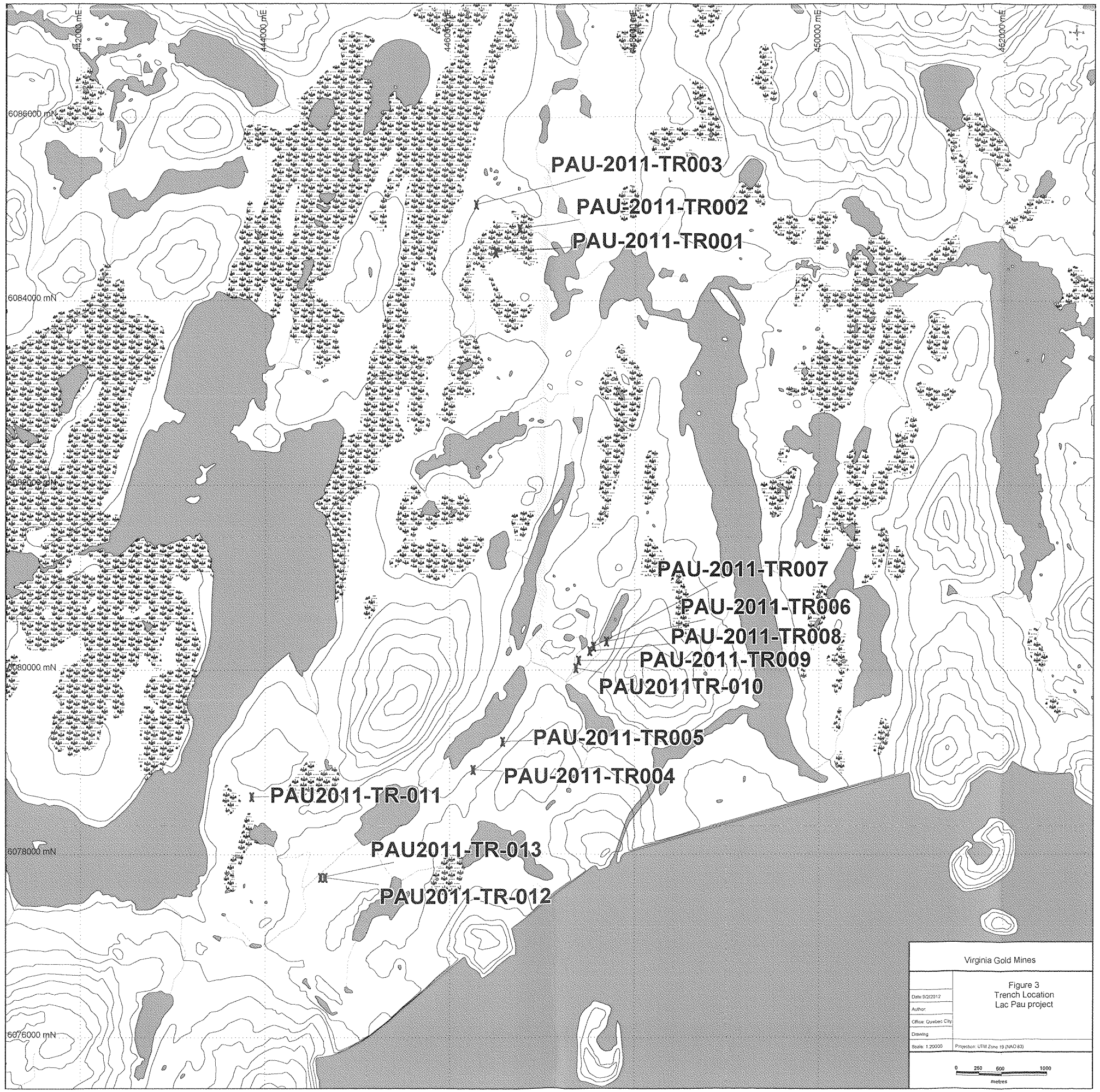
442000 mE
444000 mE
446000 mE
448000 mE
450000 mE
452000 mE
6086000 mN
6084000 mN
6082000 mN
6080000 mN
6078000 mN
6076000 mN
PAU-2011-TR003
PAU-2011-TR002
PAU-2011-TR001
PAU-2011-TR007
PAU-2011-TR006
PAU-2011-TR008
PAU-2011-TR009
PAU2011TR-010
PAU-2011-TR005
PAU-2011-TR004
PAU2011-TR-011
PAU2011-TR-013
PAU2011-TR-012
Virginia Gold Mines
Figure 3
Trench Location
Lac Pau project
Date: 9/2/2012
Author:
Office: Quebec City
Drawing:
Scale: 1:20000
Projection: UTM Zone 19 (NAD 83)
0 250 500 1000
metres

Geological Legend

Lithology

- Diabase and/or Gabbro
- Magnetic Monzo-diorite
- Monzo-diorite
- Monzo-diorite orthogneiss
- Granodiorite to granodioritic orthogneiss, low MAG
- Granodiorite à to granodioritic orthogneiss
- Tonalite
- Pegmatite
- Diatexite
- Gabbronorite

Facies

- Massive to foliated
- Porphyritic
- Protomylonitic
- Gneissic

Metasomatic unit

- Sillimanite-Chlorite-Silica alteration
- Garnet alteration
- Chlorite-K-Feldspars-Silica-Biotite±Fluorite alteration

Hydrothermalism

- Quartz vein
- Leucosome

Mineralization

- Gold-Bearing zone

Legend

- Major Showing
- NE-SW and NW-SE discontinuity
- E-W discontinuity
- Major Shear Zone
- Magnetic continuity
- Lac Pau Property
- HQ Dam
- Airstrip landing
- Gravel road

Altered granodiorite

N
W E
S

6 085 000 mN
6 080 000 mN
6 075 000 mN
6 078 000 mN

425 000 mE
430 000 mE
435 000 mE
440 000 mE
445 000 mE

Mines Virginia Inc. / IAMGOLD Corp.

Lac Pau Project
Geological interpretation
and IP location
Summer 2011

Date: 23/3/2012
Author: IS
Office: Quebec
Drawing:
Scale: 1:20000
Projection: NTM Zone 19 Nadbum Hemisphere (NAD83)

0 0.5 1 2
kilometres

Légende

× Outcrop

Virginia Gold Mines

Figure 5
Outcrops location
Lac Pau project

Date: 21/02/19
Author:
Drawing:
Scale: 1:5000
Projection: UTM Zone 19 (NAD 83)

0 25 50 75 100
Kilometers

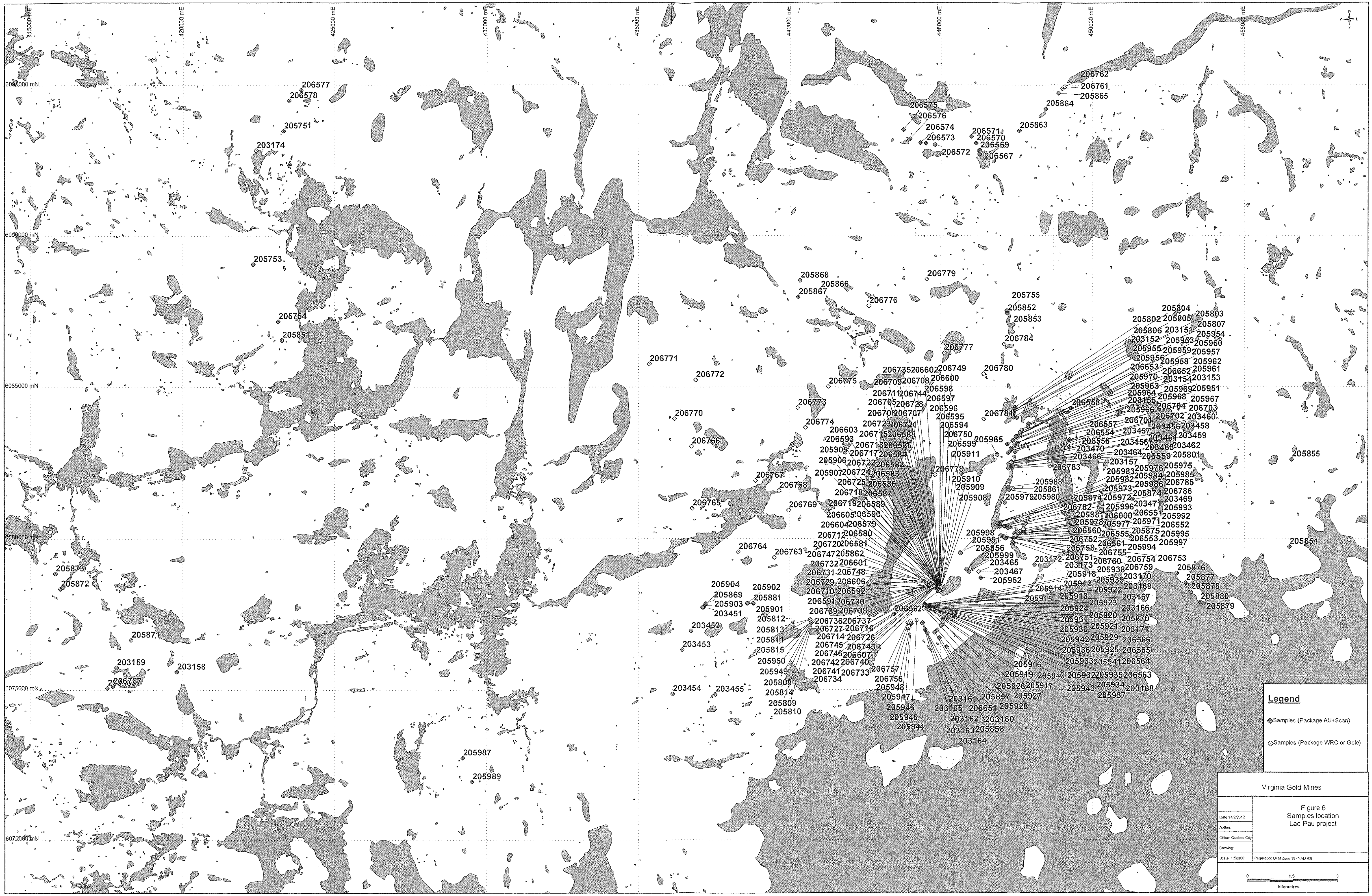

Legend
Samples (Package AU+Scan)
Samples (Package WRC or Gole)
Virginia Gold Mines
Figure 6
Samples location
Lac Pau project
Date 14/2/2012
Author:
Office: Quebec City
Drawing:
Scale: 1:50000
Projection: UTM Zone 18 (NAD 83)
Kilometres
420000 mE
425000 mE
430000 mE
435000 mE
440000 mE
445000 mE
450000 mE
455000 mE
6085000 mN
6075000 mN
205753
205754
205851
205751
203174
206577
206578
206771
206772
206770
206766
206765
206764
206763
205987
205989
205855
205854
203454
203455
203452
203453
203451
205871
203158
203159
205873
205872

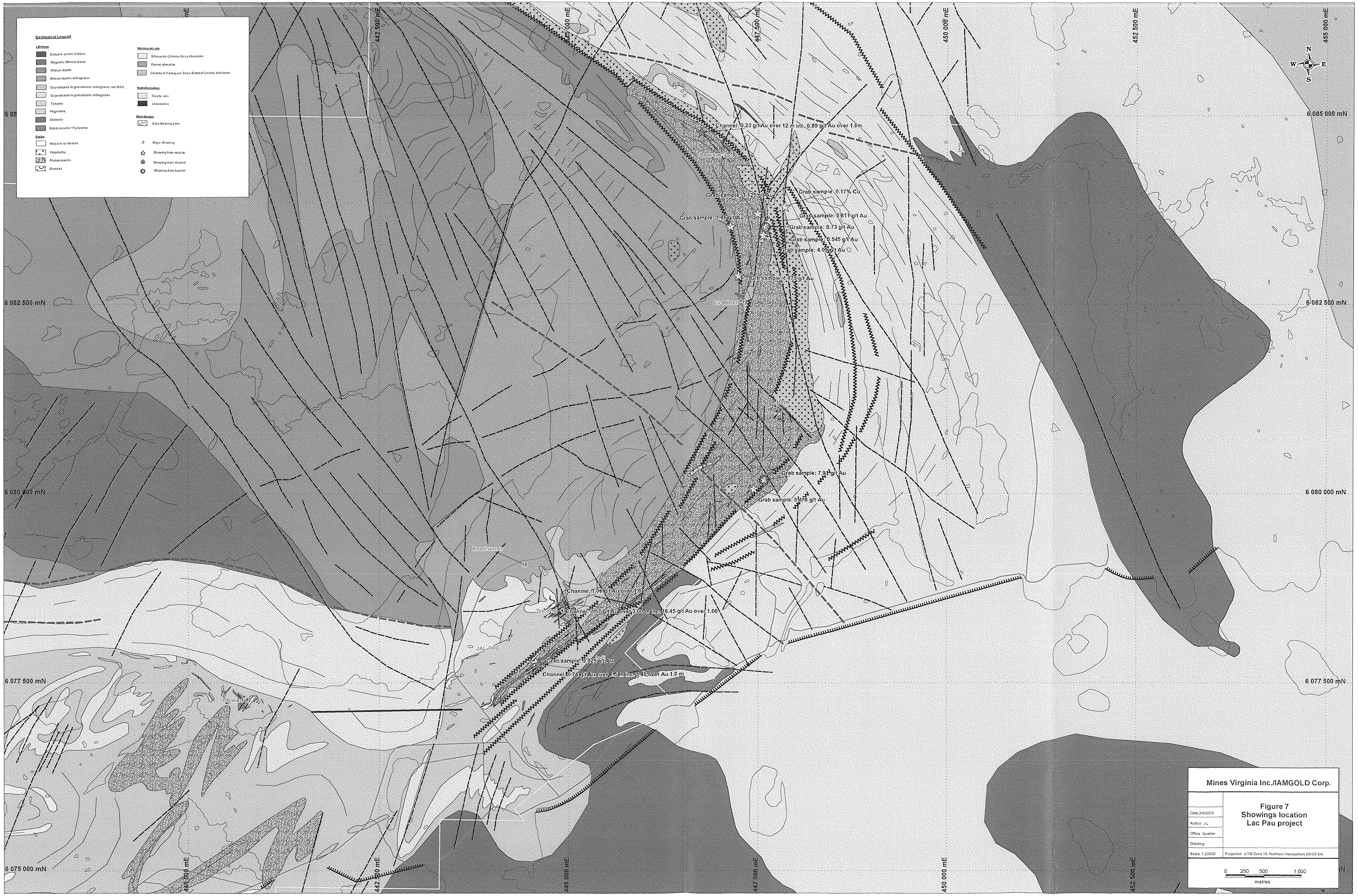
Mines Virginia Inc./IAMGOLD Corp.
Figure 7
Showings location
Lac Pau project
Date:2/4/2012
Author: J.L
Office: Quebec
Drawing
Scale. 1:20000
Projection UTM Zone 19, Northern Hemisphere (WGS 84)
0 250 500 1 000
metres
Geological Legend
Lithology
Diabase and/or Gabbro
Magnetic Monzo-diorite
Monzo-diorite
Monzo-dioritic orthogneiss
Granodiorite to granodioritic orthogneiss, low MAG
Granodiorite to granodioritic orthogneiss
Tonalite
Pegmatite
Diatexite
Gabbronorite / Pyroxenite
Facies
Massive to foliated
Porphyritic
Protomylonitic
Gneissic
Metasomatic unit
Sillimanite-Chlorite-Silica alterations
Garnet alteration
Chlorite-K-Feldspars-Silica-Biotite±Fuschite alterations
Hydrothermalism
Quartz vein
Leucosome
Mineralization
Gold-Bearing zone
Major Showing
Showing from outcrop
Showing from channel
Showing from boulder
N
W
E
S
Channel: 0.23 g/t Au over 12 m inc. 0.89 g/t Au over 1.0m
Beausac 2
Grab sample: 1.125 g/t Au
Grab sample: 0.17% Cu
Grab sample: 1.46 g/t Au
Grab sample: 0.811 g/t Au
Grab sample: 8.73 g/t Au
Grab sample: 0.545 g/t Au
Grab sample: 4.09 g/t Au
Grb sample: 1.775 g/t Au
Cu-Hébert
Grab sample: 7.91 g/t Au
Grab sample: 0.478 g/t Au
Roadrunner
Channel: 1.06 g/t Au over 1.0 m
Tricorne
Channel: 7.57 g/t Au over 3.00 m inc. 16.45 g/t Au over 1.00
JAL-PPG
Grab sample: 0.925 g/t Au
Channel 0.74 g/t Au over 6.5 m Inc. 3.48 over Au 1.0 m
442 500 mE
445 000 mE
447 500 mE
450 000 mE
452 500 mE
455 000 mE
6 085 000 mN
6 082 500 mN
6 080 000 mN
6 077 500 mN
6 075 000 mN

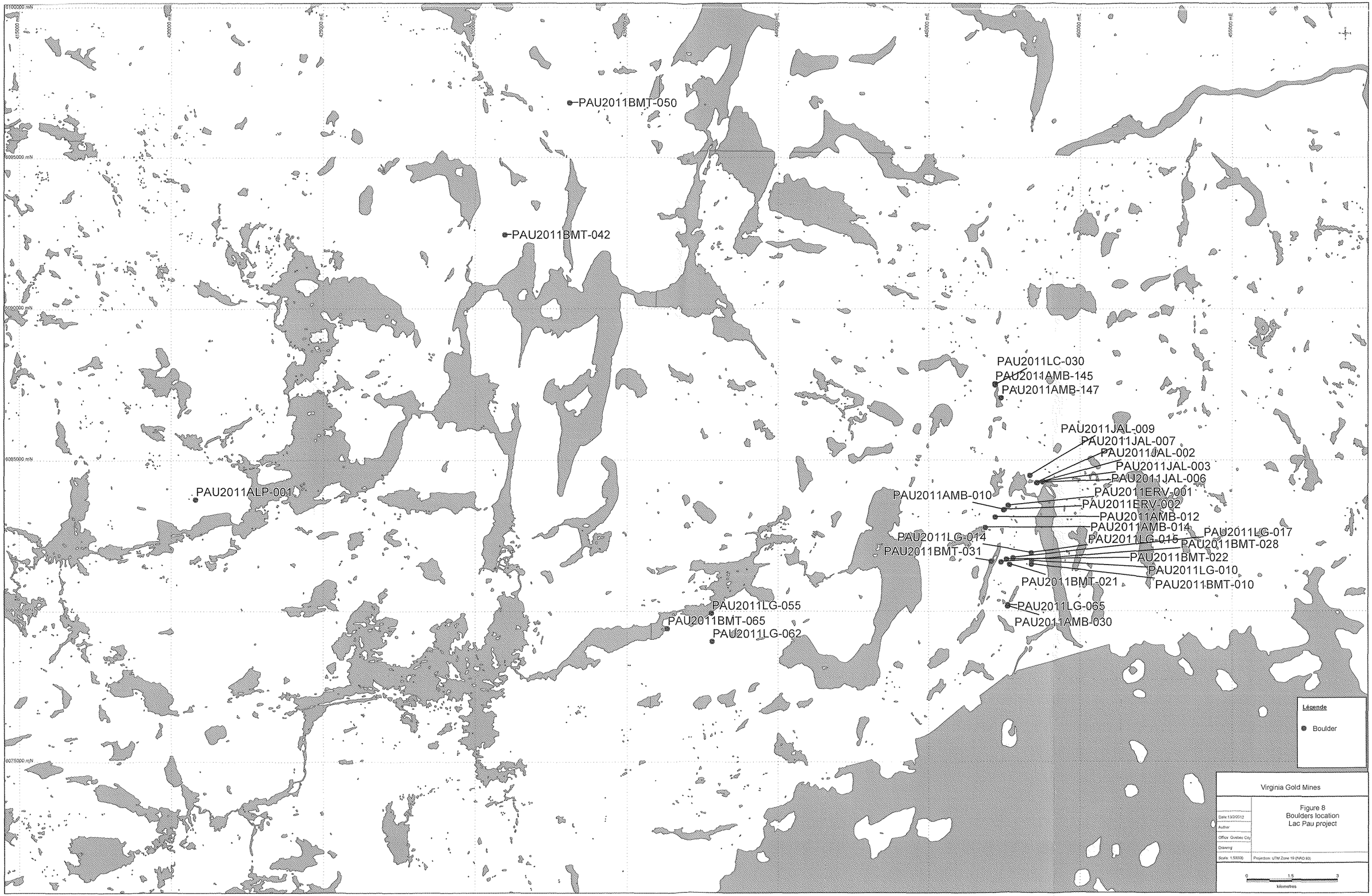
6100000 mN
6095000 mN
6090000 mN
6085000 mN
6080000 mN
6075000 mN
415000 mE
420000 mE
425000 mE
430000 mE
435000 mE
440000 mE
445000 mE
450000 mE
455000 mE
PAU2011BMT-050
PAU2011BMT-042
PAU2011ALP-001
PAU2011LG-055
PAU2011BMT-065
PAU2011LG-062
PAU2011LC-030
PAU2011AMB-145
PAU2011AMB-147
PAU2011JAL-009
PAU2011JAL-007
PAU2011JAL-002
PAU2011JAL-003
PAU2011JAL-006
PAU2011ERV-001
PAU2011AMB-010
PAU2011ERV-002
PAU2011AMB-012
PAU2011AMB-014
PAU2011LG-017
PAU2011LG-014
PAU2011LG-015
PAU2011BMT-028
PAU2011BMT-031
PAU2011BMT-022
PAU2011LG-010
PAU2011BMT-021
PAU2011BMT-010
PAU2011LG-065
PAU2011AMB-030
Légende
Boulder
Virginia Gold Mines
Figure 8
Boulders location
Lac Pau project
Date: 13/2/2012
Author:
Office: Québec City
Drawing:
Scale: 1:50000
Projection: UTM Zone 19 (NAD 83)
0
1.5
3
kilometres

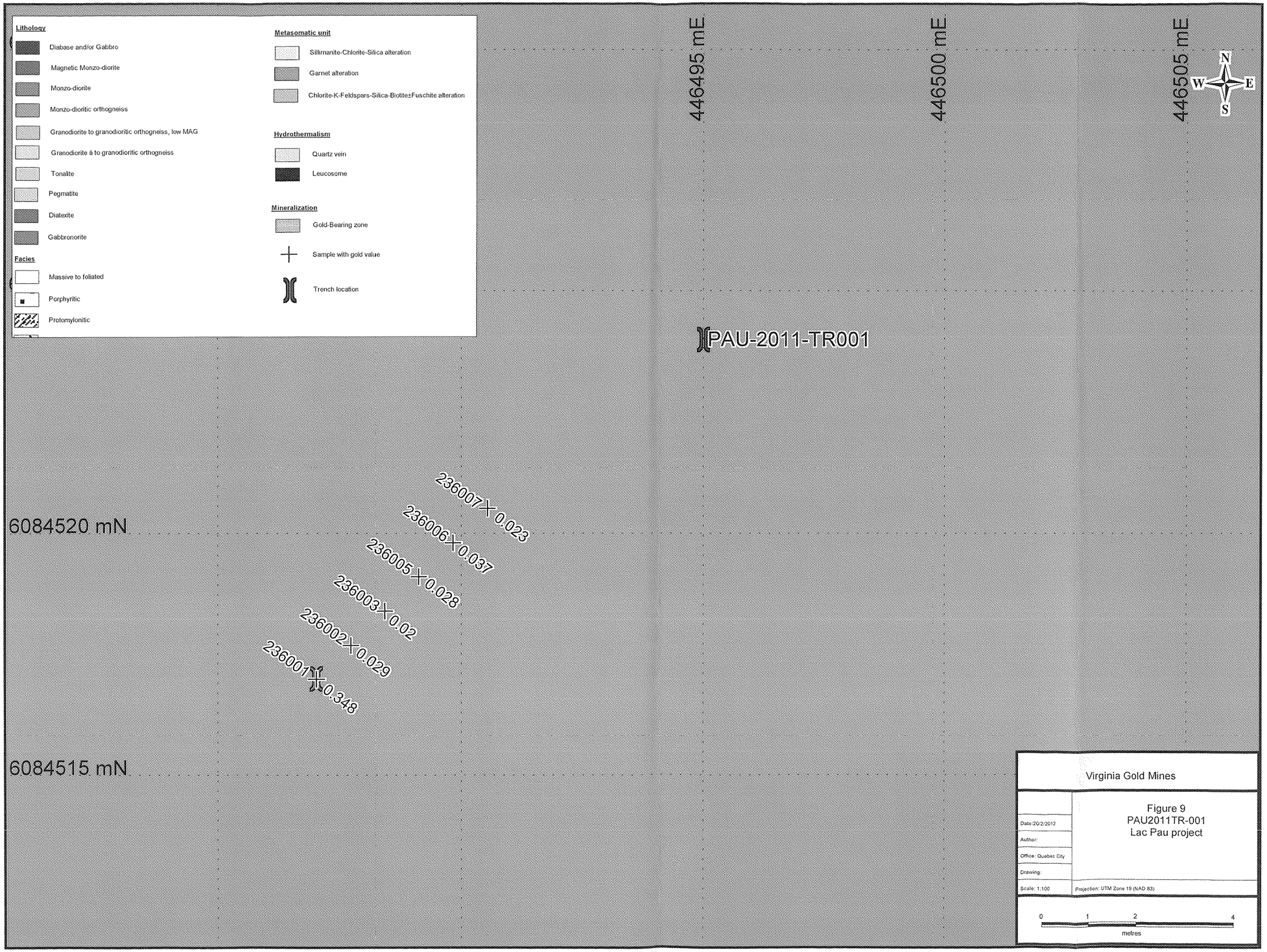
Lithology
Diabase and/or Gabbro
Magnetic Monzo-diorite
Monzo-diorite
Monzo-dioritic orthogneiss
Granodiorite to granodioritic orthogneiss, low MAG
Granodiorite à to granodioritic orthogneiss
Tonalite
Pegmatite
Diatexite
Gabbronorite
Facies
Massive to foliated
Porphyritic
Protomylonitic
Metasomatic unit
Sillimanite-Chlorite-Silica alteration
Garnet alteration
Chlorite-K-Feldspars-Silica-Biotite±Fuschite alteration
Hydrothermalism
Quartz vein
Leucosome
Mineralization
Gold-Bearing zone
Sample with gold value
Trench location
446495 mE
446500 mE
446505 mE
N
W
E
S
PAU-2011-TR001
6084520 mN
6084515 mN
236007 0.023
236006 0.037
236005 0.028
236003 0.02
236002 0.029
236001 0.348
Virginia Gold Mines
Figure 9
PAU2011TR-001
Lac Pau project
Date:20/2/2012
Author:
Office: Quebec City
Drawing:
Scale: 1:100
Projection: UTM Zone 19 (NAD 83)
0
1
2
4
metres

446740 mE
446745 mE
446750 mE
446755 mE
446760 mE

6084785 mN
6084780 mN
6084775 mN
6084770 mN

N
W
E
S

PAU2011R-002

236008 0.01
236009 0.189
236011 0.078
236012 0.891
236013 0.254
236014 0.245
236015 0.232
236016 0.153
236017 0.077
236019 0.085
236020 0.219
236021 0.145
236022 0.125
236023 0.168
236025 0.154

PAU-2011-TR002

Lithology

- Diabase and/or Gabbro
- Magnetic Monzo-diorite
- Monzo-diorite
- Monzo-dioritic orthogneiss
- Granodiorite to granodioritic orthogneiss, low MAG
- Granodiorite à to granodioritic orthogneiss
- Tonalite
- Pegmatite
- Diatexite
- Gabbronorite

Facies

- Massive to foliated
- Porphyritic
- Protomylonitic

Metasomatic unit

- Sillimanite-Chlorite-Silica alteration
- Garnet alteration
- Chlorite-K-Feldspars-Silica-Biotite±Fuschite alteration

Hydrothermalism

- Quartz vein
- Leucosome

Mineralization

- Gold-Bearing zone
- Sample with gold value
- Trench location

Virginia Gold Mines

Figure 10
PAU2011TR-002
Lac Pau project

Date: 20/2/2012
Author:
Office: Quebec City
Drawing:
Scale: 1:100
Projection: UTM Zone 19 (NAD 83)

0 1 2 4
metres

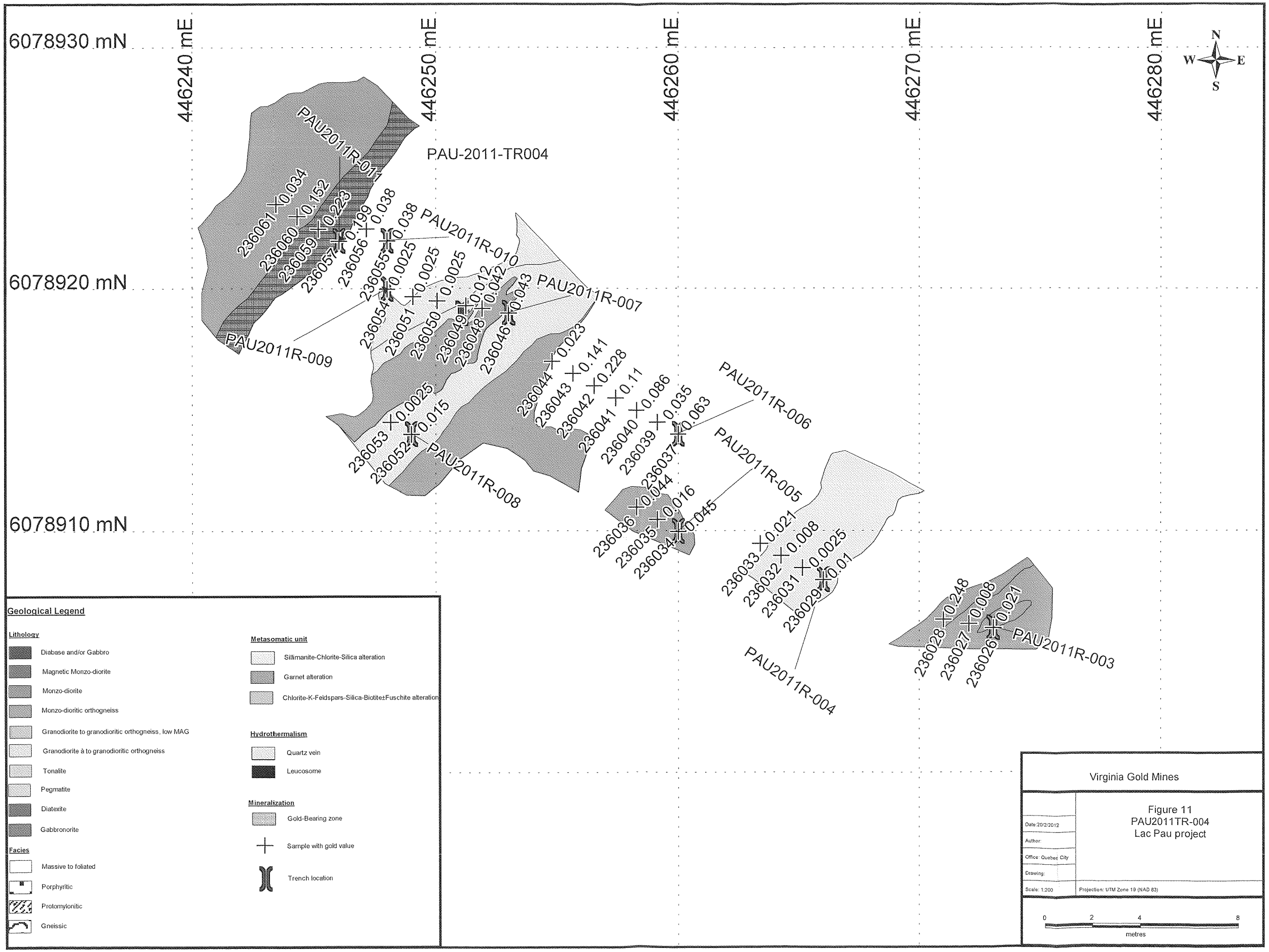
6078930 mN
6078920 mN
6078910 mN
446240 mE
446250 mE
446260 mE
446270 mE
446280 mE
N
W
E
S
PAU-2011-TR004
PAU2011R-011
PAU2011R-010
PAU2011R-009
PAU2011R-007
PAU2011R-008
PAU2011R-006
PAU2011R-005
PAU2011R-004
PAU2011R-003
236061 0.034
236060 0.152
236059 0.223
236057 0.199
236056 0.038
236055 0.038
236054 0.0025
236051 0.0025
236050 0.0025
236049 0.012
236048 0.042
236046 0.043
236044 0.023
236043 0.141
236042 0.228
236041 0.11
236040 0.086
236039 0.035
236037 0.063
236053 0.0025
236052 0.015
236036 0.044
236035 0.016
236034 0.045
236033 0.021
236032 0.008
236031 0.0025
236029 0.01
236028 0.248
236027 0.008
236026 0.021
Geological Legend
Lithology
Diabase and/or Gabbro
Magnetic Monzo-diorite
Monzo-diorite
Monzo-dioritic orthogneiss
Granodiorite to granodioritic orthogneiss, low MAG
Granodiorite à to granodioritic orthogneiss
Tonalite
Pegmatite
Diatexite
Gabbronorite
Facies
Massive to foliated
Porphyritic
Protomylonitic
Gneissic
Metasomatic unit
Sillimanite-Chlorite-Silica alteration
Garnet alteration
Chlorite-K-Feldspars-Silica-Biotite±Fuschite alteration
Hydrothermalism
Quartz vein
Leucosome
Mineralization
Gold-Bearing zone
Sample with gold value
Trench location
Virginia Gold Mines
Figure 11
PAU2011TR-004
Lac Pau project
Date:20/2/2012
Author:
Office: Quebec City
Drawing:
Scale: 1:200
Projection: UTM Zone 19 (NAD 83)
0
2
4
8
metres

446550 mE
446560 mE
446570 mE
446580 mE
446590 mE

N
W E
S

6079240 mN

6079230 mN

PAU2011R-012
PAU2011R-013
PAU2011R-014
PAU2011R-015
PAU2011R-016

236062 0.0025
236063 0.005
236065 0.0025
236066 0.0025
236067 0.0025
236068 0.0025
236069 0.006
236071 0.0025
236072 0.006
236073 0.005

PAU-2011-TR005

Geological Legend

Lithology
- Diabase and/or Gabbro
- Magnetic Monzo-diorite
- Monzo-diorite
- Monzo-dioritic orthogneiss
- Granodiorite to granodioritic orthogneiss, low MAG
- Granodiorite à to granodioritic orthogneiss
- Tonalite
- Pegmatite
- Diatexite
- Gabbronorite

Facies
- Massive to foliated
- Porphyritic
- Protomylonitic
- Gneissic

Metasomatic unit
- Sillimanite-Chlorite-Silica alteration
- Garnet alteration
- Chlorite-K-Feldspars-Silica-Biotite±Fuschite altera

Hydrothermalism
- Quartz vein
- Leucosome

Mineralization
- Gold-Bearing zone
- Sample with gold value
- Trench location

Virginia Gold Mines

Figure 12
PAU2011TR-005
Lac Pau project

Date: 20/2/2012
Author:
Office: Quebec City
Drawing:
Scale: 1:200
Projection: UTM Zone 19 (NAD 83)

0 2 4 8
metres

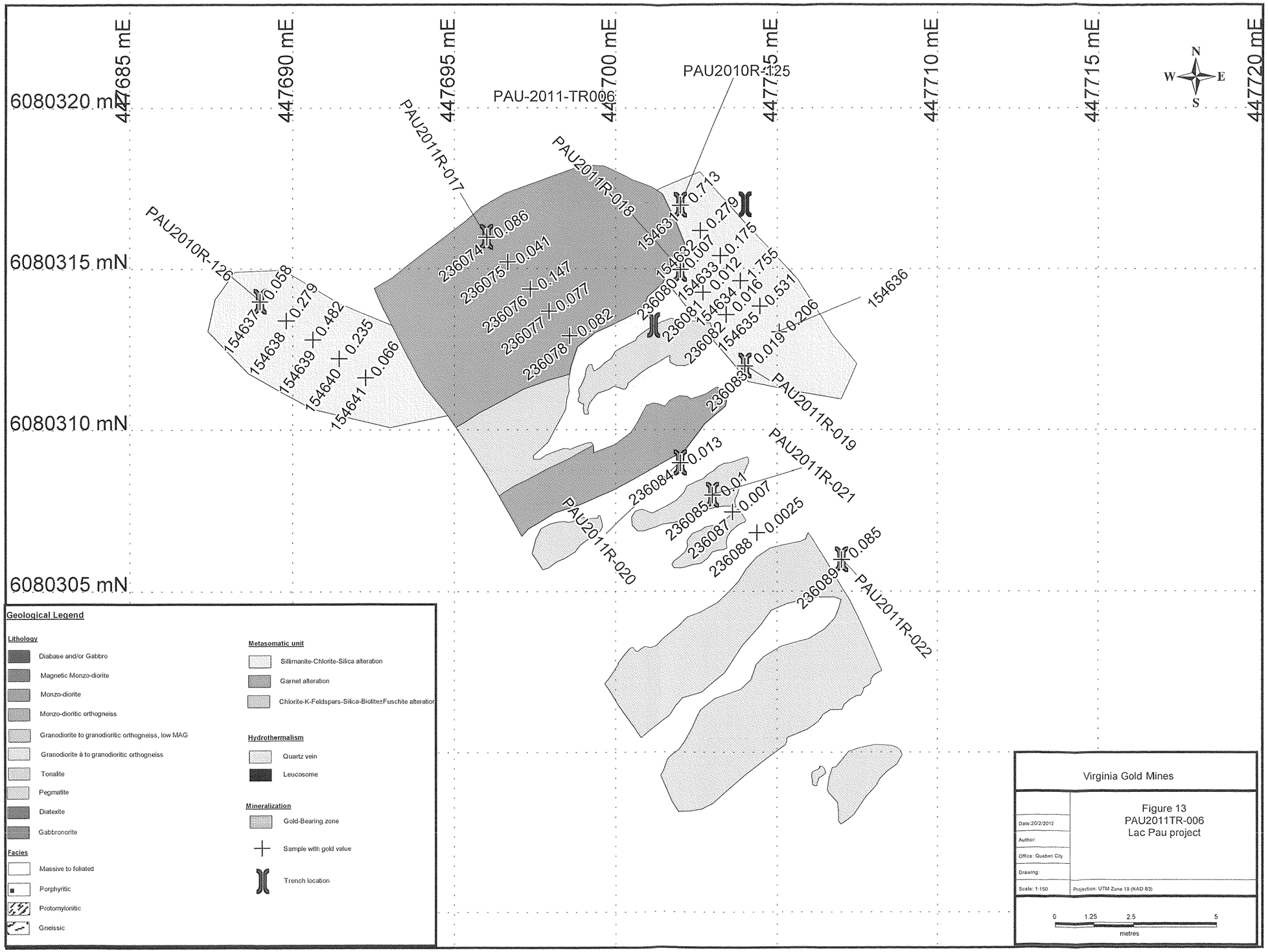
447685 mE
447690 mE
447695 mE
447700 mE
447705 mE
447710 mE
447715 mE
447720 mE
6080320 mN
6080315 mN
6080310 mN
6080305 mN
N
W
E
S
PAU2010R-125
PAU-2011-TR006
PAU2011R-017
PAU2011R-018
PAU2010R-126
154631 0.713
236074 0.086
154632 0.279
236075 0.041
154633 0.175
236076 0.147
236080 0.007
154634 0.012
236077 0.077
236081 0.016
154636 1.755
236078 0.082
154637 0.058
236082 0.531
154638 0.279
154635 0.206
154639 0.482
236083 0.019
154640 0.235
PAU2011R-019
154641 0.066
236084 0.013
PAU2011R-021
236085 0.01
236087 0.007
PAU2011R-020
236088 0.0025
236089 0.085
PAU2011R-022
Geological Legend
Lithology
Diabase and/or Gabbro
Magnetic Monzo-diorite
Monzo-diorite
Monzo-dioritic orthogneiss
Granodiorite to granodioritic orthogneiss, low MAG
Granodiorite à to granodioritic orthogneiss
Tonalite
Pegmatite
Diatexite
Gabbronorite
Facies
Massive to foliated
Porphyritic
Protomylonitic
Gneissic
Metasomatic unit
Sillimanite-Chlorite-Silica alteration
Garnet alteration
Chlorite-K-Feldspars-Silica-Biotite±Fuschite alteration
Hydrothermalism
Quartz vein
Leucosome
Mineralization
Gold-Bearing zone
Sample with gold value
Trench location
Virginia Gold Mines
Figure 13
PAU2011TR-006
Lac Pau project
Date:20/2/2012
Author:
Office: Quebec City
Drawing:
Scale: 1:150
Projection: UTM Zone 19 (NAD 83)
0
1.25
2.5
5
metres

447565 mE
447570 mE
447575 mE
447580 mE
447585 mE
447590 mE

6080255 mN

6080250 mN

6080245 mN

PAU-2011-TR007

236100 0.009
236098 0.027
236097 0.005
236096 0.007

PAU2011R-025

236095 0.0025
236094 0.0025

PAU2011R-024

236092 0.005
236091 0.0025
236090 0.0025

PAU2011R-023

N
W
E
S

Geological Legend

Lithology
- Diabase and/or Gabbro
- Magnetic Monzo-diorite
- Monzo-diorite
- Monzo-dioritic orthogneiss
- Granodiorite to granodioritic orthogneiss, low MAG
- Granodiorite à to granodioritic orthogneiss
- Tonalite
- Pegmatite
- Diatexite
- Gabbronorite

Facies
- Massive to foliated
- Porphyritic
- Protomylonitic
- Gneissic

Metasomatic unit
- Sillimanite-Chlorite-Silica alteration
- Garnet alteration
- Chlorite-K-Feldspars-Silica-Biotite±Fuschite alter

Hydrothermalism
- Quartz vein
- Leucosome

Mineralization
- Gold-Bearing zone
- Sample with gold value
- Trench location

Virginia Gold Mines

Figure 14
PAU2011TR-007
Lac Pau project

Date:20/2/2012
Author:
Office: Quebec City
Drawing:
Scale: 1:100
Projection: UTM Zone 19 (NAD 83)

0 1 2 4
metres

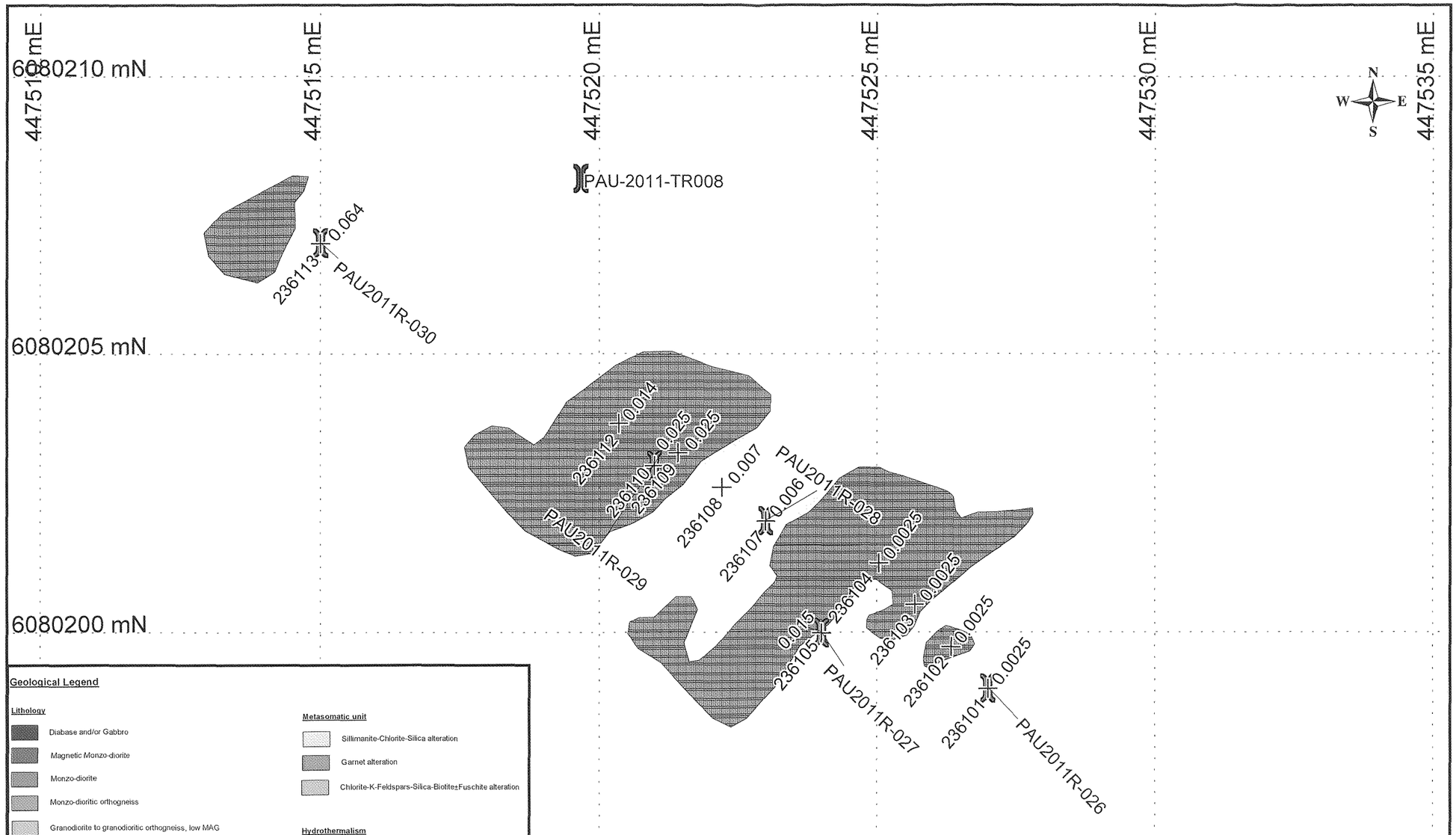

Geological Legend

Lithology

- Diabase and/or Gabbro
- Magnetic Monzo-diorite
- Monzo-diorite
- Monzo-dioritic orthogneiss
- Granodiorite to granodioritic orthogneiss, low MAG
- Granodiorite à to granodioritic orthogneiss
- Tonalite
- Pegmatite
- Diatexite
- Gabbronorite

Facies

- Massive to foliated
- Porphyritic
- Protomylonitic
- Gneissic

Metasomatic unit

- Sillimanite-Chlorite-Silica alteration
- Garnet alteration
- Chlorite-K-Feldspars-Silica-Biotite±Fuschite alteration

Hydrothermalism

- Quartz vein
- Leucosome

Mineralization

- Gold-Bearing zone
- Sample with gold value
- Trench location

Virginia Gold Mines

Figure 15
PAU2011TR-008
Lac Pau project

Date:20/2/2012
Author:
Office: Quebec City
Drawing:
Scale: 1:100
Projection: UTM Zone 19 (NAD 83)

0 1 2 4
metres

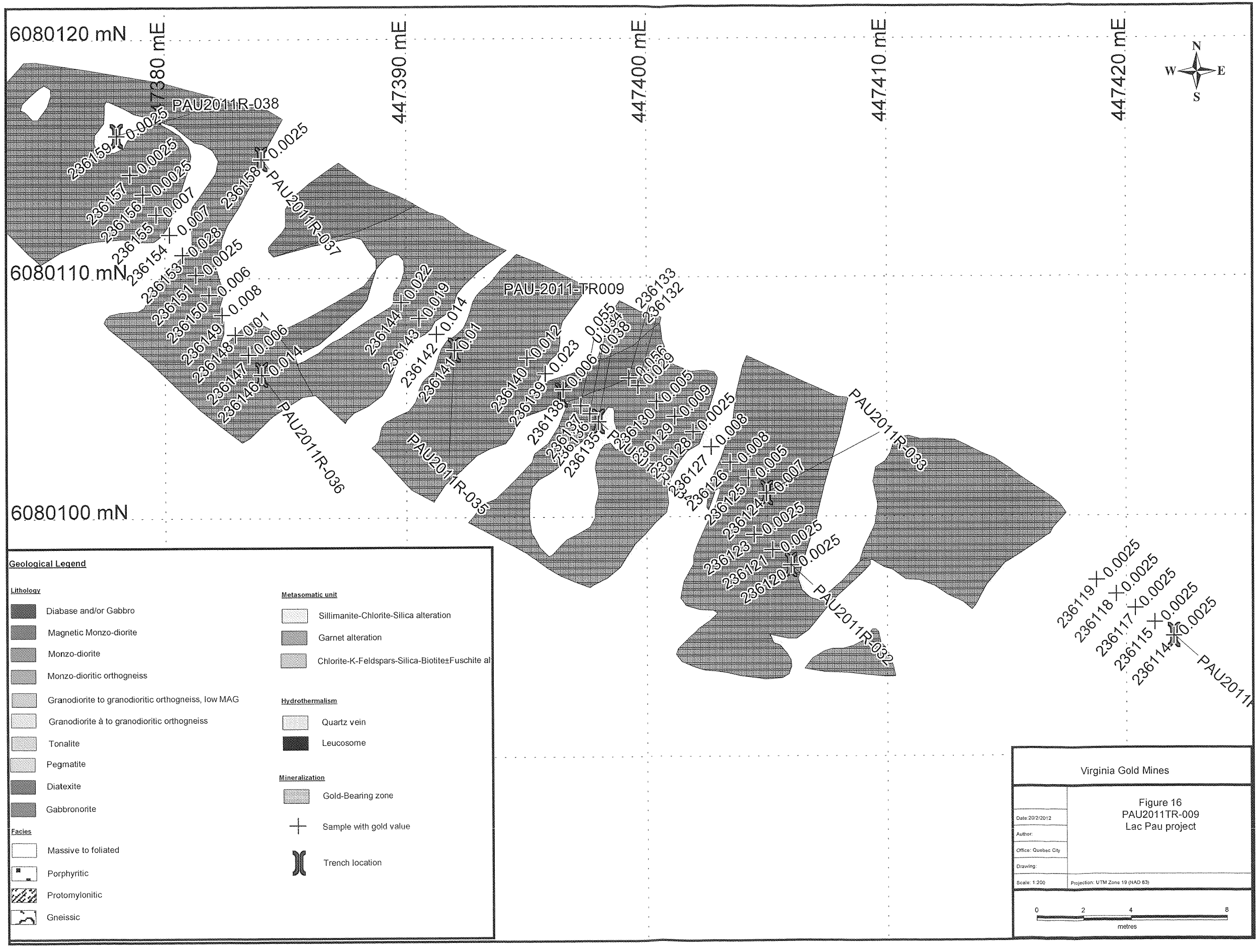
6080120 mN
6080110 mN
6080100 mN
447380 mE
447390 mE
447400 mE
447410 mE
447420 mE
N
W
E
S
PAU2011R-038
PAU2011R-037
PAU2011R-036
PAU2011R-035
PAU2011R-034
PAU2011R-033
PAU2011R-032
PAU-2011-TR009
236159 0.0025
236158 0.0025
236157 0.0025
236156 0.0025
236155 0.007
236154 0.007
236153 0.028
236152 0.0025
236151 0.006
236150 0.008
236149 0.01
236148 0.006
236147 0.014
236146 0.014
236144 0.022
236143 0.019
236142 0.014
236141 0.01
236140 0.012
236139 0.023
236138 0.006
236137 0.038
236136 0.031
236135 0.055
236133
236132
0.029
0.156
236130 0.005
236129 0.009
236128 0.0025
236127 0.008
236126 0.008
236125 0.005
236124 0.007
236123 0.0025
236121 0.0025
236120 0.0025
236119 0.0025
236118 0.0025
236117 0.0025
236115 0.0025
236114 0.0025
Geological Legend
Lithology
Diabase and/or Gabbro
Magnetic Monzo-diorite
Monzo-diorite
Monzo-dioritic orthogneiss
Granodiorite to granodioritic orthogneiss, low MAG
Granodiorite à to granodioritic orthogneiss
Tonalite
Pegmatite
Diatexite
Gabbronorite
Facies
Massive to foliated
Porphyritic
Protomylonitic
Gneissic
Metasomatic unit
Sillimanite-Chlorite-Silica alteration
Garnet alteration
Chlorite-K-Feldspars-Silica-Biotite±Fuschite al
Hydrothermalism
Quartz vein
Leucosome
Mineralization
Gold-Bearing zone
Sample with gold value
Trench location
Virginia Gold Mines
Figure 16
PAU2011TR-009
Lac Pau project
Date:20/2/2012
Author:
Office: Quebec City
Drawing:
Scale: 1:200
Projection: UTM Zone 19 (NAD 83)
0
2
4
8
metres

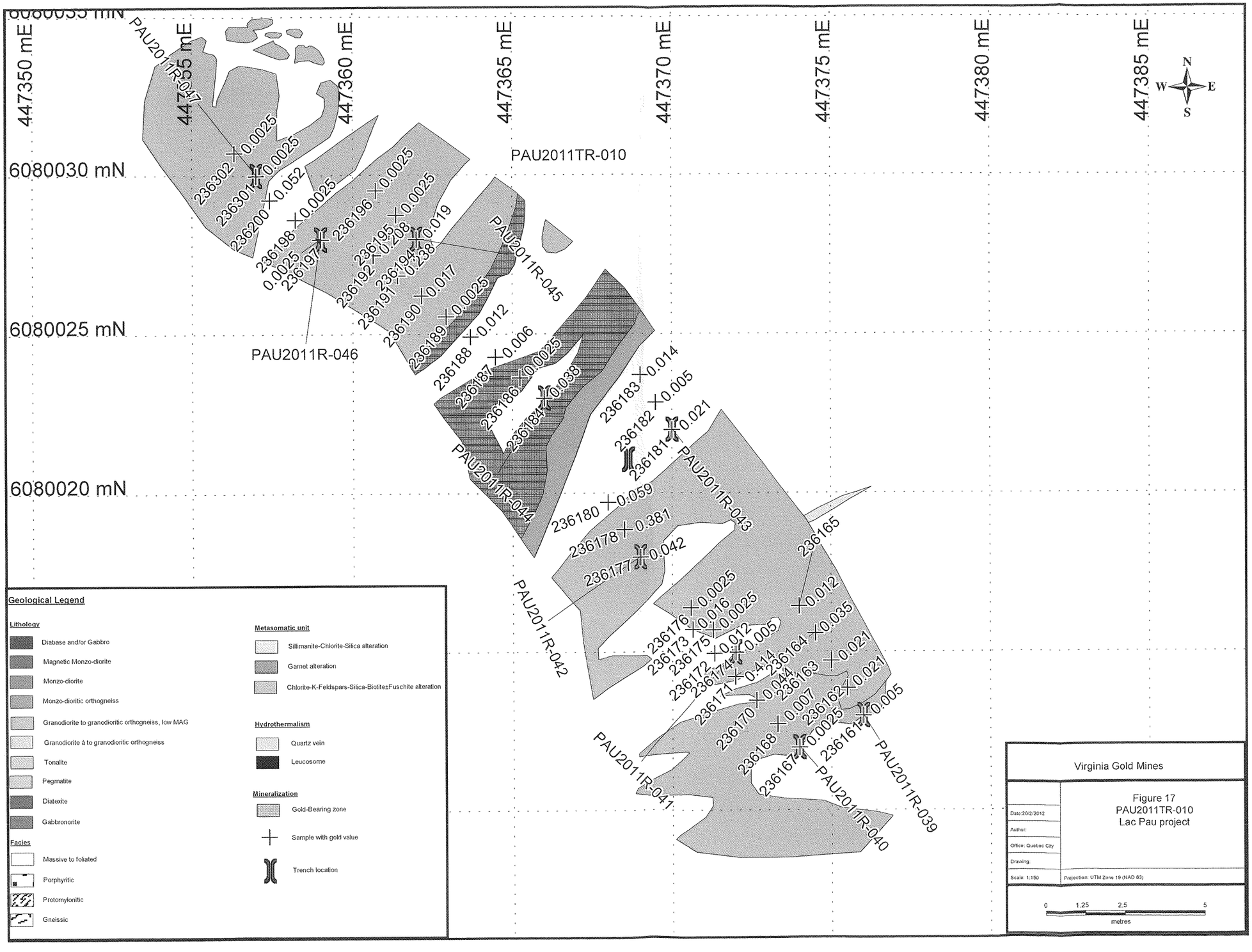
447350 mE
447355 mE
447360 mE
447365 mE
447370 mE
447375 mE
447380 mE
447385 mE
6080030 mN
6080025 mN
6080020 mN
N
W
E
S
PAU2011TR-010
PAU2011R-041
PAU2011R-042
PAU2011R-043
PAU2011R-044
PAU2011R-045
PAU2011R-046
PAU2011R-039
PAU2011R-040
236302 0.0025
236301 0.0025
236200 0.052
236198 0.0025
236197
236196 0.0025
236195 0.208
236194 0.019
236192 0.238
236191
236190 0.017
236189 0.0025
236188 0.012
236187 0.006
236186 0.0025
236184 0.038
236183 0.014
236182 0.005
236181 0.021
236180 0.059
236178 0.381
236177 0.042
236176 0.0025
236175 0.016
236173 0.0025
236172 0.012
236174 0.005
236171 0.414
236170 0.044
236168 0.007
236167 0.0025
236165
236164 0.012
236163 0.035
236162 0.021
236161 0.005
Geological Legend
Lithology
Diabase and/or Gabbro
Magnetic Monzo-diorite
Monzo-diorite
Monzo-dioritic orthogneiss
Granodiorite to granodioritic orthogneiss, low MAG
Granodiorite à to granodioritic orthogneiss
Tonalite
Pegmatite
Diatexite
Gabbronorite
Facies
Massive to foliated
Porphyritic
Protomylonitic
Gneissic
Metasomatic unit
Sillimanite-Chlorite-Silica alteration
Garnet alteration
Chlorite-K-Feldspars-Silica-Biotite±Fuschite alteration
Hydrothermalism
Quartz vein
Leucosome
Mineralization
Gold-Bearing zone
Sample with gold value
Trench location
Virginia Gold Mines
Figure 17
PAU2011TR-010
Lac Pau project
Date:20/2/2012
Author:
Office: Quebec City
Drawing:
Scale: 1:150
Projection: UTM Zone 19 (NAD 83)
0
1.25
2.5
5
metres

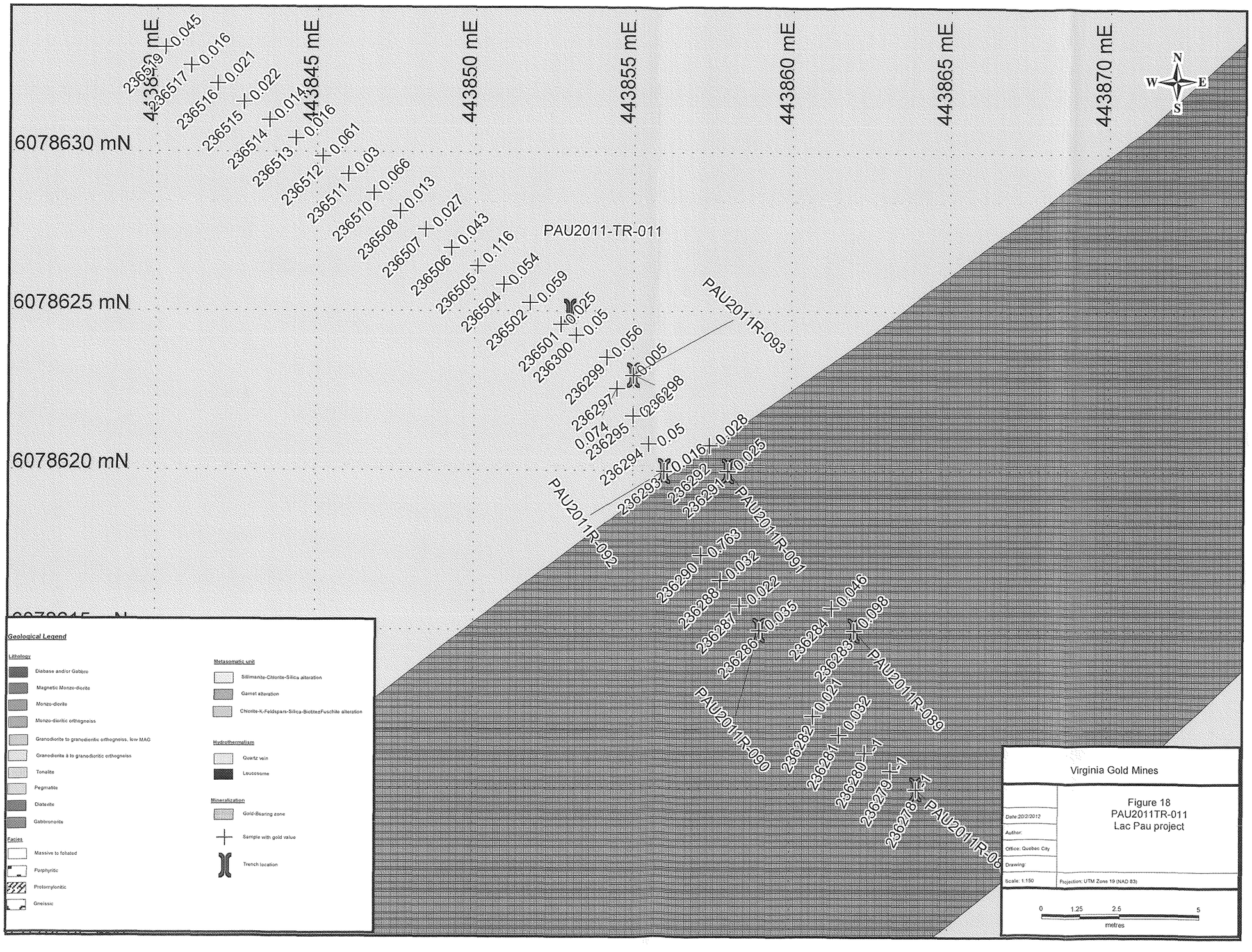
443840 mE
443845 mE
443850 mE
443855 mE
443860 mE
443865 mE
443870 mE
6078630 mN
6078625 mN
6078620 mN
N
W
E
S
PAU2011-TR-011
PAU2011R-093
PAU2011R-092
PAU2011R-091
PAU2011R-090
PAU2011R-089
PAU2011R-08
236519 0.045
236517 0.016
236516 0.021
236515 0.022
236514 0.014
236513 0.016
236512 0.061
236511 0.03
236510 0.066
236508 0.013
236507 0.027
236506 0.043
236505 0.116
236504 0.054
236502 0.059
236501 0.025
236300 0.05
236299 0.056
236297 0.005
236298
0.074
236295
236294 0.05
236293 0.016
0.028
236292
0.025
236291
236290 0.763
236288 0.032
236287 0.022
236286 0.035
236284 0.046
236283 0.098
236282 0.021
236281 0.032
236280 1
236279 1
236278 1
Geological Legend
Lithology
Diabase and/or Gabbro
Magnetic Monzo-diorite
Monzo-diorite
Monzo-dioritic orthogneiss
Granodiorite to granodioritic orthogneiss, low MAG
Granodiorite à to granodioritic orthogneiss
Tonalite
Pegmatite
Diatexite
Gabbronorite
Facies
Massive to foliated
Porphyritic
Protomylonitic
Gneissic
Metasomatic unit
Sillimanite-Chlorite-Silica alteration
Garnet alteration
Chlorite-K-Feldspars-Silica-BiotitezFuschite alteration
Hydrothermalism
Quartz vein
Leucosome
Mineralization
Gold-Bearing zone
Sample with gold value
Trench location
Virginia Gold Mines
Figure 18
PAU2011TR-011
Lac Pau project
Date:20/2/2012
Author:
Office: Quebec City
Drawing:
Scale: 1:150
Projection: UTM Zone 19 (NAD 83)
0
1.25
2.5
5
metres

Geological Legend

Lithology

- Diabase and/or Gabbro
- Magnetic Monzo-diorite
- Monzo-diorite
- Monzo-diorite orthogneiss
- Granodiorite to granodiontic orthogneiss, low MAG
- Granodiorite to granodioritic orthogneiss
- Tonalite
- Pegmatite
- Diatexite
- Gabbronorite / Pyroxenite

Facies

- Massive to foliated
- Porphyritic
- Protomylonitic
- Gneissic

Metasomatic unit

- Sillimanite-Chlorite-Silica alterations
- Garnet alteration
- Chlorite-K-Feldspars-Silica-Biotite±Fuschite alterations

Hydrothermalism

- Quartz vein
- Leucosome

Mineralization

- Gold-Bearing zone

- Trench location
- Channel location
- Colar location
- Assays with Au value

444 600 mE
444 620 mE
444 640 mE
444 660 mE

6 077 760 mN
6 077 740 mN
6 077 720 mN

PAU-11-033
PAU2011-TR-013
PAU2011-TR-012
PAU2007R-039
PAU2007R-040
PAU2007R-041

Jedi

N
W
E
S

Mines Virginia Inc./IAMGOLD Corp.	
Date: 21/3/2012	Figure 19 PAU2011TR-012 and PAU2011TR-013 Lac Pau Project
Author: J.L.	
Office: Quebec	
Drawing:	
Scale: 1:125	Projection: UTM Zone 19, Northern Hemisphe

0 2 4 8
metres

443850 mE
443860 mE
443870 mE
443880 mE
443890 mE
443900 mE
443910 mE
443920 mE
6077240 mN
6077230 mN
6077220 mN
N
W
E
S
PAU2011R-064
PAU2011R-063
PAU2011R-062
PAU2011R-061
PAU2011R-060
PAU2011R-059
PAU2011R-058
PAU2011R-057
PAU2011R-056
PAU2011R-055
PAU2011R-054
PAU2011R-053
PAU2011R-051
PAU2011R-050
PAU2011R-049
236229 0.0025
236228 0.0025
236227 0.0025
236226 0.0625
236225 0.0025
236224
236223 0.0025
236222 0.005
236221 0.0025
236220 0.011
236219
236218 0.0025
236217 0.0025
236216 0.0025
236214 0.0025
236213 0.0025
236212 0.0025
236211 0.0025
236210 0.02
236209 0.0025
236207 0.0025
236206 0.0025
236205
236203 0.0025
236202 0.0025
236201 0.0025
236340 0.923
236339 0.0025
236337 0.0025
236336 0.0025
236335
236334 0.006
236333 0.005
236332 0.0025
236330 0.0025
236329 0.005
236328 0.0025
236327 0.006
236326 0.0025
236324 0.0025
236323 0.011
236322 0.01
236321 0.012
236319 0.04
236317 0.012
236316 0.051
236315 0.054
236314 0.302
236313
236311 0.024
236310 0.006
236309 0.012
236308 0.0013
236307 0.007
236306 0.006
236305 0.006
236304 0.096
236303

Lithology

- Diabase and/or Gabbro
- Magnetic Monzo-diorite
- Monzo-diorite
- Monzo-dioritic orthogneiss
- Granodiorite to granodioritic orthogneiss, low MAG
- Granodiorite à to granodioritic orthogneiss
- Tonalite
- Pegmatite
- Diatexite
- Gabbronorite

Facies

- Massive to foliated
- Porphyritic
- Protomylonitic
- Gneissic

Metasomatic unit

- Sillimanite-Chlorite-Silica alteration
- Garnet alteration
- Chlorite-K-Feldspars-Silica-Biotite±Fuschite alterat

Hydrothermalism

- Quartz vein
- Leucosome

Mineralization

- Gold-Bearing zone
- Sample with gold value
- Trench location

Virginia Gold Mines

Figure 20
PAU2011R-049 to
PAU2011R-064
Lac Pau project

Date: 20/2/2012
Author:
Office: Quebec City
Drawing:
Scale: 1:200
Projection: UTM Zone 19 (NAD 83)

0 2 4 8
metres

443970 mE
443975 mE
443980 mE
443985 mE
443990 mE
443995 mE
444000 mE

6077285 mN
6077280 mN
6077275 mN
6077270 mN
6077265 mN
6077260 mN
6077255 mN
6077250 mN

N
W
E
S

PAU2011R-081
PAU2011R-080
PAU2011R-079
PAU2011R-078
PAU2011R-077
PAU2011R-076
PAU2011R-075
PAU2011R-074
PAU2011R-073
PAU2011R-072
PAU2011R-071
PAU2011R-070
PAU2011R-069
PAU2011R-068
PAU2011R-067
PAU2011R-066
PAU2011R-065

PAU-2009-TR-047

2362751
2362741
2362731
2362711
2362701
2362691
2362681
2362671
2362660.034
2362650.11
2362630.02
2362620.031
2362610.015
2362600.02
2362590.023
2362580.032
2362560.008
2362550.016
2362540.026
2362530.07
2362520.067
2362500.01
2362490.005
2362480.007
2362470.074
2362460.006
2362440.0025
2362430.008
2362420.009
2362400.005
2362400.012
2362390.066
2362380.009
2362370.0025
2362360.0025
2362350.007
2362330.011
2362320.03
2362310.017
2362300.005

Geological Legend

Lithology

- Diabase and/or Gabbro
- Magnetic Monzo-diorite
- Monzo-diorite
- Monzo-dioritic orthogneiss
- Granodiorite to granodioritic orthogneiss, low MAG
- Granodiorite à to granodioritic orthogneiss
- Tonalite
- Pegmatite
- Diatexite
- Gabbronorite

Facies

- Massive to foliated
- Porphyritic
- Protomylonitic
- Gneissic

Metasomatic unit

- Sillimanite-Chlorite-Silica alteration
- Garnet alteration
- Chlorite-K-Feldspars-Silica-Biotite±Fuschite alteration

Hydrothermalism

- Quartz vein
- Leucosome

Mineralization

- Gold-Bearing zone
- Sample
- Trench collar
- Trench location

Virginia Gold Mines

Figure 21
PAU2011R-065 to
PAU2011R-082
Lac Pau project

Date: 17/2/2012
Author:
Office: Quebec City
Drawing:
Scale: 1:125
Projection: UTM Zone 19 (NAD 83)

0 1.25 2.5 5
metres

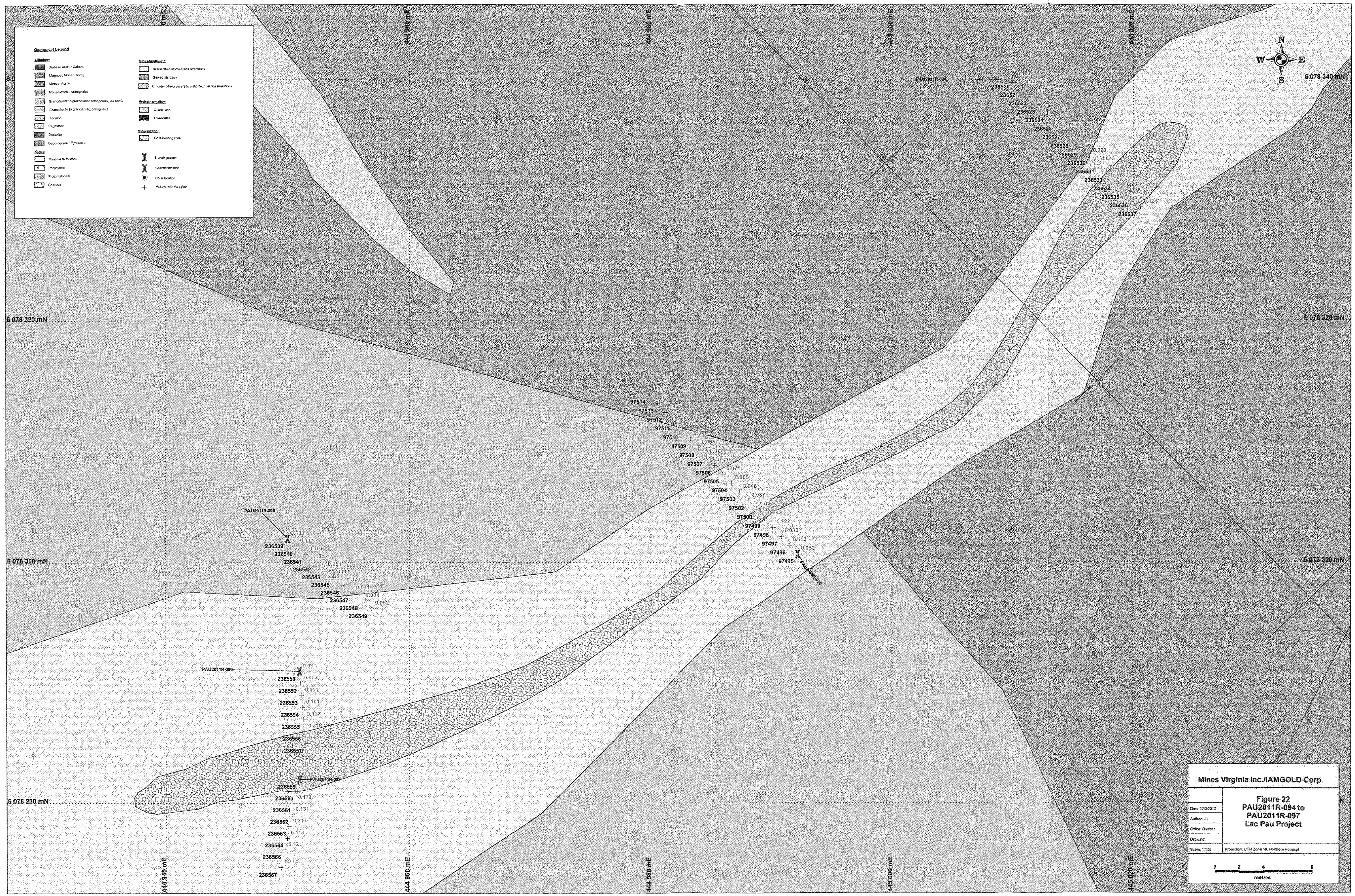
Geological Legend
Lithology
Diabase and/or Gabbro
Magnetic Monzo-diorite
Monzo-diorite
Monzo-dioritic orthogneiss
Granodiorite to granodioritic orthogneiss, low MAG
Granodiorite to granodioritic orthogneiss
Tonalite
Pegmatite
Diatexite
Gabbronorite / Pyroxenite
Facies
Massive to foliated
Porphyritic
Protomylonitic
Gneissic
Metasomatic unit
Chlorite-K-Feldspars-Silica-Biotite±Fuchsite alterations
Garnet alteration
Hydrothermalism
Quartz vein
Leucosome
Mineralization
Gold-Bearing zone
Trench location
Channel location
Collar location
Assays with Au value
444 960 mE
444 980 mE
445 000 mE
445 020 mE
444 940 mE
6 078 340 mN
6 078 320 mN
6 078 300 mN
6 078 280 mN
N
E
S
W
PAU2011R-094
236520
236521
236522
236523
236524
236526
236527
236528
236529
236530
236531
236533
236534
236535
236536
236537
0.098
0.073
0.124
97514
97513
97512
97511
97510
97509
97508
97507
97506
97505
97504
97503
97502
97500
97499
97498
97497
97496
97495
0.065
0.07
0.036
0.071
0.065
0.048
0.037
0.122
0.088
0.113
0.052
PAU2011R-095
236539
236540
236541
236542
236543
236545
236546
236547
236548
236549
0.133
0.117
0.101
0.14
0.251
0.068
0.073
0.041
0.064
0.062
PAU2011R-096
236550
236552
236553
236554
236555
236556
236557
0.08
0.062
0.091
0.101
0.137
0.318
PAU2011R-097
236559
236560
236561
236562
236563
236564
236566
236567
0.173
0.131
0.217
0.118
0.12
0.114
Mines Virginia Inc./IAMGOLD Corp.
Figure 22
PAU2011R-094 to
PAU2011R-097
Lac Pau Project
Date:22/3/2012
Author: J.L.
Office: Quebec
Drawing:
Scale: 1:125
Projection: UTM Zone 19, Northern Hemispl
0
2
4
8
metres

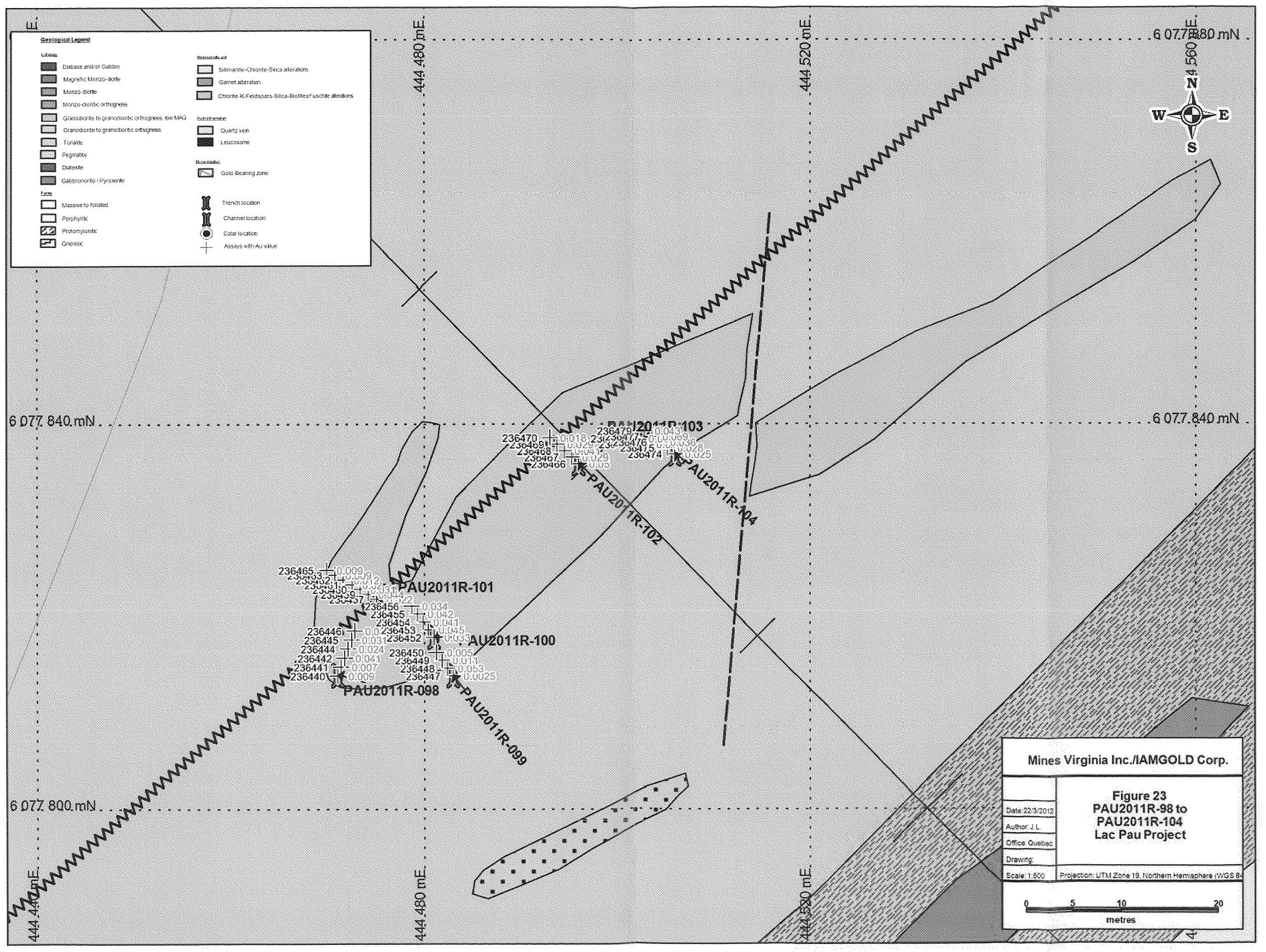
Geological Legend
Lithology
Diabase and/or Gabbro
Magnetic Monzo-diorite
Monzo-diorite
Monzo-dioritic orthogneiss
Granodiorite to granodioritic orthogneiss, low MAG
Granodiorite to granodioritic orthogneiss
Tonalite
Pegmatite
Dioritic
Gabbronorite / Pyroxenite
Fabric
Massive to foliated
Porphyritic
Protomylonitic
Gneissic
Metasomatic and
Silimanite-Chlorite-Silica alterations
Garnet alteration
Chlorite-K-Feldspars-Silica-Biotite±Fuschite alterations
Hydrothermal
Quartz vein
Leucosome
Mineralization
Gold-Bearing zone
Trench location
Channel location
Collar location
Assays with Au value
444 480 mE.
444 520 mE.
6 077 880 mN
6 077 840 mN
6 077 800 mN
N
W
E
S
PAU2011R-103
PAU2011R-104
PAU2011R-102
PAU2011R-101
PAU2011R-100
PAU2011R-098
PAU2011R-099
Mines Virginia Inc./IAMGOLD Corp.
Figure 23
PAU2011R-98 to
PAU2011R-104
Lac Pau Project
Date: 22/3/2012
Author: J.L.
Office: Quebec
Drawing:
Scale: 1:500
Projection: UTM Zone 19, Northern Hemisphere (WGS 84)
0 5 10 20
metres

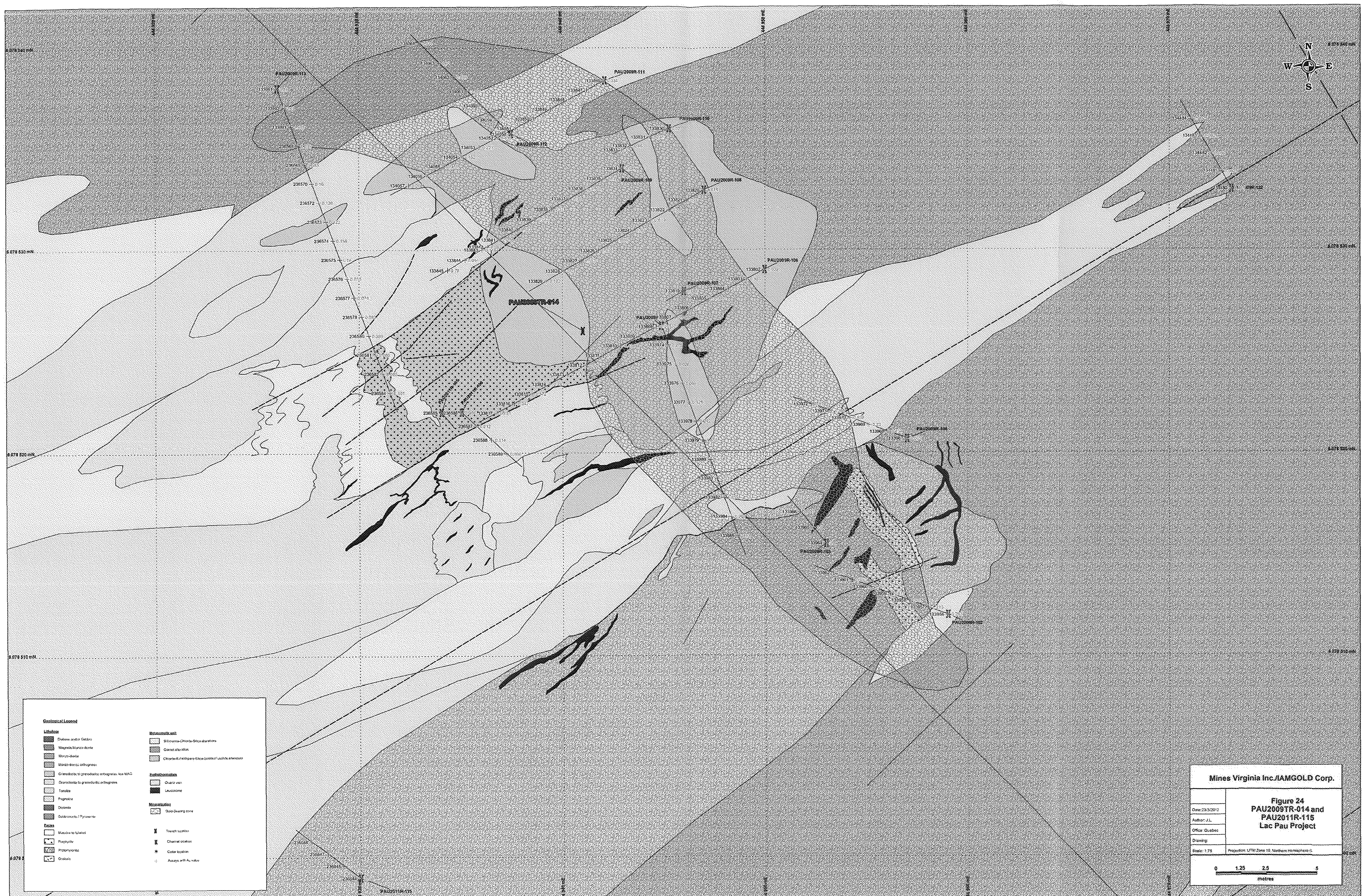
N
S
E
W
PAU2009R-113
PAU2009R-111
PAU2009R-112
PAU2009R-110
PAU2009R-109
PAU2009R-108
PAU2009R-106
PAU2009R-107
PAU2009TR-014
PAU2009R-104
PAU2009R-103
PAU2009R-102
PAU2011R-115
6 078 540 mN
6 078 530 mN
6 078 520 mN
6 078 510 mN
Geological Legend
Lithology
Diabase and/or Gabbro
Magnetic Monzo-diorite
Monzo-diorite
Monzo-dioritic orthogneiss
Granodiorite to granodioritic orthogneiss, low MAG
Granodiorite to granodioritic orthogneiss
Tonalite
Pegmatite
Diatexite
Gabbronorite / Pyroxenite
Facies
Massive to foliated
Porphyritic
Protomylonitic
Gneissic
Metasomatic unit
Garnet alteration
Hydrothermalism
Quartz vein
Leucosome
Mineralization
Gold-bearing zone
Trench location
Channel location
Collar location
Assays with Au value
Mines Virginia Inc./IAMGOLD Corp.
Figure 24
PAU2009TR-014 and
PAU2011R-115
Lac Pau Project
Date: 23/3/2012
Author: J.L.
Office: Quebec
Drawing:
Scale: 1:75
Projection: UTM Zone 19, Northern Hemisphere
0
1.25
2.5
5
metres

Geological Legend

Lithology

- Diabase and/or Gabbro
- Magnetic Monzo-diorite
- Monzo-diorite
- Monzo-diorite orthogneiss
- Granodiorite to granodioritic orthogneiss, low MAG
- Granodiorite to granodioritic orthogneiss
- Tonalite
- Pegmatite
- Dunite/ol
- Gabbronorite / Pyroxenite

Facies

- Massive to foliated
- Porphyritic
- Protomylonite
- Gneissic

Metasomatic unit

- Sillimanite-Chlorite-Silica alterations
- Garnet alteration
- Chlorite-K-Feldspars-Silica-Biotite±Fuschite alterations

Hydrothermalism

- Quartz vein
- Leucosome

Mineralization

- Gold-Bearing zone

- Trench location
- Channel location
- Collar location
- Assays with Au value

444 880 mE
444 900 mE
444 920 mE
444 940 mE
6 078 460 mN
6 078 440 mN
6 078 420 mN
6 078 400 mN

N
W
E
S

Mines Virginia Inc./IAMGOLD Corp.	
Date: 29/3/2012	Figure 25 PAU2009TR-011 Lac Pau Project
Author:	
Office: Quebec	
Drawing:	
Scale: 1:125	Projection: UTM Zone 19, Northern Hemisph

0 2 4 8
metres

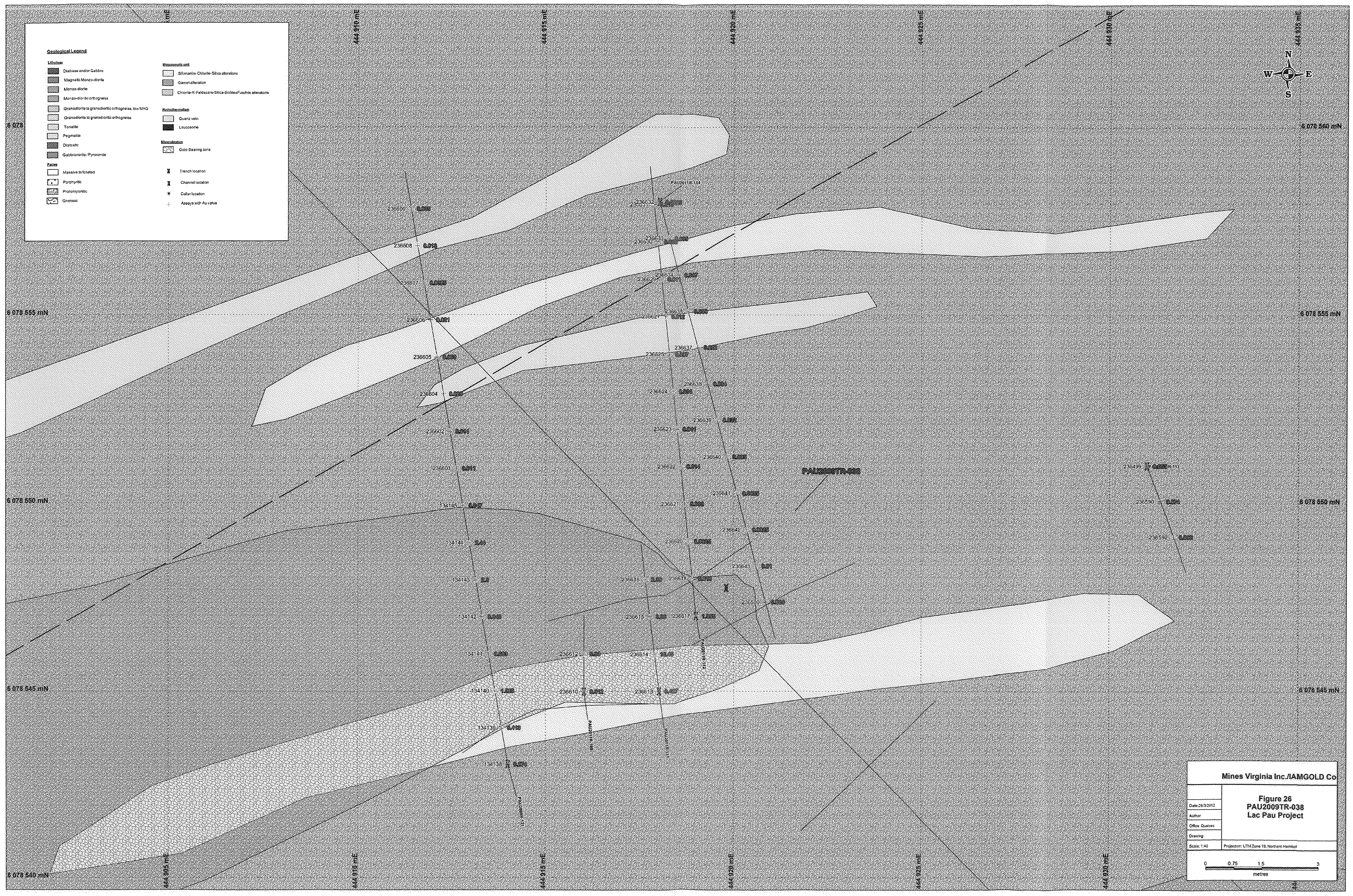

Figure 26
PAU2009TR-038
Lac Pau Project

Appendix 1 - Claims listing

INFORMATION AVAILABLE UPON REQUEST SUBMITTED TO VIRGINIA MINES INC.

info@minesvirginia.com

Toll free number: 800 476-1853

Appendix 2 – List of abbreviations used for geological descriptions, Lac Pau project

Appendix 2 : List of abbreviations

Source	Domaine	Code	Signification	Référence
VIA	Alteration	ALB	Albitisation	
VIA	Alteration	CAR	Carbonatation	
VIA	Alteration	CHL	Chloritasation	
VIA	Alteration	FRE	Fresh-Unaltered	
VIA	Alteration	HEM	Hematisation	
VIA	Alteration	KSP	Potassic Ait	
VIA	Alteration	SER	Sericitisation	
VIA	Alteration	SIL	Sil icification	
VIA	Alteration	SUL	Sulfurisation	
VIA	Contrôle	CTC	... associé à un contact	
VIA	Contrôle	CTL	... associé au litaqe	
VIA	Contrôle	BFR	... bordure de fraqments	
VIA	Contrôle	BCO	... bordures de coussins	
VIA	Contrôle	PSC	... dans le plan de la schistosité	
VIA	Contrôle	ZCI	... dans une zone de cisaillement	
VIA	Contrôle	FRP	... en plaquage de fracture	
VIA	Contrôle	VEI	... en veines et veinules	
VIA	Contrôle	GTE	... grid texture	
VIA	Contrôle	PEN	... pénétrant - pervasive	
VIA	Contrôle	RAM	... remplissaqe d'amyqdules	
VIA	Contrôle	STO	... stockwerk	
VIA	Contrôle	VAR	... variable - moUled	
VIA	Contrôle	ZAN	... zones anastomosée	
SIGEOM	Minéralisation	Ag	Argent natif (visible)	PR02000-08
SIGEOM	Minéralisation	AS	Arsénopyrite	PR02000-08
SIGEOM	Minéralisation	Bi	Bismuth	PR02000-08
SIGEOM	Minéralisation	BM	Bismuthinite	PR02000-08
SIGEOM	Minéralisation	BS	Bismutite	PR02000-08
SIGEOM	Minéralisation	BN	Bornite	PR02000-08
SIGEOM	Minéralisation	BG	Boulangerite	PR02000-08
SIGEOM	Minéralisation	WO	Bournonite	PR02000-08
SIGEOM	Minéralisation	CT	Chalcocite(ne)	PR02000-08
SIGEOM	Minéralisation	CP	Chalcopyrite	PR02000-08
SIGEOM	Minéralisation	CM	Chromite	PR02000-08
SIGEOM	Minéralisation	CE	Cobaltite	PR02000-08
SIGEOM	Minéralisation	NB	Colu m bite/N iobite	PR02000-08
SIGEOM	Minéralisation	TO	Columbo-tantalite	PR02000-08
SIGEOM	Minéralisation	CV	Covellite	PR02000-08
SIGEOM	Minéralisation	CF	Cubanite	PR02000-08
SIGEOM	Minéralisation	Cu	Cuivre natif (visible)	PR02000-08
SIGEOM	Minéralisation	CU	Cuprite	PR02000-08
SIGEOM	Minéralisation	DG	Digenite	PR02000-08
SIGEOM	Minéralisation	EM	Électrum	PR02000-08
SIGEOM	Minéralisation	EG	Enarqite	PR02000-08
SIGEOM	Minéralisation	Fe	Fer	PR02000-08
SIGEOM	Minéralisation	FM	Ferrimolybdite	PR02000-08
SIGEOM	Minéralisation	GH	Gahnite	PR02000-08
SIGEOM	Minéralisation	GL	Galène	PR02000-08
SIGEOM	Minéralisation	GO	Goethite	PR02000-08
SIGEOM	Minéralisation	HM	Hématite	PR02000-08
SIGEOM	Minéralisation	IM	Ilménite	PR02000-08
SIGEOM	Minéralisation	LM	Limonite	PR02000-08
SIGEOM	Minéralisation	LG	Loellinqite	PR02000-08
SIGEOM	Minéralisation	MG	Magnétite	PR02000-08
SIGEOM	Minéralisation	MC	Malachite	PR02000-08

SIGEOM	Minéralisation	MS	Marcasite	PR02000-08

Source	Domaine	Code	Signification	Référence
SIGEOM	Minéralisation	MK	Merenskyite	PR02000-08
SIGEOM	Minéralisation	NS	Millerite	PR02000-08
SIGEOM	Minéralisation	OP	Minéraux opaques	PR02000-08
SIGEOM	Minéralisation	MR	Minéraux radioactifs	PR02000-08
SIGEOM	Minéralisation	MO	Molybdénite	PR02000-08
SIGEOM	Minéralisation	MB	Molybdite(dine)	PR02000-08
SIGEOM	Minéralisation	UN	Nickeline	PR02000-08
SIGEOM	Minéralisation	VG	Or natif (visible)	
SIGEOM	Minéralisation	OF	Oxyde de fer	PR02000-08
SIGEOM	Minéralisation	PB	Pechblende	PR02000-08
SIGEOM	Minéralisation	PD	Pentlandite	PR02000-08
SIGEOM	Minéralisation	PY	Pyrite	PR02000-08
SIGEOM	Minéralisation	PM	Pyrochlore	PR02000-08
SIGEOM	Minéralisation	PO	Pyrrhotine	PR02000-08
SIGEOM	Minéralisation	SW	Scheelite	PR02000-08
SIGEOM	Minéralisation	SG	Sélénite	PR02000-08
SIGEOM	Minéralisation	Se	Sélénium	PR02000-08
SIGEOM	Minéralisation	S	Souffre	PR02000-08
SIGEOM	Minéralisation	HS	Spécula rite	PR02000-08
SIGEOM	Minéralisation	SP	Sphalérite	PR02000-08
SIGEOM	Minéralisation	SB	Stibine/Stibnite	PR02000-08
SIGEOM	Minéralisation	HD	Stilbite (Heulandite)	PR02000-08
SIGEOM	Minéralisation	SF	Sulfures	PR02000-08
SIGEOM	Minéralisation	OT	T étraferroplatine	PR02000-08
SIGEOM	Minéralisation	TH	Tétrahédrite	PR02000-08
SIGEOM	Minéralisation	TR	Thorianite	PR02000-08
SIGEOM	Minéralisation	TI	Thorite	PR02000-08
SIGEOM	Minéralisation	NM	Titanomagnétite	PR02000-08
SIGEOM	Minéralisation	UR	Uraninite	PR02000-08
SIGEOM	Minéralisation	UP	Uranophane	PR02000-08
SIGEOM	Minéralisation	UI	Uranopilite	PR02000-08
SIGEOM	Minéralisation	UH	Uranothorianite	PR02000-08
SIGEOM	Minéralisation	UT	Uranothorite	PR02000-08
SIGEOM	Minéralisation	GU	Uvarovite	PR02000-08
SIGEOM	Minéralisation	WF	Wolframite	PR02000-08
SIGEOM	Minéralogie	AV	Acanthite	PR02000-08
SIGEOM	Minéralogie	AC	Actinote	PR02000-08
SIGEOM	Minéralogie	EC	Aeschynite - Y	PR02000-08
SIGEOM	Minéralogie	AE	Agate	PR02000-08
SIGEOM	Minéralogie	BP	Aikinite	PR02000-08
SIGEOM	Minéralogie	KA	Akermanite	PR02000-08
SIGEOM	Minéralogie	AB	Albite	PR02000-08
SIGEOM	Minéralogie	AL	Allanite	PR02000-08
SIGEOM	Minéralogie	TP	Altaïte	PR02000-08
SIGEOM	Minéralogie	AI	Amazonite	PR02000-08
SIGEOM	Minéralogie	AH	Améthyste	PR02000-08
SIGEOM	Minéralogie	AO	Amiante (Asbestos)	PR02000-08
SIGEOM	Minéralogie	AM	Amphibole	PR02000-08
SIGEOM	Minéralogie	NT	Anatase	PR02000-08
SIGEOM	Minéralogie	AD	Andalousite	PR02000-08
SIGEOM	Minéralogie	AA	Andésine	PR02000-08
SIGEOM	Minéralogie	GD	Andradite	PR02000-08
SIGEOM	Minéralogie	LR	Anglésite	PR02000-08
SIGEOM	Minéralogie	AY	Anhydrite	PR02000-08

SIGEOM	Minéralogie	AK	Ankérite	PR02000-08
SIGEOM	Minéralogie	NG	Annabergite	PR02000-08

Source	Domaine	Code	Signification	Référence
SIGEOM	Minéralogie	AN	Anorthite	PR02000-08
SIGEOM	Minéralogie	AT	Anthophyllite	PR02000-08
SIGEOM	Minéraloqie	Sb	Antimoine	PR02000-08
SIGEOM	Minéraloqie	AP	Apatite	PR02000-08
SIGEOM	Minéraloqie	OA	Araqonite	PR02000-08
SIGEOM	Minéralogie	AG	Augite	PR02000-08
SIGEOM	Minéralogie	AU	Autunite	PR02000-08
SIGEOM	Minéralogie	NF	Awaruite	PR02000-08
SIGEOM	Minéralogie	AX	Axinite	PR02000-08
SIGEOM	Minéralogie	AZ	Azurite	PR02000-08
SIGEOM	Minéraloqie	BR	Barytine	PR02000-08
SIGEOM	Minéraloqie	BA	Bastnaesite	PR02000-08
SIGEOM	Minéraloqie	BL	Béryl	PR02000-08
SIGEOM	Minéralogie	BF	Bétafite	PR02000-08
SIGEOM	Minéralogie	BO	Biotite	PR02000-08
SIGEOM	Minéralogie	BI	Birnessite	PR02000-08
SIGEOM	Minéralogie	BD	Boltwoodite	PR02000-08
SIGEOM	Minéralogie	DI	Braggite	PR02000-08
SIGEOM	Minéraloqie	BE	Brannerite	PR02000-08
SIGEOM	Minéraloqie	BV	Bravoite	PR02000-08
SIGEOM	Minéraloqie	BU	Britholite	PR02000-08
SIGEOM	Minéralogie	BH	Brochantite	PR02000-08
SIGEOM	Minéralogie	BC	Brucite	PR02000-08
SIGEOM	Minéralogie	BT	Bytownite	PR02000-08
SIGEOM	Minéralogie	CA	Calaverite	PR02000-08
SIGEOM	Minéralogie	CO	Calcédoine	PR02000-08
SIGEOM	Minéraloqie	CC	Calcite	PR02000-08
SIGEOM	Minéraloqie	CB	Carbonate	PR02000-08
SIGEOM	Minéraloqie	CJ	Cattierite	PR02000-08
SIGEOM	Minéralogie	WD	Cérussite	PR02000-08
SIGEOM	Minéralogie	OS	Cervantite	PR02000-08
SIGEOM	Minéralogie	ZB	Chabazite(Chabasite)	PR02000-08
SIGEOM	Minéralogie	DN	Chamosite	PR02000-08
SIGEOM	Minéralogie	CH	Chert	PR02000-08
SIGEOM	Minéraloqie	CO	Chloanthite	PR02000-08
SIGEOM	Minéraloqie	CL	Chlorite	PR02000-08
SIGEOM	Minéraloqie	CR	Chloritoïde	PR02000-08
SIGEOM	Minéralogie	HR	Chondrodite	PR02000-08
SIGEOM	Minéralogie	CY	Chrysocolle	PR02000-08
SIGEOM	Minéralogie	CS	Chrysotile	PR02000-08
SIGEOM	Minéralogie	UC	Clarkeite	PR02000-08
SIGEOM	Minéralogie	CI	Clevelandite	PR02000-08
SIGEOM	Minéraloqie	HO	Clinohypersthene	PR02000-08
SIGEOM	Minéraloqie	CX	Clinopyroxène	PR02000-08
SIGEOM	Minéraloqie	CZ	Clinozoïsite	PR02000-08
SIGEOM	Minéralogie	UB	Coffinite	PR02000-08
SIGEOM	Minéralogie	00	Coopérite	PR02000-08
SIGEOM	Minéralogie	CD	Cordiérite	PR02000-08
SIGEOM	Minéralogie	CN	Corindon	PR02000-08
SIGEOM	Minéralogie	PI	Cosalite	PR02000-08
SIGEOM	Minéraloqie	CK	Cryptomelane	PR02000-08
SIGEOM	Minéraloqie	CG	Cumminqtonite	PR02000-08
SIGEOM	Minéraloqie	ZU	Cyrtolite	PR02000-08

SIGEOM	Minéralogie	DT	Danaite	PR02000-08
SIGEOM	Minéralogie	DL	Devilline	PR02000-08
SIGEOM	Minéralogie	DP	Diopside	PR02000-08

Source	Domaine	Code	Signification	Référence
SIGEOM	Minéralogie	DJ	Djurleite	PR02000-08
SIGEOM	Minéralogie	DM	Dolomite	PR02000-08
SIGEOM	Minéraloqie	TG	Dravite	PR02000-08
SIGEOM	Minéraloqie	DS	Dravite-Schorlite	PR02000-08
SIGEOM	Minéraloqie	ES	Enstatite	PR02000-08
SIGEOM	Minéralogie	EP	Epidote	PR02000-08
SIGEOM	Minéralogie	ER	Erythrite	PR02000-08
SIGEOM	Minéralogie	EU	Eudialyte	PR02000-08
SIGEOM	Minéralogie	EX	Euxénite - (Y)	PR02000-08
SIGEOM	Minéralogie	FA	Fayalite	PR02000-08
SIGEOM	Minéraloqie	FP	Feldspath	PR02000-08
SIGEOM	Minéraloqie	FN	Feldspath noir	PR02000-08
SIGEOM	Minéraloqie	FK	Feldspath potassique	PR02000-08
SIGEOM	Minéralogie	FV	Feldspath vert/brun	PR02000-08
SIGEOM	Minéralogie	FD	Feldspathoïde	PR02000-08
SIGEOM	Minéralogie	FT	Ferghanite	PR02000-08
SIGEOM	Minéralogie	FS	Fergusonite	PR02000-08
SIGEOM	Minéralogie	FB	Fibrolite	PR02000-08
SIGEOM	Minéraloqie	AF	Fluorapatite	PR02000-08
SIGEOM	Minéraloqie	FL	Fluorite (fluorine)	PR02000-08
SIGEOM	Minéraloqie	FO	Forstérite	PR02000-08
SIGEOM	Minéralogie	FR	Franklinite	PR02000-08
SIGEOM	Minéralogie	FG	Freibergite	PR02000-08
SIGEOM	Minéralogie	Fe	Fuchsite	PR02000-08
SIGEOM	Minéralogie	Ne	Gaspéite	PR02000-08
SIGEOM	Minéralogie	GT	Gédrite	PR02000-08
SIGEOM	Minéraloqie	NA	Gersdorffite	PR02000-08
SIGEOM	Minéraloqie	Ge	Glaucophane	PR02000-08
SIGEOM	Minéraloqie	GP	Graphite	PR02000-08
SIGEOM	Minéralogie	GF	Greenalite	PR02000-08
SIGEOM	Minéralogie	GK	Greenockite	PR02000-08
SIGEOM	Minéralogie	GR	Grenat	PR02000-08
SIGEOM	Minéralogie	GM	Grenat manganésifère	PR02000-08
SIGEOM	Minéralogie	GA	Grenat-almandin	PR02000-08
SIGEOM	Minéraloqie	GG	Grenat-qrossulaire	PR02000-08
SIGEOM	Minéraloqie	GY	Grenat-pyrope	PR02000-08
SIGEOM	Minéraloqie	GN	Grunérite	PR02000-08
SIGEOM	Minéralogie	UD	Gudmundite	PR02000-08
SIGEOM	Minéralogie	GB	Gummite	PR02000-08
SIGEOM	Minéralogie	GI	Gunningite	PR02000-08
SIGEOM	Minéralogie	GE	Gypse	PR02000-08
SIGEOM	Minéralogie	HL	Halite	PR02000-08
SIGEOM	Minéraloqie	HZ	Heazlewoodite	PR02000-08
SIGEOM	Minéraloqie	HG	Hédenberqite	PR02000-08
SIGEOM	Minéraloqie	HE	Hemimorphite	PR02000-08
SIGEOM	Minéralogie	He	Hercynite	PR02000-08
SIGEOM	Minéralogie	HK	Holmquistite	PR02000-08
SIGEOM	Minéralogie	HB	Hornblende	PR02000-08
SIGEOM	Minéralogie	HT	Hydrocerussite	PR02000-08
SIGEOM	Minéralogie	HN	Hydromagnésite	PR02000-08
SIGEOM	Minéraloqie	ZH	Hydrozincite	PR02000-08
SIGEOM	Minéraloqie	HP	Hypersthène	PR02000-08

SIGEOM	Minéraloqie	ID	Idaite	PR02000-08
SIGEOM	Minéralogie	IG	Iddingsite	PR02000-08
SIGEOM	Minéralogie	IR	Iriginite	PR02000-08
SIGEOM	Minéralogie	IF	Isoferroplatine	PR02000-08

Source	Domaine	Code	Signification	Référence
SIGEOM	Minéralogie	JA	Jade	PR02000-08
SIGEOM	Minéralogie	JS	Jarosite	PR02000-08
SIGEOM	Minéraloqie	JP	Jaspe	PR02000-08
SIGEOM	Minéraloqie	KL	Kaolinite	PR02000-08
SIGEOM	Minéraloqie	KS	Kasolite	PR02000-08
SIGEOM	Minéralogie	KM	Kermésite	PR02000-08
SIGEOM	Minéralogie	KK	Klockmannite	PR02000-08
SIGEOM	Minéralogie	KP	Kornérupine	PR02000-08
SIGEOM	Minéralogie	KR	Krennerite	PR02000-08
SIGEOM	Minéralogie	KN	Kyanite/Disthène	PR02000-08
SIGEOM	Minéraloqie	LB	Labradorite	PR02000-08
SIGEOM	Minéraloqie	LU	Laumontite	PR02000-08
SIGEOM	Minéraloqie	LI	Laurite	PR02000-08
SIGEOM	Minéralogie	LS	Lawsonite	PR02000-08
SIGEOM	Minéralogie	LD	Lepidocrocite	PR02000-08
SIGEOM	Minéralogie	LP	Lépidolite	PR02000-08
SIGEOM	Minéralogie	LE	Lessingite	PR02000-08
SIGEOM	Minéralogie	LC	Leucite	PR02000-08
SIGEOM	Minéraloqie	LX	Leucoxène	PR02000-08
SIGEOM	Minéraloqie	LN	Linnaéite	PR02000-08
SIGEOM	Minéraloqie	DH	Maqhémite	PR02000-08
SIGEOM	Minéralogie	IC	Magnésiochromite	PR02000-08
SIGEOM	Minéralogie	MN	Magnésite	PR02000-08
SIGEOM	Minéralogie	MM	Manganite	PR02000-08
SIGEOM	Minéralogie	MT	Mariposite	PR02000-08
SIGEOM	Minéralogie	ZF	Marmatite	PR02000-08
SIGEOM	Minéraloqie	MH	Martite	PR02000-08
SIGEOM	Minéraloqie	ME	Mélilite	PR02000-08
SIGEOM	Minéraloqie	MW	Melonite	PR02000-08
SIGEOM	Minéralogie	NE	Ménéghinite	PR02000-08
SIGEOM	Minéralogie	MP	Mésoperthite	PR02000-08
SIGEOM	Minéralogie	WH	Meymacite	PR02000-08
SIGEOM	Minéralogie	MI	Mica	PR02000-08
SIGEOM	Minéralogie	ML	Microcline	PR02000-08
SIGEOM	Minéraloqie	MA	Minéraux arqileux	PR02000-08
SIGEOM	Minéraloqie	MD	Minéraux décoratifs	PR02000-08
SIGEOM	Minéraloqie	MX	Minéraux lourds	PR02000-08
SIGEOM	Minéralogie	MF	Minéraux mafiques	PR02000-08
SIGEOM	Minéralogie	MU	Minnesotaite	PR02000-08
SIGEOM	Minéralogie	MZ	Monazite	PR02000-08
SIGEOM	Minéralogie	OM	Monticellite	PR02000-08
SIGEOM	Minéralogie	MV	Muscovite	PR02000-08
SIGEOM	Minéraloqie	NP	Néphéline	PR02000-08
SIGEOM	Minéraloqie	01	Niocalite	PR02000-08
SIGEOM	Minéraloqie	OC	Ocre	PR02000-08
SIGEOM	Minéralogie	OG	Oligoclasse	PR02000-08
SIGEOM	Minéralogie	OV	Olivine	PR02000-08
SIGEOM	Minéralogie	OR	Orthoclase (orthose)	PR02000-08
SIGEOM	Minéralogie	OX	Orthopyroxène	PR02000-08
SIGEOM	Minéralogie	OL	Ottrelite	PR02000-08
SIGEOM	Minéraloqie	OH	Oxyhornblende (Hornblende brune)	PR02000-08

SIGEOM	Minéraloqie	PE	Paraqonite	PR02000-08
SIGEOM	Minéraloqie	PT	Penninite/Pennine	PR02000-08
SIGEOM	Minéralogie	II	Péristérite	PR02000-08
SIGEOM	Minéralogie	PK	Perovskite	PR02000-08
SIGEOM	Minéralogie	PR	Perthite	PR02000-08

Source	Domaine	Code	Signification	Référence
SIGEOM	Minéralogie	PZ	Petzite	PR02000-08
SIGEOM	Minéralogie	PA	Phénacite/Phénakite	PR02000-08
SIGEOM	Minéraloqie	PH	Phloqopite	PR02000-08
SIGEOM	Minéraloqie	PU	Phosphuranylite	PR02000-08
SIGEOM	Minéraloqie	AR	Picrolite	PR02000-08
SIGEOM	Minéralogie	PC	Pistachite	PR02000-08
SIGEOM	Minéralogie	PG	Plagioclase	PR02000-08
SIGEOM	Minéralogie	ZP	Pollucite	PR02000-08
SIGEOM	Minéralogie	PJ	Posniakite	PR02000-08
SIGEOM	Minéralogie	PN	Préhnite	PR02000-08
SIGEOM	Minéraloqie	PP	Pumpellyite	PR02000-08
SIGEOM	Minéraloqie	PS	Pyrolusite	PR02000-08
SIGEOM	Minéraloqie	PL	Pyrophyllite	PR02000-08
SIGEOM	Minéralogie	PX	Pyroxène	PR02000-08
SIGEOM	Minéralogie	QZ	Quartz	PR02000-08
SIGEOM	Minéralogie	QB	Quartz bleu	PR02000-08
SIGEOM	Minéralogie	RD	Rhodochrosite	PR02000-08
SIGEOM	Minéralogie	RN	Rhodonite	PR02000-08
SIGEOM	Minéraloqie	RB	Riebeckite	PR02000-08
SIGEOM	Minéraloqie	RM	Romanechite	PR02000-08
SIGEOM	Minéraloqie	RC	Roscoelite	PR02000-08
SIGEOM	Minéralogie	RZ	Rozénite	PR02000-08
SIGEOM	Minéralogie	RL	Rutile	PR02000-08
SIGEOM	Minéralogie	FF	Safflorite	PR02000-08
SIGEOM	Minéralogie	SK	Samarskite	PR02000-08
SIGEOM	Minéralogie	UL	Samarskite - (Y)	PR02000-08
SIGEOM	Minéraloqie	SA	Sanidine	PR02000-08
SIGEOM	Minéraloqie	SH	Sapphirine	PR02000-08
SIGEOM	Minéraloqie	SC	Scapolite	PR02000-08
SIGEOM	Minéralogie	TF	Schorl ite(Schorl)	PR02000-08
SIGEOM	Minéralogie	VS	Sénarmontite	PR02000-08
SIGEOM	Minéralogie	SR	Séricite	PR02000-08
SIGEOM	Minéralogie	ST	Serpentine	PR02000-08
SIGEOM	Minéralogie	SD	Sidérite(sidérose)	PR02000-08
SIGEOM	Minéraloqie	SI	Sidérotil	PR02000-08
SIGEOM	Minéraloqie	SM	Sillimanite	PR02000-08
SIGEOM	Minéraloqie	DW	Sklodowskite	PR02000-08
SIGEOM	Minéralogie	TW	Smaltite/Smaltine	PR02000-08
SIGEOM	Minéralogie	ZO	Smithsonite	PR02000-08
SIGEOM	Minéralogie	SS	Sodalite	PR02000-08
SIGEOM	Minéralogie	DY	Soddyite	PR02000-08
SIGEOM	Minéralogie	GS	Spessartine	PR02000-08
SIGEOM	Minéraloqie	SN	Sphène/Titanite	PR02000-08
SIGEOM	Minéraloqie	SL	Spinelle	PR02000-08
SIGEOM	Minéraloqie	SO	Spodumène	PR02000-08
SIGEOM	Minéralogie	NN	Stannite	PR02000-08
SIGEOM	Minéralogie	SY	Starkéyite	PR02000-08
SIGEOM	Minéralogie	SU	Staurotide	PR02000-08
SIGEOM	Minéralogie	TS	Stéatite	PR02000-08
SIGEOM	Minéralogie	ON	Stibiconite	PR02000-08

SIGEOM	Minéraloqie	SE	Stilpnomélane	PR02000-08
SIGEOM	Minéraloqie	SV	Sylvanite	PR02000-08
SIGEOM	Minéraloqie	SZ	Szomolnokite	PR02000-08
SIGEOM	Minéralogie	TC	Talc	PR02000-08
SIGEOM	Minéralogie	TN	Tantalite	PR02000-08
SIGEOM	Minéralogie	TB	Tellurobismuthite	PR02000-08

Source	Domaine	Code	Signification	Référence
SIGEOM	Minéralogie	TT	Tennantite	PR02000-08
SIGEOM	Minéralogie	TE	Tenorite	PR02000-08
SIGEOM	Minéraloqie	TD	Tétradymite	PR02000-08
SIGEOM	Minéraloqie	ZT	Thomsonite	PR02000-08
SIGEOM	Minéraloqie	HU	Thucholite	PR02000-08
SIGEOM	Minéralogie	TZ	Topaze	PR02000-08
SIGEOM	Minéralogie	TU	Torbernite	PR02000-08
SIGEOM	Minéralogie	TL	Tourmaline	PR02000-08
SIGEOM	Minéralogie	TA	Tourmaline zincifère	PR02000-08
SIGEOM	Minéralogie	TM	Trémolite	PR02000-08
SIGEOM	Minéraloqie	US	Ulv6spinel	PR02000-08
SIGEOM	Minéraloqie	VA	Valentinite	PR02000-08
SIGEOM	Minéraloqie	VL	Valleriite	PR02000-08
SIGEOM	Minéralogie	VR	Vermiculite	PR02000-08
SIGEOM	Minéralogie	W	Vésuvianite	PR02000-08
SIGEOM	Minéralogie	VO	Viola rite	PR02000-08
SIGEOM	Minéralogie	WM	Willemite	PR02000-08
SIGEOM	Minéralogie	WS	Wilsonite	PR02000-08
SIGEOM	Minéraloqie	WL	Wollastonite	PR02000-08
SIGEOM	Minéraloqie	WN	Wulfenite	PR02000-08
SIGEOM	Minéraloqie	TX	Xénotime-(Y)	PR02000-08
SIGEOM	Minéralogie	ZL	Zéolite	PR02000-08
SIGEOM	Minéralogie	ZN	Zincite	PR02000-08
SIGEOM	Minéralogie	ZC	Zircon	PR02000-08
SIGEOM	Minéralogie	ZS	Zoïsite	PR02000-08
SIGEOM	OrganoFossile	XX	Autres	PR02000-08
SIGEOM	OrqanoFossile	XB	Bioclastes	PR02000-08
SIGEOM	OrqanoFossile	YB	Brachiopodes	PR02000-08
SIGEOM	OrqanoFossile	YZ	Bryozoaires	PR02000-08
SIGEOM	OrganoFossile	YC	Céphalopodes	PR02000-08
SIGEOM	OrganoFossile	XC	Ciment	PR02000-08
SIGEOM	OrganoFossile	YA	Conulaires	PR02000-08
SIGEOM	OrganoFossile	YX	Coraux	PR02000-08
SIGEOM	OrganoFossile	YR	Crinoïdes	PR02000-08
SIGEOM	OrqanoFossile	YD	Échinodermes	PR02000-08
SIGEOM	OrqanoFossile	YE	Éponqes	PR02000-08
SIGEOM	OrqanoFossile	yy	Fossile	PR02000-08
SIGEOM	OrganoFossile	YT	Gastéropodes	PR02000-08
SIGEOM	OrganoFossile	YG	Graptolites	PR02000-08
SIGEOM	OrganoFossile	XH	Hydrocarbures	PR02000-08
SIGEOM	OrganoFossile	XL	Liant	PR02000-08
SIGEOM	OrganoFossile	XR	Lithoclastes	PR02000-08
SIGEOM	OrqanoFossile	XG	Matière orqanique	PR02000-08
SIGEOM	OrqanoFossile	XM	Matrice	PR02000-08
SIGEOM	OrqanoFossile	XT	Oncolites	PR02000-08
SIGEOM	OrganoFossile	XO	Oolites	PR02000-08
SIGEOM	OrganoFossile	YO	Ostracodes	PR02000-08
SIGEOM	OrganoFossile	YP	Pélécipodes	PR02000-08

SIGEOM	OrganoFossile	XP	Pellets	PR02000-08
SIGEOM	OrganoFossile	XD	Péloïdes	PR02000-08
SIGEOM	OrganoFossile	YN	Plantes	PR02000-08
SIGEOM	OrganoFossile	YK	Poissons	PR02000-08
SIGEOM	OrganoFossile	YS	Stromatoïdes	PR02000-08
SIGEOM	OrganoFossile	YI	Stromatoporoïdes	PR02000-08
SIGEOM	OrganoFossile	YF	Traces fossiles	PR02000-08
SIGEOM	OrganoFossile	YL	Trilobites	PR02000-08
Source	**Domaine**	**Code**	**Signification**	**Référence**
SIGEOM	Roche	14QA	Aillikite	MB96-28
SIGEOM	Roche	11K	Alaskite	MB96-28
SIGEOM	Roche	140A	Alnoite	MB96-28
SIGEOM	Roche	V2J	Andésite	MB96-28
SIGEOM	Roche	S12C	Anhydrite	MB96-28
SIGEOM	Roche	13G	Anorthosite	MB96-28
SIGEOM	Roche	13T	Anorthosite à hyperstène	MB96-28
SIGEOM	Roche	13GR	Anorthosite foidifère	MB96-28
SIGEOM	Roche	13H	Anorthosite gabbroique	MB96-28
SIGEOM	Roche	13GQ	Anorthosite quartzifère	MB96-28
SIGEOM	Roche	11F	Aplite	MB96-28
SIGEOM	Roche	S2	Arénite	MB96-28
SIGEOM	Roche	S2D	Arénite arkosique	MB96-28
SIGEOM	Roche	S2E	Arénite lithique	MB96-28
SIGEOM	Roche	S2A	Arénite Quartizitique	MB96-28
SIGEOM	Roche	S1C	Arkose	MB96-28
SIGEOM	Roche	S2C	Arkose	MB96-28
SIGEOM	Roche	S7J	Bafflestone	MB96-28
SIGEOM	Roche	V3B	Basalte	MB96-28
SIGEOM	Roche	V3E	Basalte à olivine	MB96-28
SIGEOM	Roche	V3C	Basalte à quartz	MB96-28
SIGEOM	Roche	V3A	Basalte andésitique/Andésite basaltique	MB96-28
SIGEOM	Roche	V3F	Basalte magnésien	MB96-28
SIGEOM	Roche	V3H	Basanite	MB96-28
SIGEOM	Roche	V3HP	Basanite phonolitique	MB96-28
SIGEOM	Roche	V2FB	Benmoréite	MB96-28
SIGEOM	Roche	V3J	Bonninite	MB96-28
SIGEOM	Roche	S71	Boundstone	MB96-28
SIGEOM	Roche	S5	Brèche	MB96-28
SIGEOM	Roche	S5G	Brèche Intraformationnel	MB96-28
SIGEOM	Roche	S5H	Brèche Intraformationnel Fermé	MB96-28
SIGEOM	Roche	S51	Brèche Intraformationnel Ouvert	MB96-28
SIGEOM	Roche	S5A	Brèche Monogénique	MB96-28
SIGEOM	Roche	S5B	Brèche Monogénique Fermé	MB96-28
SIGEOM	Roche	S5C	Brèche Monoqénique Ouvert	MB96-28
SIGEOM	Roche	S5D	Brèche Polyqénique	MB96-28
SIGEOM	Roche	S5E	Brèche Polygénique Fermé	MB96-28
SIGEOM	Roche	S5F	Brèche Polygénique Ouvert	MB96-28
SIGEOM	Roche	S7	Calcaire	MB96-28
SIGEOM	Roche	S7C	Calcarénite	MB96-28
SIGEOM	Roche	S7A	Calcilulite	MB96-28
SIGEOM	Roche	14QC	Calciocarbonatite	MB96-28
SIGEOM	Roche	S7D	calcirudite	MB96-28
SIGEOM	Roche	S7B	calcisiltite	MB96-28
SIGEOM	Roche	140C	Camptonite	MB96-28
SIGEOM	Roche	14Q	Carbonatite	MB96-28
SIGEOM	Roche	11P	Charnockite (Granite à hyperstène)	MB96-28
SIGEOM	Roche	110	Charnockite à feldspath alcalin	MB96-28
SIGEOM	Roche	S10	Chert	MB96-28

SIGEOM	Roche	S10B	Chert Carbonaté	MB96-28
SIGEOM	Roche	S10F	Chert Ferruqineux	MB96-28
SIGEOM	Roche	S10E	Chert Graphiteux/Carboné	MB96-28
SIGEOM	Roche	S10A	Chert Oxydé	MB96-28
SIGEOM	Roche	S10C	Chert Silicaté	MB96-28
SIGEOM	Roche	S10D	Chert Sulfuré	MB96-28
SIGEOM	Roche	S6H	Clayshale	MB96-28

Source	Domaine	Code	Signification	Référence
SIGEOM	Roche	S61	Clayslate	MB96-28
SIGEOM	Roche	S6G	Claystone	MB96-28
SIGEOM	Roche	14C	Clinopyroxénite	MB96-28
SIGEOM	Roche	14F	Clinopyroxénite à olivine	MB96-28
SIGEOM	Roche	V1BC	Commendite	MB96-28
SIGEOM	Roche	S4	Conglomérat	MB96-28
SIGEOM	Roche	S4G	Conglomérat intraformationnel	MB96-28
SIGEOM	Roche	S4H	Conglomérat intraformationnel Fermé	MB96-28
SIGEOM	Roche	S41	Conglomérat intraformationnel Ouvert	MB96-28
SIGEOM	Roche	S4A	Conglomérat monogénique	MB96-28
SIGEOM	Roche	S4B	Conglomérat monoqénique fermé	MB96-28
SIGEOM	Roche	S4C	Conglomérat monogénique Ouvert	MB96-28
SIGEOM	Roche	S4D	Conglomérat polygénique	MB96-28
SIGEOM	Roche	S4E	Conglomérat polygénique Fermé	MB96-28
SIGEOM	Roche	S4F	Conglomérat polygénique Ouvert	MB96-28
SIGEOM	Roche	V1D	Dacite	MB96-28
SIGEOM	Roche	140D	Damtjernite	MB96-28
SIGEOM	Roche	13B	Diabase	MB96-28
SIGEOM	Roche	13M	Diabase à olivine	MB96-28
SIGEOM	Roche	13F	Diabase à quatrz	MB96-28
SIGEOM	Roche	12J	Diorite	MB96-28
SIGEOM	Roche	120	Diorite à hyperstène	MB96-28
SIGEOM	Roche	12JR	Diorite foidifère	MB96-28
SIGEOM	Roche	12JF	Diorite foidique	MB96-28
SIGEOM	Roche	121	Diorite quartzifère	MB96-28
SIGEOM	Roche	S8C	Dolarénite	MB96-28
SIGEOM	Roche	S8A	Dololutite	MB96-28
SIGEOM	Roche	S8	Dolomite	MB96-28
SIGEOM	Roche	S8D	Dolorudite	MB96-28
SIGEOM	Roche	S8B	Dolosilite	MB96-28
SIGEOM	Roche	14M	Dunite	MB96-28
SIGEOM	Roche	In	Enderbite (Tonalite à hyperstène)	MB96-28
SIGEOM	Roche	S12	Évaporite	MB96-28
SIGEOM	Roche	S11	Exhalite	MB96-28
SIGEOM	Roche	140F	Ferrocarbonatite	MB96-28
SIGEOM	Roche	13D	Ferrogabbro	MB96-28
SIGEOM	Roche	11N	Filon/Veine de quartz	MB96-28
SIGEOM	Roche	V41	Foidite	MB96-28
SIGEOM	Roche	V41P	Foidite phonolitique	MB96-28
SIGEOM	Roche	V41T	Foidite téphritique	MB96-28
SIGEOM	Roche	14S	Foidolite	MB96-28
SIGEOM	Roche	S9	Formation de fer	MB96-28
SIGEOM	Roche	S9C	Formation de fer Carbonatée	MB96-28
SIGEOM	Roche	S9A	Formation de fer indéterminée	MB96-28
SIGEOM	Roche	S9B	Formation de fer oxydée	MB96-28
SIGEOM	Roche	S9D	Formation de fer Silicatée	MB96-28
SIGEOM	Roche	S9E	Formation de fer Sulfurée	MB96-28
SIGEOM	Roche	13A	Gabbro	MB96-28

SIGEOM	Roche	13K	Gabbro à olivine	MB96-28
SIGEOM	Roche	13E	Gabbro à quartz	MB96-28
SIGEOM	Roche	131	Gabbro anorthosite	MB96-28
SIGEOM	Roche	13AR	Gabbro foidifère	MB96-28
SIGEOM	Roche	130	Gabbronorite	MB96-28
SIGEOM	Roche	13R	Gabbronorite à olivine	MB96-28
SIGEOM	Roche	S7H	Grainstone	MB96-28
SIGEOM	Roche	11B	Granite	MB96-28

Source	Domaine	Code	Signification	Référence
SIGEOM	Roche	11A	Granite à feldspath alcalin	MB96-28
SIGEOM	Roche	111	Granitoide riche en quartz	MB96-28
SIGEOM	Roche	11C	Granodiorite	MB96-28
SIGEOM	Roche	11S	Grano-diotite à hyperstène	MB96-28
SIGEOM	Roche	11H	Granophyre	MB96-28
SIGEOM	Roche	S1	Grès	MB96-28
SIGEOM	Roche	S1D	Grès Arkosique	MB96-28
SIGEOM	Roche	S1B	Grès Feldspathique	MB96-28
SIGEOM	Roche	S1E	Grès Lithique	MB96-28
SIGEOM	Roche	S1F	Grès Lithique subfeldspathitique	MB96-28
SIGEOM	Roche	S1A	Grès Quartzique	MB96-28
SIGEOM	Roche	S12D	Gypse	MB96-28
SIGEOM	Roche	S12A	Halite	MB96-28
SIGEOM	Roche	14L	Harzburgite	MB96-28
SIGEOM	Roche	V3DH	Hawaiite	MB96-28
SIGEOM	Roche	14A	Hornblendite	MB96-28
SIGEOM	Roche	V2JI	Icelandite	MB96-28
SIGEOM	Roche	V3AI	Icelandite basaltique	MB96-28
SIGEOM	Roche	11	Intrusion felsique	MB96-28
SIGEOM	Roche	12	Intrusion Intermédiaire	MB96-28
SIGEOM	Roche	13	Intrusion mafique	MB96-28
SIGEOM	Roche	14	Intrusion ultramafique	MB96-28
SIGEOM	Roche	S10J	Jaspe, Jaspilite	MB96-28
SIGEOM	Roche	12P	Jotunite (Monzodiorite à hyperstène)	MB96-28
SIGEOM	Roche	130K	Kersantite	MB96-28
SIGEOM	Roche	14P	Kimberlite	MB96-28
SIGEOM	Roche	14PA	Kimberlite (croupe 1)	MB96-28
SIGEOM	Roche	14PB	Kimberlite (qroupe II)	MB96-28
SIGEOM	Roche	V4A	Komatiite	MB96-28
SIGEOM	Roche	V4D	Komatiite dunitique	MB96-28
SIGEOM	Roche	V4C	Komatiite péridotitique	MB96-28
SIGEOM	Roche	V4B	Komatiite pyroxénitique	MB96-28
SIGEOM	Roche	14R	Lamproite	MB96-28
SIGEOM	Roche	130	Lamprophyre mafique	MB96-28
SIGEOM	Roche	140	l.amprophvre ultrabasique	MB96-28
SIGEOM	Roche	V2FL	Latite	MB96-28
SIGEOM	Roche	V2LR	Latite foidifère	MB96-28
SIGEOM	Roche	V2E	Latite quartzifère	MB96-28
SIGEOM	Roche	13P	Leuconorite	MB96-28
SIGEOM	Roche	14K	Lherzolite	MB96-28
SIGEOM	Roche	14QM	Magnésiocarbonatite	MB96-28
SIGEOM	Roche	120	Mangérite (Monzonite à hyperstène)	MB96-28
SIGEOM	Roche	V4E	Meimechite	MB96-28
SIGEOM	Roche	V4F	Melilitite	MB96-28
SIGEOM	Roche	V4FO	Melilitite à olivine	MB96-28
SIGEOM	Roche	14T	Mélilitolite	MB96-28
SIGEOM	Roche	130M	Minette	MB96-28

SIGEOM	Roche	140M	Monchiquite	MB96-28
SIGEOM	Roche	12H	Monzodiorite	MB96-28
SIGEOM	Roche	12HR	Monzodiorite foidifère	MB96-28
SIGEOM	Roche	12HF	Monzodiorite foidique	MB96-28
SIGEOM	Roche	12G	Monzodiorite quartzifère	MB96-28
SIGEOM	Roche	13C	Monzoqabbro	MB96-28
SIGEOM	Roche	13CR	Monzogabbro foidifère	MB96-28
SIGEOM	Roche	13CF	Monzogabbro foidique	MB96-28
SIGEOM	Roche	13CQ	Monzogabbro quartzifère	MB96-28

Source	Domaine	Code	Signification	Référence
SIGEOM	Roche	11M	Monzo-Granite	MB96-28
SIGEOM	Roche	11R	Monzo-granite à hyperstène	MB96-28
SIGEOM	Roche	12F	Monzonite	MB96-28
SIGEOM	Roche	12FR	Monzonite foidifère	MB96-28
SIGEOM	Roche	12E	Monzonite quartzifère	MB96-28
SIGEOM	Roche	13S	Monzonorite	MB96-28
SIGEOM	Roche	12K	Monzosyénite	MB96-28
SIGEOM	Roche	12KF	Monzosyénite foidique	MB96-28
SIGEOM	Roche	OB	Mort Terrain (Overburden)	
SIGEOM	Roche	S6	Mudrock	MB96-28
SIGEOM	Roche	S6E	Mudshale	MB96-28
SIGEOM	Roche	S6F	Mudslate	MB96-28
SIGEOM	Roche	S6D	Mudstone	MB96-28
SIGEOM	Roche	S7E	Mudstone	MB96-28
SIGEOM	Roche	V3GM	Mugéargite	MB96-28
SIGEOM	Roche	V41N	Néphélinite	MB96-28
SIGEOM	Roche	13J	Norite	MB96-28
SIGEOM	Roche	13L	Norite à olivine	MB96-28
SIGEOM	Roche	14E	Orthopyroxénite	MB96-28
SIGEOM	Roche	14H	Orthopyroxénite à olivine	MB96-28
SIGEOM	Roche	S7G	Packstone	MB96-28
SIGEOM	Roche	V1BP	Pantellérite	MB96-28
SIGEOM	Roche	11G	Pegmatite (granitique)	MB96-28
SIGEOM	Roche	141	Péridotite	MB96-28
SIGEOM	Roche	V2G	Phonolite	MB96-28
SIGEOM	Roche	V2GT	Phonolite téphritique	MB96-28
SIGEOM	Roche	V4H	Pic rite	MB96-28
SIGEOM	Roche	V4G	Picrobasalte	MB96-28
SIGEOM	Roche	140P	Polzénite	MB96-28
SIGEOM	Roche	14B	Pyroxénite	MB96-28
SIGEOM	Roche	11J	Quartzolite (Silexite)	MB96-28
SIGEOM	Roche	V1C	Rhyodacite	MB96-28
SIGEOM	Roche	V1B	Rhyolite	MB96-28
SIGEOM	Roche	V1A	Rhyolite à feldspath alcalin	MB96-28
SIGEOM	Roche	V4M	Roche volcanique ultramafique à melilite	MB96-28
SIGEOM	Roche	S7K	Rudstone	MB96-28
SIGEOM	Roche	140S	Sannaite	MB96-28
SIGEOM	Roche	S	Sédiments	MB96-28
SIGEOM	Roche	14N	Serpentinite	MB96-28
SIGEOM	Roche	V3GS	Shoshonite	MB96-28
SIGEOM	Roche	S6B	Siltshale	MB96-28
SIGEOM	Roche	S6C	Siltslate	MB96-28
SIGEOM	Roche	S6A	Siltsone	MB96-28
SIGEOM	Roche	130S	Spessartite	MB96-28
SIGEOM	Roche	S2B	SubArkose	MB96-28
SIGEOM	Roche	S2F	Sublitharénite	MB96-28

SIGEOM	Roche	S12E	Sulfate	MB96-28
SIGEOM	Roche	F1	Sulfures Massifs	MB96-28
SIGEOM	Roche	F2	Sulfures semi-Massifs	MB96-28
SIGEOM	Roche	12D	Syénite	MB96-28
SIGEOM	Roche	12B	Syénite à feldspath alcalin	MB96-28
SIGEOM	Roche	12N	Syénite à hyperstène	MB96-28
SIGEOM	Roche	12DR	Syénite foidifère	MB96-28
SIGEOM	Roche	12BR	Syénite foidifère à feldspath alcalin	MB96-28
SIGEOM	Roche	12DF	Syénite foidique	MB96-28
SIGEOM	Roche	12C	Syénite quartzifère	MB96-28

Source	Domaine	Code	Signification	Référence
SIGEOM	Roche	12A	Syénite quartzifère à feldspath alcalin	MB96-28
SIGEOM	Roche	12M	Syénite quartzifère à feldspath alcalin avec hyperstène	MB96-28
SIGEOM	Roche	11L	Syéno-qranite	MB96-28
SIGEOM	Roche	11Q	Syéno-qranite à hyperstène	MB96-28
SIGEOM	Roche	S12B	Sylvite	MB96-28
SIGEOM	Roche	V31	Téphrite	MB96-28
SIGEOM	Roche	V31P	Téphryte phonolitique	MB96-28
SIGEOM	Roche	S4J	Tillite	MB96-28
SIGEOM	Roche	11D	Tonalite	MB96-28
SIGEOM	Roche	V2F	Trachyandésite	MB96-28
SIGEOM	Roche	V3G	Trachyandésite basaltique	MB96-28
SIGEOM	Roche	V3D	Trachybasalte	MB96-28
SIGEOM	Roche	V3DK	Trachybasalte potassique	MB96-28
SIGEOM	Roche	V1E	Trachydacite	MB96-28
SIGEOM	Roche	V2D	Trachyte	MB96-28
SIGEOM	Roche	V2B	Trachyte à feldspath alcalin	MB96-28
SIGEOM	Roche	V2DC	Trachyte commenditique	MB96-28
SIGEOM	Roche	V2DR	Trachyte foidifère	MB96-28
SIGEOM	Roche	V2BR	Trachyte foidifère à feldspath alcalin	MB96-28
SIGEOM	Roche	V2DP	Trachyte pantellétique	MB96-28
SIGEOM	Roche	V2C	Trachyte quartzifère	MB96-28
SIGEOM	Roche	V2A	Trachyte quartzifère à feldspath alcalin	MB96-28
SIGEOM	Roche	13N	Troctolite	MB96-28
SIGEOM	Roche	11E	Trondhjémite	MB96-28
SIGEOM	Roche	130V	Vogesite	MB96-28
SIGEOM	Roche	V	Volcanite	
SIGEOM	Roche	V1	Volcanite felsique	MB96-28
SIGEOM	Roche	V2	Volcanite Intermédiaire	MB96-28
SIGEOM	Roche	V3	Volcanite mafique	MB96-28
SIGEOM	Roche	V4	Volcanite ultramafique	MB96-28
SIGEOM	Roche	S3	Wacke	MB96-28
SIGEOM	Roche	S3C	Wacke Arkosique	MB96-28
SIGEOM	Roche	S3D	Wacke Feldspathique	MB96-28
SIGEOM	Roche	S3E	Wacke Lithique	MB96-28
SIGEOM	Roche	S3A	Wacke Quartzitique	MB96-28
SIGEOM	Roche	S7F	Wackestone	MB96-28
SIGEOM	Roche	14D	Websterite	MB96-28
SIGEOM	Roche	14G	Websterite à olivine	MB96-28
SIGEOM	Roche	14J	Wehrlite	MB96-28
SIGEOM	Roche Métamorphique	M23	Agmatite	MB96-28
SIGEOM	Roche Métamorphique	M16	Amphibolite	MB96-28
SIGEOM	Roche Métamorphique	M26	Brèche Tectonique	MB96-28
SIGEOM	Roche Métamorphique	M24	Cataclastite	MB96-28
SIGEOM	Roche Métamorphique	M18	Cornéenne	MB96-28
SIGEOM	Roche Métamorphique	M31	Coticule	MB96-28

SIGEOM	Roche Métamorphique	M21	Diatexite	MB96-28
SIGEOM	Roche Métamorphique	M17	Éclogite	MB96-28
SIGEOM	Roche Métamorphique	M1	Gneiss	MB96-28
SIGEOM	Roche Métamorphique	T3A	Gneiss droit (cstraiqht gneiss»)	MB96-28
SIGEOM	Roche Métamorphique	M6	Gneiss granitique	MB96-28
SIGEOM	Roche Métamorphique	T3D	Gneiss irréqulier	MB96-28
SIGEOM	Roche Métamorphique	T3B	Gneiss porphyroclastique	MB96-28
SIGEOM	Roche Métamorphique	M5	Gneiss Quartzofeldspathique	MB96-28
SIGEOM	Roche Métamorphique	T3C	Gneiss régulier	MB96-28
SIGEOM	Roche Métamorphique	M2	Gneiss Rubané	MB96-28
SIGEOM	Roche Métamorphique	M21A	Granite d'Anatexie	MB96-28

Source	Domaine	Code	Signification	Référence
SIGEOM	Roche Métamorphique	M7	Granulite	MB96-28
SIGEOM	Roche Métamorphique	M13	Marbre	MB96-28
SIGEOM	Roche Métamorphique	M20	Métatexite	MB96-28
SIGEOM	Roche Métamorphique	M22	Migmatite	MB96-28
SIGEOM	Roche Métamorphique	M25	Mylonite	MB96-28
SIGEOM	Roche Métamorphique	M3	Orthogneiss	MB96-28
SIGEOM	Roche Métamorphique	M9	Orthoschiste	MB96-28
SIGEOM	Roche Métamorphique	M4	Paragneiss	MB96-28
SIGEOM	Roche Métamorphique	M10	Paraschiste	MB96-28
SIGEOM	Roche Métamorphique	M11	Phyllade	MB96-28
SIGEOM	Roche Métamorphique	M12	Quartzite	MB96-28
SIGEOM	Roche Métamorphique	M14	Roche Calco-Silicatée	MB96-28
SIGEOM	Roche Métamorphique	M15	Roche Métasomatique (Skarn)	MB96-28
SIGEOM	Roche Métamorphique	M8	Schiste	MB96-28
SIGEOM	Roche Métamorphique	M30	Tourmalinite	MB96-28
SIGEOM	Roche Tectonite	T2E	Blastomylon ite	MB96-28
SIGEOM	Roche Tectonite	T1A	Brèche de Faille	MB96-28
SIGEOM	Roche Tectonite	T1F	Brèche d'Impact	MB96-28
SIGEOM	Roche Tectonite	T4	Brèche tectonique	MB96-28
SIGEOM	Roche Tectonite	T4B	Brèche tectonique à matrice de marbre	MB96-28
SIGEOM	Roche Tectonite	T1	Cataclastite	MB96-28
SIGEOM	Roche Tectonite	T1C	Gouge de faille	MB96-28
SIGEOM	Roche Tectonite	T1G	Impactite	MB96-28
SIGEOM	Roche Tectonite	T4A	Mélange tectonique	MB96-28
SIGEOM	Roche Tectonite	T1B	Microbrèche de Faille	MB96-28
SIGEOM	Roche Tectonite	T1E	Mylolisthénite	MB96-28
SIGEOM	Roche Tectonite	T2	Mylonite	MB96-28
SIGEOM	Roche Tectonite	T2B	Orthomylonite	MB96-28
SIGEOM	Roche Tectonite	T2D	Phyllonite	MB96-28
SIGEOM	Roche Tectonite	T2A	Protomylon ite	MB96-28
SIGEOM	Roche Tectonite	T1D	Pseudotachyl ite	MB96-28
SIGEOM	Roche Tectonite	T2C	Ultramylonite	MB96-28
VIA	Structure	APL	Axe de Pli	
VIA	Structure	DIA	Diaclase, Joint, Fracture	
VIA	Structure	DYK	Dyke	
VIA	Structure	FAI	Faille, Cisaillement	
VIA	Structure	FOL	Foliation	
VIA	Structure	LAM	Lamination, Rubannement, Flow banding	
VIA	Structure	LIN	Linéation	
VIA	Structure	LIT	Litage, Bedding, SO, Stratification	
VIA	Structure	PAX	Plan Axial	
VIA	Structure	SCH	Schistosité, Gneissosité, SP, S1, S2, S3	
VIA	Structure	SGL	Strie Glaciaire	
VIA	Structure	VEI	Veine	

SIGEOM	Structure	L	Axe de mullion	PR02000-08
SIGEOM	Structure	B	Axe de boudin	PR02000-08
SIGEOM	Structure	J	Axe de joint en colonne	PR02000-08
VIA	Structure	AP	Axe de pli	
SIGEOM	Structure	Q	Axe de stylolithe	PR02000-08
SIGEOM	Structure	E	Axe d'étirement	PR02000-08
SIGEOM	Structure	A	Axe d'étirement d'objet déformé	PR02000-08
SIGEOM	Structure	Y	Axe d'étirement plaquage minéral	PR02000-08
SIGEOM	Structure	M	Axe Minérale primaire (magmatique)	PR02000-08
SIGEOM	Structure	N	Axe Minérale secondaire (tectonométamorphique)	PR02000-08
VIA	Structure	LE	Linéation d'étirement	
SIGEOM	Structure	L1	Linéation d'intersection	PR02000-08

Source	Domaine	Code	Signification	Référence
SIGEOM	Structure	L2	Linéation d'intersection	PR02000-08
SIGEOM	Structure	L3	Linéation d'intersection	PR02000-08
SIGEOM	Structure	L4	Linéation d'intersection	PR02000-08
SIGEOM	Structure	L	Linéation Indéterminée	PR02000-08
VIA	Structure	LM	Linéation minérale	
SIGEOM	Structure	F	Strie de faille	PR02000-08
VIA	Structure	SG	Strie glaciaire	
SIGEOM	Structure	T	Strie intercouche	PR02000-08
VIA	Structure	CC	Clivage de crénulation	
VIA	Structure	DY	Dyke	
VIA	Structure	FA	Faille	
VIA	Structure	FR	Fracture	
VIA	Structure	LI	Litage	
VIA	Structure	PA	Plan axial	
VIA	Structure	S1	Schistosité S1	
VIA	Structure	S2	Schistosité S2	
VIA	Structure	S3	Schistosité S3	
VIA	Structure	VN	Veine	
VIA	Structure	ZC	Zone de cisaillement	
SIGEOM	Texture	AC	Aciculaire	PR02000-08
SIGEOM	Texture	AD	Adcumulat	PR02000-08
SIGEOM	Texture	AA	Affleurement caractérisé par le plissement	PR02000-08
SIGEOM	Texture	AT	Agmatitique	PR02000-08
SIGEOM	Texture	AL	Alaskitique	PR02000-08
SIGEOM	Texture	AE	Altéré	PR02000-08
SIGEOM	Texture	AO	Amas arrondis (globulaires)	PR02000-08
SIGEOM	Texture	AB	Amiboïdal(e)	PR02000-08
SIGEOM	Texture	AM	Amygdalaire	PR02000-08
SIGEOM	Texture	AM	Amygdalaire	PR02000-08
SIGEOM	Texture	AN	Anastomosé	PR02000-08
SIGEOM	Texture	AR	Antirapakivi	PR02000-08
SIGEOM	Texture	AP	Aphanitique	PR02000-08
SIGEOM	Texture	AY	Apophyse (en)	PR02000-08
SIGEOM	Texture	AS	Arborescent	PR02000-08
SIGEOM	Texture	AU	Autoclastique	PR02000-08
SIGEOM	Texture	XX	Autres	PR02000-08
SIGEOM	Texture	BA	Bancs (en)	PR02000-08
SIGEOM	Texture	BM	Bandes de cimentation	PR02000-08
SIGEOM	Texture	BS	Basal(e)	PR02000-08
SIGEOM	Texture	BE	Birds eyes	PR02000-08
SIGEOM	Texture	BI	Biseau	PR02000-08
SIGEOM	Texture	BL	Blocs (à)	PR02000-08
SIGEOM	Texture	BU	Bordure / limite de coulée	PR02000-08

SIGEOM	Texture	BV	Botryoïdal	PR02000-08
SIGEOM	Texture	BO	Boudinage	PR02000-08
SIGEOM	Texture	BC	Brèche à coussins ordinaires isolés	PR02000-08
SIGEOM	Texture	BG	Brèche à coussins peu serrés	PR02000-08
SIGEOM	Texture	BF	Brèche à méga-coussins isolés	PR02000-08
SIGEOM	Texture	BB	Brèche à mini-coussins isolés	PR02000-08
SIGEOM	Texture	BQ	Brèche de coulée / Brèche de lave	PR02000-08
SIGEOM	Texture	BH	Brèche de coussins désagrégés / brisés	PR02000-08
SIGEOM	Texture	BK	Brèche de coussins fragmentés	PR02000-08
SIGEOM	Texture	BN	Brèche d'intrusion	PR02000-08
SIGEOM	Texture	BP	Brèche pyroclastique	PR02000-08
SIGEOM	Texture	BT	Brèche tectonique	PR02000-08
SIGEOM	Texture	BR	Bréchique / Brèche	PR02000-08

Source	Domaine	Code	Signification	Référence
SIGEOM	Texture	BY	Broyage	PR02000-08
SIGEOM	Texture	CA	Cailloux 4-64 mm	PR02000-08
SIGEOM	Texture	PK	Cailloux aliqnés «pebble stringers»	PR02000-08
SIGEOM	Texture	CN	Cannelure	PR02000-08
SIGEOM	Texture	CO	Cataclastique	PR02000-08
SIGEOM	Texture	CE	Cendre (à)	PR02000-08
SIGEOM	Texture	VP	Centre volcanique/ faciès proximal	PR02000-08
SIGEOM	Texture	DN	Cheminée d'alimentation (dyke nourricier)	PR02000-08
SIGEOM	Texture	CV	Cheminée volcanique	PR02000-08
SIGEOM	Texture	CH	Chenal	PR02000-08
SIGEOM	Texture	CD	Chenal d'érosion (à)	PR02000-08
SIGEOM	Texture	CG	Chenalisé	PR02000-08
SIGEOM	Texture	CS	Cisaillé(e)	PR02000-08
VIA	Texture	CIS	Cisaillement	
SIGEOM	Texture	JC	Columnaire/ (joints en colonnes)	PR02000-08
SIGEOM	Texture	CB	Convolutions (à)	PR02000-08
SIGEOM	Texture	KO	Coronitique	PR02000-08
SIGEOM	Texture	NM	Coulé massive à noyaux saussuritisés	PR02000-08
SIGEOM	Texture	CL	Coulée	PR02000-08
SIGEOM	Texture	NC	Coulée coussinée à noyaux saussuritisés	PR02000-08
SIGEOM	Texture	FZ	Coulée fraqmentée	PR02000-08
SIGEOM	Texture	CK	Coulée massive	PR02000-08
SIGEOM	Texture	CZ	Coulée massive à surface coussinée	PR02000-08
SIGEOM	Texture	CW	Coulée massive grenue et/ou partie basale grenue de coulée	PR02000-08
SIGEOM	Texture	CO	Coussiné (coussins)	PR02000-08
SIGEOM	Texture	CO	Coussiné (coussins)	PR02000-08
SIGEOM	Texture	XP	Coussins allonqés	PR02000-08
SIGEOM	Texture	FP	Coussins aplatis	PR02000-08
SIGEOM	Texture	MD	Coussins en molaire	PR02000-08
SIGEOM	Texture	CF	Coussins fragmentés	PR02000-08
SIGEOM	Texture	CI	Coussins isolés	PR02000-08
SIGEOM	Texture	CJ	Coussins jointifs	PR02000-08
SIGEOM	Texture	CT	Crescumulat	PR02000-08
SIGEOM	Texture	CR	Cristalloblastique	PR02000-08
SIGEOM	Texture	CX	Cristaux (en)	PR02000-08
SIGEOM	Texture	CP	Cryptalquaire	PR02000-08
SIGEOM	Texture	CU	Cumulat (à)	PR02000-08
SIGEOM	Texture	CM	Cumulite	PR02000-08
SIGEOM	Texture	DS	Cupules (cdish structure»)	PR02000-08
SIGEOM	Texture	CY	Cyclique(Cyclicité)	PR02000-08

SIGEOM	Texture	DG	Désagrégés / brisés	PR02000-08
SIGEOM	Texture	DO	Diabasique	PR02000-08
SIGEOM	Texture	DB	Diablastique	PR02000-08
SIGEOM	Texture	DC	Diaclasé	PR02000-08
SIGEOM	Texture	DR	Direction de courant	PR02000-08
SIGEOM	Texture	DE	Direction d'écoulement de coulés	PR02000-08
SIGEOM	Texture	DD	Discordance	PR02000-08
SIGEOM	Texture	DK	Drusique	PR02000-08
SIGEOM	Texture	DU	Dunes	PR02000-08
SIGEOM	Texture	DW	Durchbewequnq	PR02000-08
SIGEOM	Texture	SB	Échappement (structure d')	PR02000-08
SIGEOM	Texture	ED	Écharde	PR02000-08
SIGEOM	Texture	EO	Écoulement (structure d')	PR02000-08
SIGEOM	Texture	EF	Effondrement (structure d')	PR02000-08
SIGEOM	Texture	EL	Empreinte de cannelures	PR02000-08
Source	**Domaine**	**Code**	**Signification**	**Référence**
SIGEOM	Texture	EC	Em preinte de charge (« load cast»)	PR02000-08
SIGEOM	Texture	EI	Empreinte d'impact	PR02000-08
SIGEOM	Texture	EE	En échelon	PR02000-08
SIGEOM	Texture	ES	En festons	PR02000-08
SIGEOM	Texture	EN	Enclave	PR02000-08
SIGEOM	Texture	EM	Encroûtement (ecrustiticatcn»)	PR02000-08
SIGEOM	Texture	EP	Épiclastique	PR02000-08
SIGEOM	Texture	EQ	Équigranulaire	PR02000-08
SIGEOM	Texture	ER	Excroissances	PR02000-08
SIGEOM	Texture	EX	Extrusif (ve)	PR02000-08
SIGEOM	Texture	FJ	Faille intra-formationnelle	PR02000-08
SIGEOM	Texture	FV	Faille synvolcanique	PR02000-08
SIGEOM	Texture	FD	Fente de dessication	PR02000-08
SIGEOM	Texture	FM	Fente de refroidissement	PR02000-08
SIGEOM	Texture	FI	Fibreux (se)	PR02000-08
SIGEOM	Texture	FB	Fibroblastique	PR02000-08
SIGEOM	Texture	FS	Filandré « Flaser »	PR02000-08
SIGEOM	Texture	FH	Filons-couches cogénitiques (synvolcaniques)	PR02000-08
SIGEOM	Texture	FE	Flammes	PR02000-08
SIGEOM	Texture	FL	Flué, par fluage - fluidal	PR02000-08
SIGEOM	Texture	FL	Fluidal(e) (à structure)	PR02000-08
SIGEOM	Texture	FT	Flûte (eflutecast»)	PR02000-08
SIGEOM	Texture	FX	Flûte déformée par surcharge	PR02000-08
SIGEOM	Texture	FO	Folié(e)	PR02000-08
SIGEOM	Texture	FF	Fossilifère	PR02000-08
SIGEOM	Texture	FA	Fracturé(e)	PR02000-08
SIGEOM	Texture	FC	Fractures radiales dans les coussins	PR02000-08
SIGEOM	Texture	FG	Fragmenté	PR02000-08
SIGEOM	Texture	FW	Fragments allongés «monomictes»/monogéniques	PR02000-08
SIGEOM	Texture	FU	Fragments allongés «polymictic»/polygéniques	PR02000-08
SIGEOM	Texture	FQ	Fragments aplatis «monomictic»/monogénique	PR02000-08
SIGEOM	Texture	FK	Fragments aplatis «polymictic»/polygénique	PR02000-08
SIGEOM	Texture	FR	Frites (cpencil structure») (en crayon)	PR02000-08
SIGEOM	Texture	GA	Galets (à)(64-256 mm)	PR02000-08
SIGEOM	Texture	GE	Géode	PR02000-08
SIGEOM	Texture	GB	Glomeroblastique	PR02000-08
SIGEOM	Texture	GC	Glomeroclastique	PR02000-08
SIGEOM	Texture	GX	Glomérocristallin(e)	PR02000-08
SIGEOM	Texture	GH	Glomeroporphyrique	PR02000-08
SIGEOM	Texture	NR	Gneiss à crayons	PR02000-08
SIGEOM	Texture	GD	Gneiss droit (cstraiqht gneiss»)	PR02000-08

SIGEOM	Texture	GS	Gneissique	PR02000-08
SIGEOM	Texture	GW	Gradation densimétrique	PR02000-08
SIGEOM	Texture	VG	Gradation granulométrique	PR02000-08
SIGEOM	Texture	GF	Grains fins (à) < 1 mm roches ignées	PR02000-08
SIGEOM	Texture	GG	Grains grossiers (à) >5 mm roches ignées	PR02000-08
SIGEOM	Texture	GM	Grains moyens (à) 1-5 mm roches ignées	PR02000-08
SIGEOM	Texture	GT	Grains très fins	PR02000-08
SIGEOM	Texture	GO	Grains très grossiers	PR02000-08
SIGEOM	Texture	GR	Granoblastique	PR02000-08
SIGEOM	Texture	GI	Granoclassement inverse	PR02000-08
SIGEOM	Texture	GJ	Granoclassement inverse suivi de normal	PR02000-08
SIGEOM	Texture	GN	Granoclassement normal	PR02000-08
SIGEOM	Texture	GK	Granoclassement normal suivi d'inverse	PR02000-08
SIGEOM	Texture	GQ	Granoclastique	PR02000-08
SIGEOM	Texture	GY	Granophyrique	PR02000-08

Source	Domaine	Code	Signification	Référence
SIGEOM	Texture	GU	Granules (à) (2-4 mm)	PR02000-08
SIGEOM	Texture	GP	Graphique	PR02000-08
SIGEOM	Texture	GV	Griffon	PR02000-08
SIGEOM	Texture	HA	Harrisitic	PR02000-08
SIGEOM	Texture	HE	Hélicitique	PR02000-08
SIGEOM	Texture	HU	Hétéradcumulat	PR02000-08
SIGEOM	Texture	HB	Hétéroblastique	PR02000-08
SIGEOM	Texture	HK	Hétérogène	PR02000-08
SIGEOM	Texture	HG	Hétérogranulaire	PR02000-08
SIGEOM	Texture	HC	Holocristallin(e)	PR02000-08
SIGEOM	Texture	HH	Holohyalin(e)	PR02000-08
SIGEOM	Texture	HL	Hololeucocrate	PR02000-08
SIGEOM	Texture	HM	Holomélanocrate	PR02000-08
SIGEOM	Texture	HQ	Homéoblastique	PR02000-08
SIGEOM	Texture	HJ	Homogène	PR02000-08
SIGEOM	Texture	HT	Homotactique	PR02000-08
SIGEOM	Texture	HY	Hyaloclastites	PR02000-08
SIGEOM	Texture	HR	Hyaloclastites remaniées	PR02000-08
SIGEOM	Texture	HP	Hvalopilitique	PR02000-08
SIGEOM	Texture	TH	Hyalotuf	PR02000-08
SIGEOM	Texture	HD	Hypidiomorphe	PR02000-08
SIGEOM	Texture	HX	Hypocristallin(e)	PR02000-08
SIGEOM	Texture	IM	Imbrication de cailloux, blocs	PR02000-08
SIGEOM	Texture	IP	Imprégnation	PR02000-08
SIGEOM	Texture	IS	Intersertale	PR02000-08
SIGEOM	Texture	IT	Intraclastes (à)	PR02000-08
SIGEOM	Texture	IR	Intraformationnel(le)	PR02000-08
SIGEOM	Texture	IU	Intrusif(ve) / injection	PR02000-08
SIGEOM	Texture	IC	Iridescence	PR02000-08
SIGEOM	Texture	IL	Isolés	PR02000-08
SIGEOM	Texture	JC	Joints en colonnes	PR02000-08
SIGEOM	Texture	KR	Karstique	PR02000-08
SIGEOM	Texture	LU	Labradorescence	PR02000-08
SIGEOM	Texture	LA	Laminaire (laminé)	PR02000-08
SIGEOM	Texture	LC	Laminations convolutées	PR02000-08
SIGEOM	Texture	CP	Laminations cryptalqaires	PR02000-08
SIGEOM	Texture	LQ	Laminations obliques	PR02000-08
SIGEOM	Texture	LO	Laminations ondulantes	PR02000-08
SIGEOM	Texture	LL	Laminations ondulantes lenticulaires	PR02000-08
SIGEOM	Texture	LP	Laminations parallèles	PR02000-08

SIGEOM	Texture	LI	Lapilli (à)	PR02000-08
SIGEOM	Texture	TO	Lapillistone	PR02000-08
SIGEOM	Texture	LT	Lattes (en)	PR02000-08
SIGEOM	Texture	LV	Lave / coulée de lave	PR02000-08
SIGEOM	Texture	LK	Lave en blocs	PR02000-08
SIGEOM	Texture	LF	Lépidoblastique	PR02000-08
SIGEOM	Texture	LX	Leucocrate	PR02000-08
SIGEOM	Texture	LS	Leucosome	PR02000-08
SIGEOM	Texture	SA	Lité(e), stratifiée e)	PR02000-08
SIGEOM	Texture	AG	Lits amalgamés	PR02000-08
SIGEOM	Texture	LN	Lits d'épaisseur moyenne (10 à 25 cm)	PR02000-08
SIGEOM	Texture	LG	Lits épais (>25 cm)	PR02000-08
SIGEOM	Texture	LD	Lits lenticulaires	PR02000-08
SIGEOM	Texture	LM	Lits minces (1-10 cm)	PR02000-08
SIGEOM	Texture	LB	Lobe	PR02000-08
SIGEOM	Texture	MC	Mégacoussins (à)	PR02000-08

Source	Domaine	Code	Signification	Référence
SIGEOM	Texture	MP	Mégaporphyrique	PR02000-08
SIGEOM	Texture	MX	Mélanocrate	PR02000-08
SIGEOM	Texture	MS	Mélanosome	PR02000-08
SIGEOM	Texture	MK	Mésocrate	PR02000-08
SIGEOM	Texture	MF	Mésocumulat	PR02000-08
SIGEOM	Texture	ME	Métamorphisé	PR02000-08
SIGEOM	Texture	ML	Miarolitique	PR02000-08
SIGEOM	Texture	MT	Micritique	PR02000-08
SIGEOM	Texture	MB	Microbrèche	PR02000-08
SIGEOM	Texture	MI	Microlitique	PR02000-08
SIGEOM	Texture	MR	Microporphvrique	PR02000-08
SIGEOM	Texture	MU	Minicoussins (à)	PR02000-08
SIGEOM	Texture	MZ	Mobilisat	PR02000-08
SIGEOM	Texture	MM	Monogénique «Monomictic»	PR02000-08
SIGEOM	Texture	MO	Mosaïque	PR02000-08
SIGEOM	Texture	MN	Mylonitique	PR02000-08
SIGEOM	Texture	MY	Myrmékitique	PR02000-08
SIGEOM	Texture	NB	Nébulitique	PR02000-08
SIGEOM	Texture	NE	Nématoblastique	PR02000-08
SIGEOM	Texture	NS	Néosome	PR02000-08
SIGEOM	Texture	NY	Noyaux	PR02000-08
SIGEOM	Texture	OC	Ocellaire	PR02000-08
SIGEOM	Texture	OE	Oeillé(e)	PR02000-08
SIGEOM	Texture	01	Oïkocryst (à)	PR02000-08
SIGEOM	Texture	00	Oolitique	PR02000-08
SIGEOM	Texture	OP	Ophitique	PR02000-08
SIGEOM	Texture	OR	Orbiculaire	PR02000-08
SIGEOM	Texture	OU	Orthocumulat	PR02000-08
SIGEOM	Texture	PS	Paléosome	PR02000-08
SIGEOM	Texture	PE	Paléosurface d'érosion	PR02000-08
SIGEOM	Texture	PA	Panidiomorphe	PR02000-08
SIGEOM	Texture	PV	Patron d'interférence	PR02000-08
SIGEOM	Texture	PG	Pegmatitique	PR02000-08
SIGEOM	Texture	PL	Pellets (à)	PR02000-08
SIGEOM	Texture	PD	Péloïdes	PR02000-08
SIGEOM	Texture	PT	Perlitique	PR02000-08
SIGEOM	Texture	LR	Peu serrés (loosely packed)	PR02000-08
SIGEOM	Texture	PH	Phanéritique	PR02000-08
SIGEOM	Texture	PI	Phénocristique	PR02000-08

SIGEOM	Texture	PZ	Plis ptygmatiques	PR02000-08
SIGEOM	Texture	PU	Plutonique	PR02000-08
SIGEOM	Texture	PC	Poecilitique	PR02000-08
SIGEOM	Texture	PB	Poeciloblastique	PR02000-08
SIGEOM	Texture	PM	Polygénique j«polymictic»	PR02000-08
SIGEOM	Texture	PN	Ponce	PR02000-08
SIGEOM	Texture	PP	Porphyre	PR02000-08
SIGEOM	Texture	PO	Porphyrique	PR02000-08
SIGEOM	Texture	PO	Porphyroblastique	PR02000-08
SIGEOM	Texture	PJ	Porphyroclastique	PR02000-08
SIGEOM	Texture	PX	Prismatique	PR02000-08
SIGEOM	Texture	PF	Protoclastique	PR02000-08
SIGEOM	Texture	PR	Pyroclastique	PR02000-08
SIGEOM	Texture	RO	Radeaux (en)	PR02000-08
SIGEOM	Texture	RK	Rapakivique	PR02000-08
SIGEOM	Texture	RG	Régolite	PR02000-08
SIGEOM	Texture	RN	Remanié(e)	PR02000-08

Source	Domaine	Code	Signification	Référence
SIGEOM	Texture	RL	Remplacement	PR02000-08
SIGEOM	Texture	RF	Réniforme	PR02000-08
SIGEOM	Texture	RE	Réticulé(e)	PR02000-08
SIGEOM	Texture	RC	Rides de courant	PR02000-08
SIGEOM	Texture	RP	Rides de plage	PR02000-08
SIGEOM	Texture	RM	Rill mark(s)	PR02000-08
SIGEOM	Texture	RI	Rip-up clast(s)	PR02000-08
SIGEOM	Texture	RQ	Ruban de quartz	PR02000-08
SIGEOM	Texture	RU	Rubané(e)	PR02000-08
SIGEOM	Texture	RA	Rubanement concentrique	PR02000-08
SIGEOM	Texture	LJ	Rubanement de diffusion (cl.ieseqano rinqs»)	PR02000-08
SIGEOM	Texture	RS	Rubanement symétrique	PR02000-08
SIGEOM	Texture	RT	Rubanement tectonique	PR02000-08
SIGEOM	Texture	SD	Saccaroïdale (granoblastique)	PR02000-08
SIGEOM	Texture	SC	Schisteux	PR02000-08
SIGEOM	Texture	SH	Schlieren	PR02000-08
SIGEOM	Texture	SR	Scoriacé(e)	PR02000-08
SIGEOM	Texture	SV	shaUercone	PR02000-08
SIGEOM	Texture	SL	Siump	PR02000-08
SIGEOM	Texture	SM	Sommital(e)	PR02000-08
SIGEOM	Texture	SP	Sphérolitique	PR02000-08
SIGEOM	Texture	SX	Spinifex (à)	PR02000-08
SIGEOM	Texture	SN	Stratifications / laminations obliques planaires	PR02000-08
SIGEOM	Texture	SQ	Stratifications / laminations obliques tangentielles	PR02000-08
SIGEOM	Texture	SF	Stratifications entrecroisées defosse	PR02000-08
SIGEOM	Texture	ST	Stratifiée e) / stratiforme	PR02000-08
SIGEOM	Texture	SG	Streaky mafiques en trait	PR02000-08
SIGEOM	Texture	SI	Strie	PR02000-08
SIGEOM	Texture	SK	Stromatic	PR02000-08
SIGEOM	Texture	SU	Stromatolitique	PR02000-08
SIGEOM	Texture	DW	Structure «durchbewegung »	PR02000-08
SIGEOM	Texture	ET	Structure de percement (cpiercement»)	PR02000-08
SIGEOM	Texture	PW	Structure en peigne (ecomb»)	PR02000-08
SIGEOM	Texture	SY	Stylolites	PR02000-08
SIGEOM	Texture	SO	Subophitique	PR02000-08
SIGEOM	Texture	SE	Surface d'érosion	PR02000-08
SIGEOM	Texture	TA	Tabulaire	PR02000-08
SIGEOM	Texture	TT	Talus (de)	PR02000-08

SIGEOM	Texture	TE	Tectonique	PR02000-08
SIGEOM	Texture	YH	Tectonique hétéroclastique	PR02000-08
SIGEOM	Texture	YL	Tectonite en L	PR02000-08
SIGEOM	Texture	YS	Tectonite en LIS	PR02000-08
SIGEOM	Texture	YZ	Tectonite en S	PR02000-08
SIGEOM	Texture	YM	Tectonite homoclastique	PR02000-08
SIGEOM	Texture	TF	Tracesfossiles (trous de vers, etc.)	PR02000-08
SIGEOM	Texture	TR	Trachytique / trachytoïde	PR02000-08
SIGEOM	Texture	TP	Trempe (de)	PR02000-08
SIGEOM	Texture	TM	Tuf à blocs	PR02000-08
SIGEOM	Texture	TZ	Tuf à blocs et tuf à lapilli	PR02000-08
SIGEOM	Texture	TD	Tuf à cendre	PR02000-08
SIGEOM	Texture	TX	Tuf à cristaux	PR02000-08
SIGEOM	Texture	TL	Tuf à lapilli	PR02000-08
SIGEOM	Texture	TY	Tuf à lapilli et tuf à blocs	PR02000-08
SIGEOM	Texture	TC	Tuf cherteux	PR02000-08
SIGEOM	Texture	TG	Tuf graphiteux	PR02000-08
SIGEOM	Texture	TI	Tuf lithique	PR02000-08

urce	Domaine	Code	Signification	Référence
SIGEOM	Texture	TS	Tuf soudé	PR02000-08
SIGEOM	Texture	TU	Tufacé	PR02000-08
SIGEOM	Texture	TB	Turbidite (voir quide des qéofiches)	PR02000-08
SIGEOM	Texture	VA	Variolitique	PR02000-08
SIGEOM	Texture	VE	Vesiculaire	PR02000-08
SIGEOM	Texture	VI	Vitreux(se)	PR02000-08
SIGEOM	Texture	VO	Volcanique	PR02000-08
SIGEOM	Texture	VC	Volcanoclastites	PR02000-08
SIGEOM	Texture	XB	Xénoblastique	PR02000-08
SIGEOM	Texture	XM	Xénomorphe	PR02000-08
SIGEOM	Texture	ZS	Zone de cisaillement	PR02000-08
SIGEOM	Texture	ZC	Zone de contact	PR02000-08
SIGEOM	Texture	ZD	Zone de déformation	PR02000-08
SIGEOM	Texture	ZF	Zone de faille	PR02000-08
SIGEOM	Texture	ZM	Zone minéralisée	PR02000-08
SIGEOM	Texture	ZR	Zone rouillée	PR02000-08
SIGEOM	Texture	AI	Amas irréguliers, agrégats	PR02000-08
SIGEOM	Texture	OI	Colloforme	PR02000-08
SIGEOM	Texture	CC	Concrétion(s) nodules	PR02000-08
SIGEOM	Texture	DT	Dendritique	PR02000-08
SIGEOM	Texture	DI	Disséminé	PR02000-08
SIGEOM	Texture	FN	Filonien	PR02000-08
SIGEOM	Texture	RB	Framboïdal	PR02000-08
SIGEOM	Texture	ID	Idiomorphe	PR02000-08
SIGEOM	Texture	IG	Intergranulaire	PR02000-08
SIGEOM	Texture	IE	lenticulaire	PR02000-08
SIGEOM	Texture	MA	Massif(ve)	PR02000-08
SIGEOM	Texture	NO	Nodulaire	PR02000-08
VIA	Texture	SSM	Semi-Massif	
SIGEOM	Texture	SW	Stockwerk	PR02000-08
SIGEOM	Texture	SJ	Stratoïde (estratabound»)	PR02000-08
SIGEOM	Texture	SS	Stringer	PR02000-08
SIGEOM	Texture	PY	Structure en cocarde (crustification , «cockade»)	PR02000-08
VIA	Texture	VN	Veine	

Appendix 3 – Outcrop description

INFORMATION AVAILABLE UPON REQUEST SUBMITTED TO VIRGINIA MINES INC.

info@minesvirginia.com

Toll free number: 800 476-1853

Appendix 4 – Grabs and boulders sample results

INFORMATION AVAILABLE UPON REQUEST SUBMITTED TO VIRGINIA MINES INC.

info@minesvirginia.com

Toll free number: 800 476-1853

Appendix 5 – Channel assay results

INFORMATION AVAILABLE UPON REQUEST SUBMITTED TO VIRGINIA MINES INC.

info@minesvirginia.com

Toll free number: 800 476-1853

Appendix 6 – Grab sample whole rock analysis (WRA) results

INFORMATION AVAILABLE UPON REQUEST SUBMITTED TO VIRGINIA MINES INC.

info@minesvirginia.com

Toll free number: 800 476-1853

Appendix 7 – Structure measurement table

INFORMATION AVAILABLE UPON REQUEST SUBMITTED TO VIRGINIA MINES INC.

info@minesvirginia.com

Toll free number: 800 476-1853

Appendix 8 – Assays certificates (Volume 2)

INFORMATION AVAILABLE UPON REQUEST SUBMITTED TO VIRGINIA MINES INC.

info@minesvirginia.com

Toll free number: 800 476-1853

Appendix 9 – Standards certificates

INFORMATION AVAILABLE UPON REQUEST SUBMITTED TO VIRGINIA MINES INC.

info@minesvirginia.com

Toll free number: 800 476-1853